UNIVERSITÀ
DI PAVIA

Dipartimento di Biologia e Biotecnologie "L. Spallanzani"

RNA metabolism and DNA damage in neurodegeneration: a new pathological relationship in Amyotrophic Lateral Sclerosis patients.

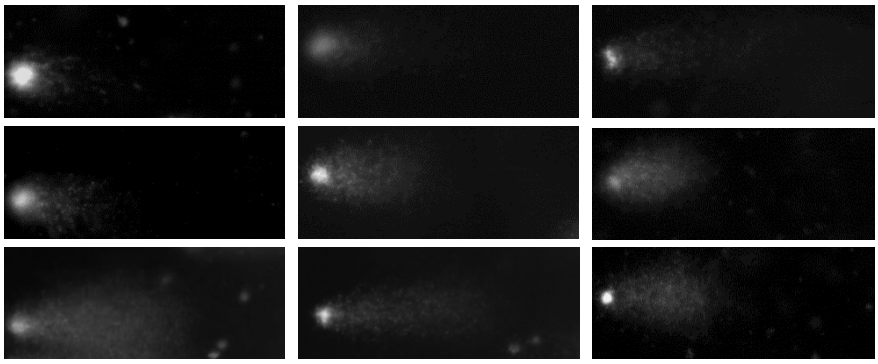

Maria Garofalo

Dottorato di Ricerca in
Genetica, Biologia Molecolare e Cellulare
Ciclo XXXIV – A.A. 2018-2021

TABLE OF CONTENTS

1. ABSTRACT

Neurodegenerative disorders, such as Alzheimer's disease (AD), Parkinson's disease (PD) and Amyotrophic Lateral Sclerosis (ALS), among others, are characterized by the progressive degeneration of the structure and function of the central or peripheral nervous system. Despite our knowledge has increased in the last years, their etiopathogenesis remains unknown since they are characterized by the interplay between many different processes and molecules. A central role of RNA metabolism has emerged in these diseases, involving both mRNAs processing and non coding RNAs biogenesis.

Nevertheless, the exact contribution of RNA metabolism dysregulation to neurodegenerative disorders is still unknown. Therefore, we performed a whole transcriptome analysis in Peripheral Blood Mononuclear Cells (PBMCs) of unmutated sporadic ALS patients (sALS), AD patients and PD patients compared to healthy controls. The aim was to intersect resulting differentially expressed (DE) genes for pointing out possible common grounds or differences in the pathways dysregulated in our casuistry. A total of 380 DE genes were found in sALS patients, 293 long noncoding RNAs (lncRNAs) and 87 mRNAs. In AD patients a total of 23 DE genes emerged, 19 protein coding genes and 4 lncRNAs. While in PD patients 5 genes only emerged from this analysis. Despite none of the gene was commonly DE in the three cohorts of patients, through KEGG and GO analyses we found common enriched pathways and biological processes in sALS and AD. These data provided insights into the different involvement of RNA metabolism and gene expression alterations in PBMCs of most common neurodegenerative disorders.

Because of the significance of whole transcriptome analysis conducted on sALS patients, we decide to enlarge this cohort and respective healthy control to perform a DE genes analysis. We further confirmed that RNA deregulation represents a good discriminant factor for pathological and healthy condition even in PBMCs.

The involvement of wild-type Superoxide Dismutase 1 (SOD1) in ALS sporadic cases has been investigates given its reduced expression in lysates from PBMCs in discordance with the abnormal upregulation of its transcript. SOD1 is the first gene associated to familial cases of ALS and is a soluble cytosolic enzyme, whose, aggregation cell toxicity and contributes to ALS pathogenesis. A fraction of the protein is also localized into the nucleus (nSOD1), where it seems involved in regulation of gene participating in the oxidative stress response and DNA repair. It has been suggested that nSOD1 could act as a scavenger enzyme also in the nucleus regulating the oxidative stress response, while

its cytoplasmic retention, due to genetic mutations or posttranslational modifications, could enhance cell vulnerability to oxidation and DNA damage. SOD1 distribution in sALS PBMCs lead to identify two subgroups of patients: those with High nSOD1 and those with Low nSOD1. The protein re-localization causes a reduction of DNA damage when SOD1 is accumulated as soluble protein within the nucleus (nSOD1), while it associates to an extensive DNA damage when SOD1 aggregated in the cytoplasm. In addition, a positive correlation between longer survival and higher amount of soluble SOD1 in the nucleus was described and this has suggested that SOD1 may exert a protective role against neurodegeneration when located within the nucleus, while aggregated cytoplasmic SOD1 could be impaired in its protective activity, and potentially harmful.

Thus, we investigated transcriptional pathways activated by nSOD1 in PBMCs of sALS patients by their stratification in relation to an "high" or a "low" level of soluble nSOD1. PBMCs from sALS patients (n=18) and healthy controls (n=12) were collected to perform RNA-sequencing experiments and differential expression analysis. We obtained different gene expression patterns for High and Low nSOD1 patients. Differentially expressed genes in High nSOD1 casuistry form a cluster similar to controls compared to Low nSOD1 group. Pathways activated in High nSOD1 patients relate to the upregulation of HSP70 molecular chaperones, possibly ensuring the correct protein folding and DNA repair processes. Also, investigating the possible effect of higher soluble nSOD1 and HSP70, we demonstrated that in this condition the DNA damage is reduced even under oxidative stress condition. While in Low nSOD1 group the upregulation of KDM4C and S100B may be responsible for reduced DNA damage sensing and increased neuroinflammation.

In conclusion, our findings highlight the importance of nuclear localization of soluble SOD1 as a protective mechanism in sALS patients. This different distribution confers differences in RNA regulation between the two groups of patients, leading to pathways supporting "protection" when nSOD1 is high, and "perturbation" of crucial biological systems when nSOD1 is low. Moreover, we demonstrated in vitro that high nSOD1 and HSP70 correspond to reduced DNA damage even under oxidative stress conditions, thus confirming that nuclear SOD1 aggregation or exclusion observed for mutant SOD1 may cause a loss of its protective activity in nuclear compartment.

2. ABBREVIATIONS

ALS: Amyotrophic Lateral Sclerosis

sALS: sporadic Amyotrophic Lateral Sclerosis

AD: Alzheimer's disease

PD: Parkinson's disease

lncRNA: long non coding RNA

ncRNA: non coding RNA

PBMCs: Peripheral Blood Mononuclear Cells

ROS: Reactive Oxygen species

SOD1: Superoxide Dismutase 1

nSOD1: nuclear Superoxide Dismutase 1

HSPs: Heat Shock Proteins

HSF1: Heat Shock Factor 1

NGS: Next Generation Sequencing

DE: differentially expressed

PCA: Principal Component Analysis

GO: Gene Ontology

KEGG: Kyoto Encyclopedia of Genes and Genomes

3. INTRODUCTION

3.1. Amyotrophic Lateral Sclerosis (ALS)

Amyotrophic Lateral Sclerosis (ALS) is a rare, adult-onset, progressive and fatal neurodegenerative disorder characterized by loss of upper and lower motor neurons controlling voluntary muscles in the spinal cord, motor cortex and brainstem [1]. Neuronal degeneration results in muscle denervation, hence weakness, atrophy and eventually paralysis. Respiratory failure generally causes the death within 3-5 years after onset [2]. The first description of ALS dates back to 1824 with the surgeon Sir Charles Bell. However, it is only in 1869 that the French neurologist Jean Martin Charcot establishes ALS as a unique disorder and distinguishes it from other diseases with similar presentations, providing a platform in clinicopathologic correlations that helped define ALS for all neurologists [3]. Because of the muscle fibers atrophy, he named the disease "Amyotrophic", "Lateral" as the areas of the anterior and lateral cortico-spinal tracts, where affected motor neurons are located, and "Sclerosis" as "hardening", a consequence of gliosis that replaces the degenerated motor neurons [4].

The site of onset of ALS are usually limbs, where the first symptoms are often unilateral and focal. However, patients develop heterogenous symptoms depending on the involved motor neurons: spasticity, hyperreflexia, modest weakness, Babinski and Hoffman signs, and emotional lability are caused by degeneration of the upper motor neurons in the cerebral cortex and in the brainstem; fasciculation, cramps, muscle atrophy and marked weakness are caused by loss of lower neurons, from the spinal cord to the muscles. Moreover, 15% of ALS patients develop extra motor system associated symptoms, such as neuronal loss in the frontotemporal cortex leading to cognitive and behavioral impairment, features frontotemporal dementia (FTD) too [5]. Also, bulbar-onset of ALS exists and it is mostly associated with language and cognitive damage [6]. The heterogeneity of ALS symptoms is present also among members of the same family carrying the same mutation [5].

The pathological hallmark of ALS is denervation and atrophy of muscle due to loss of spinal motor neurons. Swelling of the perikaryal and proximal axons is also observed, as the accumulation of phosphorylated neurofilaments, Bunina bodies and Lewy body-like inclusions, and the deposition of inclusions of ubiquitinated material in these axons [7]. In addition, the activation and proliferation of astrocytes and microglia are also common in ALS. At present, there is no primary therapy for ALS. Riluzole, a presumed glutamate antagonist that may reduce excitotoxicity, and edaravone, a free radical scavenger, are the only drug approved by the US Food and Drug Administration for the treatment of ALS, but their exact mechanism of action is still unclear. Riluzole appears to prolong ALS survival by a few months on average, although when given at an early

stage or to younger patients, it might prove more effective [8]. Edaravone showed efficacy in a small subset of people with ALS, showing a significantly smaller decline of ALSFRS-R (ALS Functional Rating Scale) score compared with placebo [9], but its use was suspended in Europe. Many factors contribute to the delay in developing effective treatments. Although ALS has a large genetic component, many of the gene variants that cause or predispose an individual to develop ALS remain unknown. Additionally, many cellular processes are implicated in ALS disease progression, therefore determining which are causative is a difficult challenge [10]. The diagnosis depends on electrodiagnostic testing (EMG and NCV). The El Escorial criteria help standardize diagnosis for clinical research studies [5].

The incidence of ALS in European populations and populations of European descent has been estimated at 2·6–3·0 cases per 100 000 people. The global incidence of ALS has tended to slightly increase over the years, especially in Western societies, probably in part due to the progressive aging of the population, nevertheless ALS remains rare [11]. In contrast, other population-based studies have measured the lowest incidence in East Asia to be 0.89 per 100,000 per year and in South Asia to be 0.79 per 100,000 per year. A large part of Africa, Latin America and Asia does not have any population-based studies. The origin of geographic difference in ALS incidence is a matter of debate. Probably, this is partly due to genes and partly due to environmental risk factors [12]. Lifetime risk is about 1:350 for men and 1:400 for women, thus it is more common in men than in women by a factor between 1.2 and 1.5 [13]. The rate of disease progression is more rapid in patients with an older age at onset, a bulbar site of onset, cognitive impairment, and certain genotypes. The average age of onset is 58-60 years and the average survival from onset to death is 3-5 years [14].

3.1.1. Genetics of ALS

ALS can occur sporadically, without any family history (sALS; 90-95% of patients), while a small percentage of ALS cases are considered familial (fALS; 5-10%), where the disease has mostly been found to be inherited in an autosomal dominant manner [15].

The first gene linked with fALS cases is *SOD1* (superoxide dismutase 1), this association was identified in 1993 [16]. Then, thanks to advances in sequencing technology like Next Generation Sequencing (NGS), other genes have been identified to have a link with ALS. For instance, the hexanucleotide repeat expansion in *C9ORF72*, previously described in FTD, has been also observed in ALS cases. So far, more than thirty genes and loci were linked to fALS, but also to some sALS (Table 1). The four most commonly mutated genes in ALS are *C9ORF72*, *SOD1*, *TDP43* and *FUS*. Their frequency depends on ancestral origins: in fact, most European fALS patients present mutations of the *C9ORF72* (33.7%), *SOD1* (14.8%), *TDP43* (4.2%) and *FUS* (2.8%) genes, and other known or unknown genes in 44.5% of fALS cases. Most of these genes have dominant

inheritance, not always with full penetrance, whereas some of them have recessive (*SOD1, FUS*) or even X-linked inheritance [17].

Gene	Protein	Inheritance
SOD1	Superoxide dismutase 1	AD, AR
TDP43	TAR DNA-binding protein 43	AD
FUS/TLS	Fusion malignant liposarcoma	AD, AR
C9ORF72	Chromosome 9 open reading frame 72	AD
VAPB	Vesicle-associated membrane protein B	AD
ANG	Angiogenin	AD
FIG4	FIG4 phosphoinositide 5-phosphatase	AD
OPTN	Optineurin	AD, AR
ATXN2	Ataxin-2	AD
VCP	Valosin-containing protein	AD
UBQLN2	Ubiquilin 2	X-linked

Table 1. Genes involved in ALS. AD = Autosomal Dominant; AR = Autosomal Recessive.

The role of many contributory pathogenic mechanisms has been highlighted thanks to the discover of gene mutations, such as oxidative stress and RNA processing, transport, and translation. Moreover, ubiquitin–proteasome system, protein trafficking, and impaired cytoskeletal function have also been involved in ALS pathogenesis because of rare genetics variants implicated in these pathways. All these dysregulated pathways contribute to the loss of motor neurons [18], rather than just one isolated mechanism.

In sALS cases, mutations are rarely reported: *C9orf72* mutations account for 3–7%, *SOD1* mutations for 1%, and *TARDBP* and *FUS* for even less, thereby suggesting that pathogenic genetic factors are absent in 9/10 cases of sALS. In this population, genetic factors act through predisposing patients toward developing ALS, thus corresponding to genetic susceptibility factors [19]. However, clinical manifestations of sALS and fALS are highly similar, despite the heterogeneity of ALS symptoms represented by age of onset and disease duration. In conclusion, family history and genetics are the primer factors discriminating between sALS and fALS [2].

3.2. Pathogenesis

Causative pathogenic mechanisms of ALS are still to be elucidates, especially in sALS. It is now clear that multiple factors, and not isolated event, take part to development and progression of the disease [20]. Some of them are disturbances in RNA metabolism, impaired protein homeostasis, nucleocytoplasmic transport defects, impaired DNA

repair, excitotoxicity, mitochondrial dysfunction, oxidative stress, axonal transport disruption, neuroinflammation, oligodendrocyte dysfunction, and vesicular transport defects (Figure 1). These events associated to known mutated genes and are interconnected. In fact, nucleocytoplasmic transport impairment of RNA-binding proteins, such as TDP-43 and FUS, cause their mislocalization in the cytoplasm, that in turn causes alterations in transport and metabolism of RNA molecules, affecting also stress granules dynamics [21]. The aberrant aggregation of TDP-43 and SOD1, that accumulate in the cytoplasm, is a demonstration of proteostasis impairment, also represented by disruptive protein clearance pathway and autophagy. DNA repair mechanism are also affected in ALS and, interestingly, many ALS-linked proteins are involved in this mechanism (FUS, TDP-43, TAF15, SETX and EWSR1) [22]. Mitochondrial dysfunction also takes part to molecular pathogenesis of ALS, that causes an increase of reactive oxygen and nitrogen species (ROS/RNS) formation [23]. Importantly, mitochondrial damage was proposed as an initiating factor of ALS because of the interaction of several ALS-linked proteins with mitochondria (SOD1, TDP-43, and FUS). Axonal transport defects as a result of neurofilament accumulation and cytoskeletal disorganization have been implicated in ALS. The secretion of inflammatory proteins by activated microglia leads to the potentially neurotoxic activation of astrocytes, which may contribute to the death of neurons and oligodendrocytes. Finally, oligodendrocyte dysfunction may lead to reduced support for neurons [2].

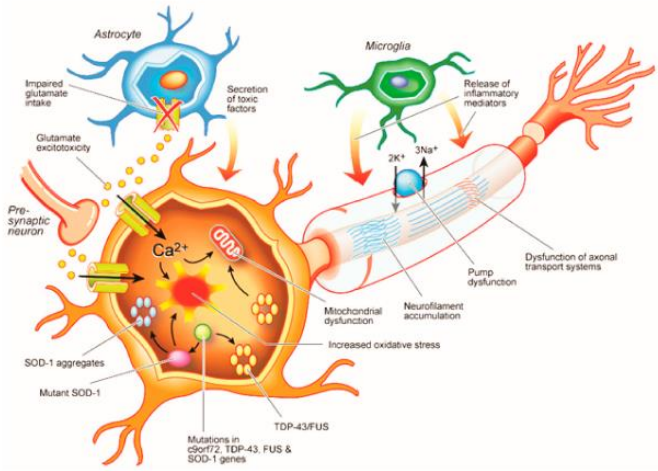

Figure 1. Amyotrophic Lateral Sclerosis (ALS) molecular and genetic alteration are outlined. Dysfunction of the astrocytic excitatory amino acid transporter 2 (EAAT2) causing excitotoxicity, resulting in Ca^{2+}-dependent enzymatic pathways activation, drives neurodegeneration. RNA metabolism leading to aberrant protein translation and aggregates, is linked to mutations in C9ORF72, TDP-43 and FUS. Oxidative stress is increased because of SOD1 mutation, inducing mitochondrial dysfunction that in turn causes defective axonal transportation. Neuroinflammation mechanisms are also present because of microglia activation, resulting in neurotoxicity (Modified from Van De Bos et al., Int. J. Mol. Sci., 2019).

3.2.1. Impaired proteostasis

The presence of cytoplasmic inclusions or aggregates in degenerating motor neurons and surrounding oligodendrocytes is one of the pathological hallmarks of ALS. They are not only present in the spinal cord, but also in other brain regions such as the frontal and temporal cortices, hippocampus and cerebellum. Lewy body-like hyaline inclusion (or skein-like inclusions), ubiquitinated aggregates, are the predominant aggregates found in ALS. They appear as randomly oriented filaments covered by fine granules. Other aggregates subclasses typical of ALS are Bunina bodies, small eosinophilic ubiquitin-negative inclusions, that consist of amorphous electron-dense material surrounded by tubular and vesicular structures, and round hyaline inclusions. In close proximity to ubiquitinated inclusions, neurofilamentous inclusions are also found [24].

Protein misfolding and accumulation are detectable in both fALS and sALS patients, but their presence is due to gene mutations in the first case and to aberrant post-translational modifications in the second case [25]. The most commonly ALS-linked genes (*SOD1*, *C9ORF72*, *TARDBP* and *FUS*) all give rise to proteins that are found to aggregate in the neurons of ALS patients [2]. When in cytoplasmic aggregated state, these proteins may be non-functional and even toxic because of sequestration of multiple binding partners and interactomes, essential for neuronal function. FUS and TDP-43, for example, interact and colocalize with many different proteins, including small nuclear ribonucleoprotein particles (snRNPs). Molecular chaperones, the UPS, and the autophagy-lysosome system function to monitor protein quality and protect cells from dysfunctional, misfolded, or denatured proteins. The presence of ubiquitin, p62 and molecular chaperones in ALS aggregates implicates a role for all these three systems in ALS pathophysiology [24]. For degradation of soluble misfolded proteins, a proteolytic system, called UPS, in which substrates are tagged with ubiquitin, unfolded and cleaved into short peptides though the proteasome, is the first line of defense [26]. The fact that proteins present in ALS aggregates are ubiquitinated, may indicate that they are marked for degradation by the UPS. However, they are eventually found as deposits when their aggregation exceeds UPS capacity [24]. Also, autophagy is involved in the degradation and recycling of proteins. Misfolded proteins can be specifically degraded by chaperone mediated autophagy (CMA), which is a branch of the autophagy-lysosome system. In this system substrates are selectively recognized by Hsc70 and transported to lysosomes, where they will be degraded by hydrolases.

Some misfolded proteins are directed to macroautophagy, in particular those that escape the UPS and the CMA. Macroautophagy is a degradation system in which substrates are segregated into autophagosomes which then fuse with lysosomes for degradation. In addition, ALS mutant proteins that escape UPS and autophagy, form intracellular inclusions containing Ubiquitin and Ubiquitin ligases, as found in fALS mice and in spinal cord of sALS patients. These insoluble inclusions are visible in the brain stem and spinal cord from the onset and their progressive accumulation is observable until latera stages of the disease [26]. Upregulation of molecular chaperones is indicative of importance of modulators of protein aggregation and protein degradation pathway as

ALS toxicity hallmarks. Chaperons partially counteract protein aggregation through the increase of solubility of FUS and TDP-43 [24].

Although large inclusions are clinical hallmarks of ALS symptoms, it is still unclear if aggregate formation directly causes neuronal toxicity, if it is only an innocuous consequence of the neurodegenerative process or if it is a defense mechanism to reduce the concentration of toxic proteins [27].

3.2.2. Mitochondrial disfunction

The mitochondrion is a double-membrane-bound organelle found in the cytoplasm of almost all eukaryotic cells whose primary function is to generate large quantities of energy in the form of adenosine triphosphate (ATP). Other functions of mitochondria are calcium storage for cell signaling activities, heat generation, mediation of cell growth and death and contribution to cellular stress response, such as autophagy and apoptosis [28]. All the above listed functions can be directly linked to mechanisms involved in ALS, such as dysregulation of intracellular Ca^{2+}, homeostasis, oxidative stress, glutamate excitotoxicity, apoptosis and axonal transport disruption. Thus, a crucial role in motor neuron degeneration can be attributed to mitochondria, as mitochondrial damages are well documented in both sporadic and familial ALS. Aggregated, swollen, vacuolated or fragmented mitochondria were observed when considering mitochondrial morphology in cell or animal models of fALS [29]. Also, biochemical analyses have delineated defects in the respiratory chain complexes I and IV in sALS [30] and fALS [31]. The maintenance of the mitochondrial membrane potential relies on the activity of the different complexes of the electron transport chain and therefore mitochondrial depolarization has been additionally observed [23].

In transgenic mouse models of ALS, increased oxidative and/or nitrosative stress were observed. These studies highlighted increased oxidative damage to mitochondrial proteins, lipids and DNA. The explanation for these events lies in the excess of activity od mutant SOD1[32], increased levels of ROS produced by mitochondria following inhibition of complex I or increased NADPH oxidase (NOX) activity through mutant SOD1 interacting with Rac1, a NOX regulator [29].

Also, ATP synthesis is impaired and mitochondrial Ca^{2+} buffering is reduced in cells expressing various SOD1 mutations. The latter is essential for controlling neurotransmitter release [33, 34]. Cytosolic Ca^{2+} overloading and ATP shortage in motor neurons may pose a sustained metabolic stress on mitochondria, accelerating cellular ageing and ultimately lowering the threshold for apoptosis [29].

Apoptosis is also partially controlled by mitochondria and changes in the ratio between anti- and proapoptotic members of the Bcl-2 family have also been documented in ALS. In spinal cord of ALS patients, decreased levels of the anti-apoptotic factors Bcl-2 and

Bcl-xL, and increased levels of the death-promoting factors Bax, Bid and Bcl-xS were found. This imbalance leads to scarce survival of motor neurons, pointing out that mitochondria-dependent apoptosis is a predominant pathway in motor neuron degeneration in ALS [35].

Whether mitochondrial dysfunction and pathology represent primary or secondary pathological events is unknown, as mitochondrial abnormalities can both result from and cause oxidative toxicity. It is likely that mitochondrial function modifies the course of motor neuron degeneration [7].

3.2.3. Excitotoxicity

Glutamate receptor overstimulation is a pathological process called excitotoxicity, that causes neuronal damage and/or degeneration. Glutamate, released from presynaptic terminals to act on post- and presynaptic glutamate receptors, like AMPA and NMDA, is an excitatory neurotransmitter [2]. Neurons are damaged through excessive stimulation of glutamate receptors when glutamate levels are high at extracellular levels. This can be due to excessive presynaptic glutamate release or as a consequence of impaired glutamate reuptake [36]. Electrophysiological studies in upper and lower motor neurons have highlighted the altered glutamatergic signaling in ALS. The evidence consist in elevated presence of fasciculation [37] as a result of aberrant discharge of lower motor neurons on to the muscle fibers they innervate [38]. Altered glutamate levels were also observed in post-mortem ALS tissue and in cerebrospinal fluid [39].

Motor neurons are highly susceptible to excitotoxicity because of their enhanced expression of calcium permeable AMPA receptors, due to lack of GluR2 subunit, necessary to resist calcium entry. In fact, when these cells are subjected to glutamate stimulation, intracellular free calcium levels quickly increase. This is due to a high glutamate-induced calcium influx in combination with low calcium-buffering capacity, resulting from low levels of the calcium-buffering proteins parvalbumin and calbindin D28K [40]. This process is favorable in physiological conditions, since motor neurons can benefit of calcium transients with rapid relaxation times, especially during high-frequency rhythmic activity, but expose the motor neurons to excessive influx of calcium ions. As a consequence, mitochondria take control of calcium metabolism, that however saturates because of excessive stimulation and result in persistent increase in cytosolic calcium levels [41]. In ALS this vulnerability is even increased, leading to activation of Ca^{2+}-sensitive proteases, protein kinases/phosphatases, phospholipases and NOS, causing the opening of mitochondrial membrane transition pore, osmotic swelling and rupture of outer mitochondrial membrane [42].

Mutations in SOD1 lead to interference in GluR2 mRNA expression, that in turn causes reduction in protein expression. Thus, calcium permeable AMPA receptors on the motor neuron membrane are altered and neurons are highly exposed to excitotoxicity [43].

GluR2 expression is also altered in neurons derived from sALS patients, where receptor levels are also lower [44]. Moreover, glutamate release augmentation in spinal cord was also observed in SOD1/G93A(+) mice, due to increased size of the readily releasable pool of vesicles and release facilitation, supported by plastic changes of specific presynaptic mechanisms [45, 46].

Glutamate transported dysfunctions has been deeply investigated in ALS. It was found that glutamate transporter EAAT2 expression is reduced in the cortex and spinal cord of both fALS and sALS patients [47]. EEAT2 may by downregulated at transcriptional, translational and post-translational level [48] because of impaired RNA processing [49] or oxidative damage [50]. This might be one of the hypotesis supporting the elevated glutamate levels in the synaptic cleft. However, EEAT2 dysfunction has not yet been elucidated. It may represent a driving factor or a downstream complication of ALS [38].

Riluzole, the only drug which has proved effective against disease progression in ALS patients, has anti-glutamate properties. This is considered indirect evidence for a pathogenic role of excitotoxicity in ALS. However, other anti-glutamate treatments tested in ALS were less successful [51].

3.2.4. Axonal transport defects

The movement and spatiotemporal distribution of intracellular cargo such as lipids, proteins, mRNA, membrane-bound vesicles, and organelles along the axon is defined axonal transport. This process ensures the long-distance communication between cell body and synaptic terminals, the maintenance of the cell and its functionality [10]. Cargoes transport can be termed anterograde when it goes from the cell body to the synapse, and retrograde when it goes from the synapse to the cell body. The polarity of microtubule partially regulates the directionality, that is exploited by molecular motor proteins: kinesins are responsible for anterograde transporting while dynein moves cargoes in the retrograde direction [52].

Axonal transport defects are proposed to trigger degeneration causing death of neuronal cells in several neurodegenerative disease, such as ALS. The mechanism throughout which axonal degeneration occurs remains to be elucidated, but there are evidence supporting its potential role as degeneration inductor. Electron microscopy and neuropathological studies of post-mortem ALS samples revealed abnormal accumulations of phosphorylated neurofilaments, mitochondria and lysosomes in the proximal axon of large motor neurons [53] and axonal spheroids containing a variety of vesicles, lysosomes, and mitochondria as well as neurofilaments and microtubules [54], highlighting axonal transports defects in ALS. Further experiments, especially metabolic labelling experiments, showed a significant decrease in the slow anterograde transport of cytoskeletal elements in SOD1G37R transgenic mice before the onset of neurodegeneration symptoms [55]. Moreover, slow and fast axonal transport were found

to be impaired in SOD1G93A transgenic mice [56]. This evidence suggests a role of these disrupted mechanism in ALS.

Mechanisms causing perturbations in axonal transport in sALS and fALS have been mostly investigated on mutant SOD1-related ALS, such as reductions in microtubule stability, mitochondrial damage, pathogenic signaling that alters phosphorylation of molecular motors to regulate their function or of cargoes, such as neurofilaments, to disrupt their association with motors [57].

In spinal cord and brain tissue of sALS patients, tissue spheroids show positive staining for MAP6 [58], that protects microtubule from depolymerization, thus associated to with normal microtubule in healthy neurons. However, when MAP6 accumulated in the spheroids, stable microtubules are disrupted as their mediated transport is. Furthermore, disruption of anterograde transport by misfolded human SOD1H46R protein involves p38 MAP Kinase activation and therefore kinesin-1 phosphorylation, inhibiting its translocation along microtubules [59].

3.2.5. Glial activation and neuroinflammation

Microglia, first line of immune defense in brain and spinal cord, and astrocyte activation, overproduction of inflammatory cytokines and infiltration of T lymphocytes are characteristics of neuroinflammation associated with neuronal loss [2]. Since the role of microglia is to sense the surrounding environment and respond to “danger signal” from damage tissue [60], their activation, through CD14, toll-like receptors and scavenger receptors dependent pathway, is caused by the release of misfolded proteins from motor neurons, such as mutant SOD1[61]. Neurons that are dying and do not normally function, release ATP in the extracellular space, thus activating microglia through the ionotropic and metabotropic purinergic receptors [62]. Upon activation, either neurotoxic or neuroprotective function can be exerted by microglia, depending on the state of activation and disease stage. In fact, protective phenotype of microglia is displayed at the early slow progressive stage, where it provides tissue repair and regeneration, and interaction with protective signals. On the other hand, when the disease progresses, “danger signals” are released by injured motor neurons. In this case microglia acquires a neurotoxic phenotype with enhanced secretion of NOX2, ROS, and proinflammatory cytokines.

Also, in astrocytes the expression of ALS-linked genes in observable [63]. These cells’ function is to contribute to trophic support for neurons, but they also exert homeostatic functions in the CNS. The toxicity of astrocytes’ expression mSOD1 for normal motor neurons has been demonstrated in both in vitro and in vivo studies [64]. Excess glutamate from synaptic cleft is cleared by astrocytes through glutamate transporters. The loss of glutamate transport EAAT2 in astrocytes leads to inefficient uptake of glutamate, resulting in motor neurons excitotoxicity [65]. This toxic mechanism was observed in

sALS and fALS patients as well as in mSOD1 mice. Astrocytes can also regulate the expression of GluR2 through secretion of factors that enhance its expression in motor neurons, thus protecting them from AMPA receptor mediated excitotoxicity. When SOD1 is mutated, the protective effect of GluR2 is abolished [65]. Other inflammatory mediators, such as prostaglandin E2, leukotriene B4, nitric oxide, and NOX2, were reported to exert toxic effects on motor neurons [66]. These molecules, secreted by astrocytes, were detected in both post-mortem tissues from ALS cases and SOD1G93A mice. Also, in SOD1G93A mouse model, CD4+ T cells are observed in lumbar spinal cords at early stages of the disease. Genetic removal of CD4+ T cells accelerates disease progression with upregulated expression of NOX2 and proinflammatory cytokines. Therefore, CD4+ T cells exert neuroprotective functions, probably due to their interactions with microglia and astrocytes [67]. At the end stage of ALS, when the immune response shifts from neuroprotective to neurotoxic, cytotoxic CD8+ T cells are mostly present [68].

Ultimately, oligodendrocytes are proposed to contribute to axonal degeneration through changes in the production of the metabolite lactate. These cells are the myelinating cells in the CNS responsible for producing the myelin sheath that insulates the axons of nerves and neurons. The dominant lactate transporter in the brain, MCT1, that is highly enriched within oligodendroglia, results reduced in the motor cortex in mouse models of ALS and in ALS patients [69].

For all these reasons, ALS has to be considered not only a motor neuron disease but also a pathology involving neuronal neighboring cells.

3.2.6. Nucleocytoplasmic transport defects

The redistribution of nuclear proteins to cytoplasm inclusion is one of the most marked pathological features of ALS [70]. This aberrant system causes dysfunction in nucleocytoplasmic transport. Aggregated proteins are found as aggregated in neurons of ALS, especially the most commonly mutated in ALS, such as SOD1, TARDBP, FUS, and C9ORF72 [71]. In fact, the formation of these inclusions can be attributed to mutations that reshape conformational stability or even vary their Nuclear Localization Signal (NLS), thus enhancing their tendency to aggregate in the cytoplasm [72]. In addition to the important role of mutations in these genes, this defect can also be observable in patients that do not carry ALS-associated mutation and are diagnosed with sALS. In this scenario, proteins cannot reach the nucleus, thus resulting in negative effects for the neuronal cell, whatever the biological function of these proteins is [71]. Examples of these consequences include impaired DNA repair mechanism and altered RNA transport and metabolism, which will be further discussed.

3.2.7. Impaired DNA repair

An important mechanism contributing to ALS pathogenesis is the impairment of DNA repair. Due to their high metabolic turnover, neurons are particularly vulnerable to DNA damage. Moreover, their transcription-associated continuously open chromatin state paired with the inability to perform replication-coupled DNA repair such as homologous recombination (HR) contribute to this susceptibility. In fact, postmitotic neurons mostly exploit non-homologous end joining (NHEJ) for Double Strand Breaks repair [73]. Some of the ALS associated proteins, such as TDP43 and FUS, are also involved in repair of transcription-associated DNA damage [2]. For instance, TDP43 interact with proteins involved in NHEJ repair when recruited to DNA damage sites. Mutations in *TDP43*, leading to its mislocalization and aggregation in cytoplasm, also cause loss of recruitment of NHEJ downstream proteins. Thus, the accumulation of unrepaired DSBs [74]. Moreover, FUS operates on homologous recombination and NHEJ related repair mechanisms, hence having a role in DSB restitution. When FUS is inactive in neural cells, a drastic decline in repair efficiency is observed accompanied by a deregulation of chromosomal stability on telomere level [73].

3.2.8. Oxidative stress

One the most critical initiating factors of ALS pathogenesis is oxidative stress [2]. Biomarkers of oxidative stress are present in regions of the CNS that are considered meaningful in ALS, thus suggesting that this process is intensively implicated in moto neuron degeneration [75]. ROS and RNS are oxygen- and nitrogen- carrying metabolites which may or may not contain a free radical but share the ability to oxidize other cellular components because of the presence of unpaired electron in their outer orbit that enhance their reactivity [76, 77]. Hydrogen peroxide, peroxynitrite, nitric oxide, superoxide anions, hydroxyl and monoxide radicals are the most common reactive molecules [78]. Generation of many by-products as peroxides, alcohols, aldehydes and ketones, that can be toxic in cells is often considered a dangerous event involving ROS and RNS [79]. However, these processes are inevitable and important in cells from a biological point of view [76]. In fact, mitochondrial H_2O_2 is generated by monoamine oxidase when metabolizing neurotransmitter, and $O_2^{\cdot-}$ and H_2O_2 derived from NAPDH oxidase participate to essential neuronal progenitors maintenance [80]. Neurons seem to be uncommonly susceptible to oxidative stress and stress-induced damage, even though in other cells ROS/RNS production only causes oxidative insults when excessively present. This may be due to intrinsic properties of neuronal cells [76]. In fact, due to their high aerobic metabolism, they are enriched in mitochondria that help neurons in responding to high energy demands [81]. However, this has dangerous implications due to the

several redox centers contained in the mitochondrial electron transport chain, that may leak electrons to molecular oxygen and serve as primary source of ROS production [82]. In the brain, Fe^{2+} is quite present, and expose the area to reaction between $O_2^{\cdot-}$ and H_2O_2 that may form hydroxyl radicals, highly reactive with neuronal membrane lipids [76, 80]. The latter contain highly polyunsaturated fatty-acid side-chains, extremely susceptible to lipid peroxidation [83]. These disruptive mechanisms have a great impact on neuronal cell health, mostly because these are post-mitotic cells with a limited capacity for regeneration, thus the accumulation of oxidative stress induced damage may last the lifetime of the cell [76]. Thanks to antioxidant enzymes, such as SOD, catalase, glutathione peroxidase and glutathione reductase, cells have evolved defense and repair mechanism for dealing with oxidative stress and associated damage [84]. These are modest in the brain. In fact, compared to other cell, such as hepatocytes, in most brain regions levels of catalase are low [85], and it appears to be located in small peroxisomes, where it may not efficiently deal with H_2O_2 deriving from other compartments of the cell [83]. Cytosolic glutathione is imported through glutathione transporters to balance intra-organelle levels of ROS. Neurons only express one glutathione transporter, on the contrary astrocytes express two of the, and this affect mitochondrial glutathione levels and resistance to oxidative and nitrosative stress [76]. Dismutation of $O_2^{\cdot-}$ to H_2O_2 is accelerated by SOD enzymes, helping to diminish direct damage by $O_2^{\cdot-}$. Also, inhibition of metal ion-dependent autoxidation reactions is mediated by SOD1 enzymes, that are generally propagated via $O_2^{\cdot-}$ [83]. A good percentage of fALS cases, about 20%, have defect in the gene encoding SOD [84]. The mutant protein form protein aggregates, with itself or even with other proteins, that may cause both loss of enzymatic activity and acquisition of toxic properties. Since the role of SOD in clearance of $O_2^{\cdot-}$, when its functionality is lost, levels of oxidative stress are increased [75].

TDP43 is also involved in oxidative stress. In fact, recent studies conducted on cellular models has demonstrated that upon oxidative insult, TDP43 delocalizes from nucleus to cytoplasm and enhanced its predisposition to aggregate. Thus, alteration of several steps in RNA processing are observed [86]. Delocalization and aggregation hallmarks are also found concerning another RNA binding protein, FUS. Together with TDP43, they colocalize in Stress Granules (SG), both in ALS patients and in cellular models. Eukaryotic cells display SGs when are under various stress, such as oxidative stress, heat shock or glucose deprivation. This mechanism is activated to promptly modulate gene expression, allowing the prioritized translation of stress response genes by storing housekeeping mRNAs until stress conditions persist. Since ALS motor neurons endure oxidative stress, the permanence of SGs might become detrimental and might lead to the entrapping of active endogenous form of FUS and TDP-43 in stable aggregates and consequential loss of function of these two nuclear proteins [87]. These SG may also sequester a subset of mRNAs thus inducing cell dysfunction or serve as nucleation site for larger protein aggregates as the ones found in ALS patients [88].

3.2.9. Superoxide Dismutase 1 (SOD1)

Monomeric SOD1 enzyme, transcribed from *SOD1* gene located on chromosome 21q22.11, works for dismutate the free superoxide radicals with the aim of reducing oxidative stress. More than 180 mutations have been discovered on this gene, including single point mutations, deletions, insertions and truncation mutations throughout its exons, explaining the toxic function of SOD1 [89]. DNA/RNA metabolism, ATP production, Ca^{2+} release, axonal transport and more are pathways affected by the toxicity of mutant SOD1. It deposits as insoluble aggregates in motor neurons because of conformational instability of its mutant form, representing a crucial hallmark of SOD1-associated fALS cases [7].

The involvement of altered wtSOD1 in sALS pathogenesis has also been investigated, due to the evidence that a 32-kDa covalently cross-linked SOD1-containing protein species are present in spinal cord extracts of sALS patients [90]. In fact, many of the binding and toxic properties of ALS-linked mutant SOD1 are gained by wtSOD1 through oxidative damage [91]. Therefore, an evolving hypothesis has proposed a common neurodegenerative pathway shared by at least some fALS and sALS cases, that involves cytotoxic and non-native conformers of SOD1. Moreover, in post-mortem CNS tissue of both sALS and fALS without SOD1 mutations, misfolded forms of human wtSOD1 have also been detected [92].

The over-expression of SOD1 mRNA was also reported on PBMCs obtained from sALS patients [93], in contrast to the unaltered soluble SOD1 protein expression level found in the cytoplasm [94], suggesting that the missing SOD1 may translocate and re-localize in different compartments. Indeed, in a sub-group of sALS patients, SOD1 was present in the nuclear compartment at higher levels, while, in the remaining ALS subjects, perinuclear/cytoplasm insoluble SOD1 aggregates were found. In addition, a positive correlation between longer disease duration and higher amount of soluble SOD1 in the nucleus has resulted, implying a possible protective role of the protein in this compartment [95]. A study has demonstrated the lack of DNA damage in the sub-group of sALS patients characterized by high levels of soluble nuclear SOD1, and an extensive DNA damage in sALS patients with high levels of insoluble/aggregate SOD1. This confirms the hypothesis that normal soluble SOD1 could have a potential protective role in DNA damage mediated by oxidative stress, whereas aggregate SOD1 could be non-functional. In response to increased levels of H_2O_2, different mechanisms are activated in order to coordinate DNA repair, included the ATM/Chk1 and ATR/Chk2 kinase signaling cascades [96]. Chk2 could phosphorylate SOD1, leading to the translocation of the protein in the nuclear compartment (Figure 2), in order to protect the DNA. In the nucleus, SOD1 acts as transcription factor and regulates the expression of a large set of genes that are known to provide resistance to oxidative stress and promote DNA damage repair [97]. These results may open new perspectives on the stratification of sALS patients in subgroups depending on SOD1 cellular localization [95].

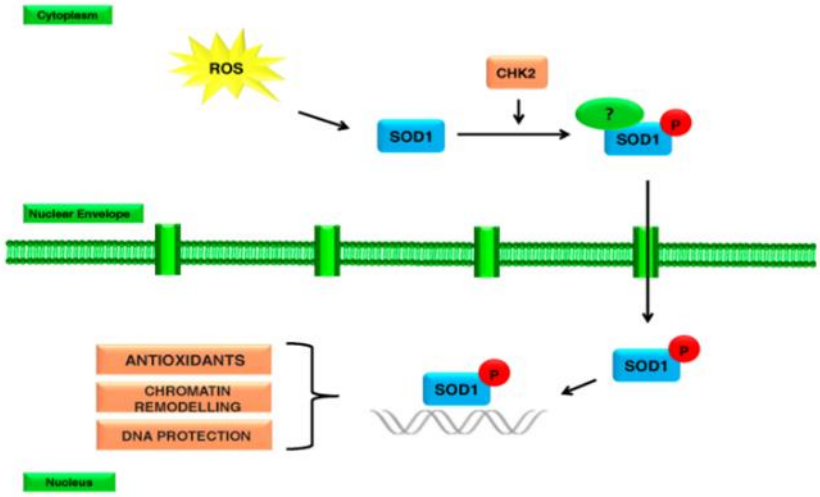

Figure 2. Representation of SOD1 translocation in the nucleus following Chk2-mediated phosphorylation. (Modified from Pansarasa et al., Int J Mol Sci., 2018).

3.2.10. Altered RNA metabolism in ALS

Approximately 97% of patients with fALS and sALS are positive for TDP-43 inclusions in the motor cortex and spinal cord, thereby establishing TDP-43 as a major protein signature for disease [98]. TDP-43 is a ubiquitously expressed heterogeneous nuclear ribonucleoprotein (hnRNP) with a nuclear localization signal and nuclear export signal that allow shuttling of the protein between the nucleus and cytoplasm, although it is predominantly located in the nucleus in healthy neurons [99]. TDP-43 has been shown to play a role in RNA metabolism, including RNA transcription, alternative splicing, pre-microRNA processing, RNA transport, and messenger RNA stability. It has the ability to bind multiple mRNAs to regulate their splicing and it is able to repress the splicing of cryptic exons [98]. These regions are normally skipped by the spliceosome due to the presence of adjacent UG microsatellite repeats, the consensus binding site of TDP-43. When TDP-43 function is lost, these cryptic exons become activated and often lead to nonsense-mediated decay of the associated mRNA. The loss of nuclear TDP-43 and the resulting splicing deficits have been reported in ALS [100]. Furthermore, TDP-43 binds to the 3′ UTR of numerous mRNAs, suggesting a role in mRNA stability and/or transport. RNA-seq analysis have reported that TDP-43 is required for regulating the expression of 239 mRNAs, many of those encoding synaptic proteins, exhibiting its important role in regulating genes involved in synaptic formation and function and in the regulation of neurotransmitter processes [101]. TDP-43 also co-purifies with various proteins that form ribonucleoprotein (RNP) complexes or RNA granules involved in mRNA transport [102]. The majority of TDP-43 granules are co-labelled by RNA dyes, indicating that they contain RNAs [103]. These granules are transported along axonal

and dendritic processes through microtubule cytoskeleton but, compared to the wild type TDP-43, its mutant forms are not as efficiently transported, with increased pausing and a preference for retrograde versus anterograde transport. This results in its increased localization in regions proximal to the cell body and depletion from the neurite tips, which contributes to an mRNA altered transport and delivery [104]. Mutations in *FUS*, an RNA-binding protein that shares structural and functional properties with TDP-43, cause rare cases of ALS. In these cases, FUS is the major pathological protein in neuronal cytoplasmic inclusions. Approximately half of ALS associated FUS mutations are located in its NLS and disrupt its normal nuclear localization[105]. The degree to which these FUS NLS mutations affect its nucleocytoplasmic transport correlates with the severity of disease in these patients [106]. FUS can bind 3′ UTRs regulating the stability of hundreds of transcripts, promoting their stabilization or destabilization [107]. In addition, FUS mutants have been shown to induce the upregulation of mRNA nonsense-mediated decay (NMD) machinery, resulting in a decrease of transcript stability and consequent reduction in translation [108]. The finding of frequent NLS mutations in ALS-linked proteins evidence that dysfunction in nucleocytoplasmic transport through the nuclear pore complex may contribute to disease initiation or progression, either through loss of nuclear functions or toxic gain of cytoplasmic function, due to increased concentration or residence time of these proteins in cytoplasmic assemblies [99]. Interestingly, also mRNA of SOD1 was found to be deregulated (over-expressed) in PBMCs obtained from sALS patients [93].

TDP-43 and FUS also play a role in the biogenesis of miRNAs, endogenous small non-coding RNAs that recognize target mRNAs through base-pairing interactions and perform gene silencing. TDP-43, in particular, was shown to associate with proteins involved in the cytoplasmic cleavage of pre-miRNA mediated by the DICER enzyme. It is thus to no surprise that dysregulation of miRNAs has been observed in ALS, including miRNAs essential for motor neuron development and maintenance, axonal growth and synaptic transmission. Thus, these miRNA alterations likely contribute to the pathological phenotype observed in ALS [109]. The discovery that ALS causative mutations frequently occur in genes coding for RNA binding proteins involved in the RNA processing, has supported the hypothesis that RNA dysregulation could be a key contributor to familiar ALS pathogenesis. Likewise, in the past years, several papers have demonstrated the involvement of an altered RNA metabolism in sporadic ALS cases. Studies based on RNAs deep sequencing have pointed out the differential expression of several coding and non-coding RNAs, resulting in a negative regulation of the RNA transcription process and transcription factors activity [110], as well as aberrant alternative splicing [111], and therefore RNA processing. Consequently, the study and the understanding of RNA metabolism alterations in ALS could provide new insights on this disease and perhaps lead to the discovery of possible therapeutic targets in this fatal disease. The best way to unravel the changes in gene expression that may be involved in ALS pathogenesis is to perform transcriptomic analysis through RNA sequencing.

3.3. RNA metabolism in other neurodegenerative diseases

RNA processing is a contributor factor in the pathogenesis of neurodegenerative diseases, such as ALS, Alzheimer's Disease (AD) and Parkinson's Disease (PD) [112–116]. Basic processes, crucial for physiological gene expression, are affected in these diseases. For instance, RNA transcription, post-transcriptional modifications, activity and functional degradation of RNA molecules are aberrant. This is caused by both alterations in RNA-binding proteins (RBPs) and in noncoding RNAs, crucial for gene expression regulation. Thus, improper RNA metabolism has a central role in pathogenesis of NDs.

3.3.1. Alzheimer's Disease

Alzheimer's Disease (AD) is a degenerative and progressive dementia that represents the most common form of senile dementia in Western area. It is characterized by progressive memory loss, deficits in cognitive abilities and behaviour impairments [117]. Several areas of both the cerebral cortex and the hippocampus are affected by this disorder. In particular, the first areas involved in AD are the frontal and the temporal lobes. Eventually, the degeneration slowly reaches other areas of the neocortex [118].

The first study describing AD was published in 1906 by Deutsch psychiatrist and neuropathologist Alois Alzheimer. Nowadays, almost 35 million people suffer from AD, and in 2030 this number is expected to grow to 70 million [119]. AD covers 50-70% of total cases of dementia and has an age-specific prevalence that tends to exponentially increase by 3% for individuals among 65 and 74 years old, to 50% in individuals older than 85 [120]. A systematic review highlighted that the prevalence of AD does not only vary according to age, but also depending on geographical distribution: in fact, in developing countries is at 3.4%. Studies on Nigerian [121] and Indian [122] population indicate a diminished disease prevalence compared to European metanalysis. North America (6.4%), Western Europe (5.4%) showed the highest prevalence of AD in population ≥60 years, followed by Latin America (4.9%), China and Western Pacific Region (4%) [123].

Sporadic form of AD represents the great majority (85-90%). Some factors have been associated to with increased risk of developing AD. For example, diabetes, smoking, obesity, dyslipidaemia and cerebrovascular diseases [124]. Familial forms of this disease have been linked to rare mutations in three genes involved in the aggregation of Aβ42: *APP*, *PSEN1*, and *PSEN2* [125–127] (Table 2). These mutations cause an increase of Aβ42 peptide levels and its aggregation during the fourth and fifth decade of life [128]. About *APP,* missense mutations in the gene and microduplication affect APP processing and aggregation [125, 126]. *PSEN* mutations, mostly single-nucleotide substitutions but also indels, lead to an increased Aβ42/Aβ40 probably due to loss of function in *PSEN* [128]. Although these mutations represent rare causes of AD, their discovery greatly

highlighted the main role of Aβ in the pathogenesis of AD. Also, *APOE4* has been identified as one of the main risk factors for AD [128]. In fact, depending on the copies of this gene, the risk curve can shift to 5 years earlier (one allele) and to 10 years earlier (two alleles). The role of *APOE4* has been linked to pathways involved in immunity, inflammation, cholesterol metabolism, or endosomal vesicle recycling [128]. The latter is not the only susceptibility gene for AD, many others have been linked to an increase of AD risk in the population [128].

Gene	Protein	Inheritance
APP	Amyloid beta precursor protein	AD
PSEN1	Presenilin 1	AD
PSEN2	Presenilin 2	AD
APOE	Apolipoprotein E	Risk factor

Table 2. Genes involved in AD. AD = Autosomal Dominant; AR = Autosomal Recessive.

On average, the duration of AD is about 8–10 years, but a preclinical and prodromal stage, which can extend over 2 decades, precedes the symptomatic clinical stages. AD has two main hallmarks (Figure 3):

- the accumulation of insoluble amyloid-β (Aβ42) in extracellular and blood vessels plaques in the extracellular spaces;
- the formation of neurofibrillary tangles in neurons due to the aggregation of the microtubule protein tau.

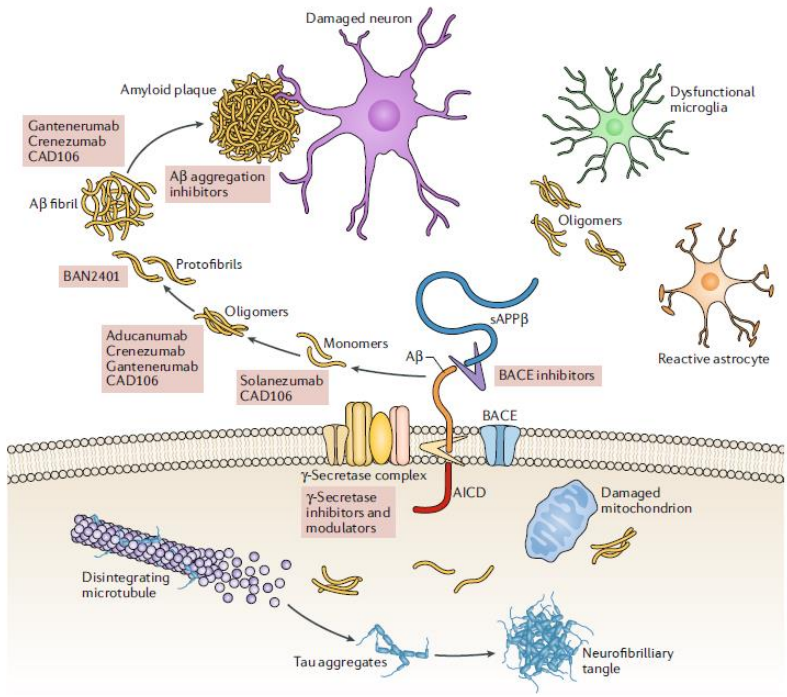

Figure 3. Graphical representation of the two main hallmarks of AD: amyloid plaques formation and neurofibrillary tangles. Also, drugs that are currently in phase III clinical development for the treatment of AD and the respective target are represented (Modified from Panza et al., Nat Rev Neurol., 2019).

The tracking of accumulation and aggregation of both Aβ and tau *in vivo* has improved the study of disease progression [118]. It has been observed that Aβ42 deposition usually precedes neurofibrillary changes, involving specific regions of the brain, in particular the frontal and temporal lobes, hippocampus and limbic system. Sometimes, AD starts from other areas, such as parietal and occipital lobes, with the accumulation of the neurofibrillary tangles in the medial temporal lobes and hippocampus, and progressively spread to other areas of the neocortex [118].

3.3.2. Altered RNA metabolism in AD

In recent studies, gene expression alterations in AD have been described. In particular, mechanisms affecting transcription of mRNA, alternative splicing and noncoding RNAs-mediated gene regulation have been investigated [129].

In the brain, several AD-causing genes were verified to be affected by splicing and disease mechanisms, including APP, PSEN1-2, APOE, or MAPT [130, 131]. Mutations in these genes cause exon skipping with the consequence of reduced expression of the

relative proteins [132], imbalance of tau translation [133] and impaired axonal transport of APP [134].

Concerning analysis of DE genes, many mRNAs and lncRNAs resulted deregulated in AD cells and tissue. Comparing AD neurons to healthy neurons, three genes were found upregulated: casein kinase 2, beta polypeptide (CSNK2B), apolipoprotein J (APOJ), and tissue inhibitor of metalloproteinase 3 (TIMP3) interleukin-1 receptor-associated kinase 1 (IRAK1). Calpain 7 (CAPN7) was instead found downregulated [135]. Other studies exploited RNA-sequencing techniques for investigating gene expressions in AD patients' brain. Resulting affected pathways were related to calcium signaling, neuroactive ligand–receptor interaction, microtubule-associated protein tau (MAPT) signaling, long term potentiation, axon guidance, synaptic transmission, DNA repair and transcription, immune response and metabolism [136, 137]. Together with deregulation of coding genes, also altered expression of lncRNAs resulted from this approach on AD cerebral areas [138]. Indeed, lncRNA n341006, involved in protein ubiquitination, was strongly downregulated [139]. The most interesting lncRNA found deregulated in AD is BACE1-AS. Being antisense to BACE1, this transcript may be involved in APP cleavage enhancing it [140]. Also Lnc-NDM29 is involved in APP synthesis since its overexpression has been linked to increase in amyloid generation [141]. BC200 is further implicated in BACE1 activity. It is upregulated in AD hippocampus and its suppression led to reduced BACE1 expression and amyloid peptide production [142]. Importantly, upregulation of MALAT-1 could have neuroprotective effects in AD together with reduced inflammatory response [143].

3.3.3. Parkinson's Disease

Parkinson's Disease (PD) is the second neurodegenerative disease (ND) after AD, and both diseases share the main risk factor: aging. PD was first described in 1817 by the English doctor Dr. James Parkinson [144]. PD is a movement disorder and the motor symptoms are related to progressive loss of nigrostriatal dopamine and, as the disease gets worse, new symptoms develop, often referred to as non-dopamine-related features, thus not responding to levodopa-therapy [145]. Observations by Braak et al. suggested that the pathology is characterized by the presence of intracytoplasmic, protein-rich inclusions named Lewy Bodies (LBs), and Lewy neurites that occurred sequentially over six phases [146]; the aggregates and the dopaminergic loss in the *Substantia Nigra pars compacta* (SNpc) represent the two hallmarks of the disease.

PD is rare before the age of 50 but its prevalence increases with aging, affecting 1% of subjects above 60 years of age and 3-5% of the over 85 years old people. From a geographical point of view, the disease mostly affects industrialized areas, such as North America, Europe, and Australia, while the incidence is lower in Cina and Asia. It has to be said that there are not data about the worldwide population yet.

The scientific interest around PD has been increasing over the past decades for the higher incidence of this disease and the discovery of new monogenic mutations probably responsible for the disease. Those mutations, however, can explain only a small percentage of cases and the majority of the patients remain classified as sporadic, thus with an unknown etiology [145]. In fact, only 10% of PD patients exhibit a positive familial history. Defined loci and genes for PD are reported in Table 3. Mutations in α-synuclein (*SNCA)*, leucine-rich repeat kinase 2 (*LRRK2*) and vacuolar sorting protein 35 (*VPS35*) genes are examples of genes responsible for autosomal-dominant PD forms, while autosomal recessive (AR) inheritance is suggested in families where several members of one generation are affected, especially siblings, but not their parents or their children. A large number of mutations in recessive PD genes have been reported to be disease-causing and some of these have been published from several groups and have become well-established while others have only been found in one or a few patients, and their significance is difficult to confirm [147].

Gene	Protein	Inheritance
SNCA	α-synuclein	AD
LRRK2	Leucine-rich repeat kinase 2	AD
VPS35	Vacuolar protein sorting 35	AD
EIF4G1	Eukaryotic translation initiation factor 4-γ 1	AD
Parkin	Parkin	AR
PINK1	PTEN-induced putative kinase 1	AR
DJ-1	DJ-1	AR
GBA	Glucosylceramidase beta	Risk factor

Table 3. Genes involved in PD. AD = Autosomal Dominant; AR = Autosomal Recessive.

Epidemiological findings, pathological observations, and genetic discoveries helped to understand the pathogenesis of PD. For example, important molecular pathways of both familial and sporadic forms have been identified by fitting genes that are associated with the disease [148]. In PD pathogenesis seem to be implied cellular pathways involved in the protein homeostatsis, called also proteostasis, such as abnormal protein aggregation, intracellular protein and membrane trafficking, impairments of the ubiquitin-proteasome and lysosomeautophagy systems. Moreover, in PD patients seems to be altered synaptic structures and also mitochondrial dysfunction has been found. For example, the impairment of mitochondria has been used to develop a toxic model of the disease, e.g., 6-hydroxydopamine (6-OHDA) and 1-methyl-4-phenyl-1,2,3,6-tetrahydropyridine (MPTP) [149] (Figure 4).

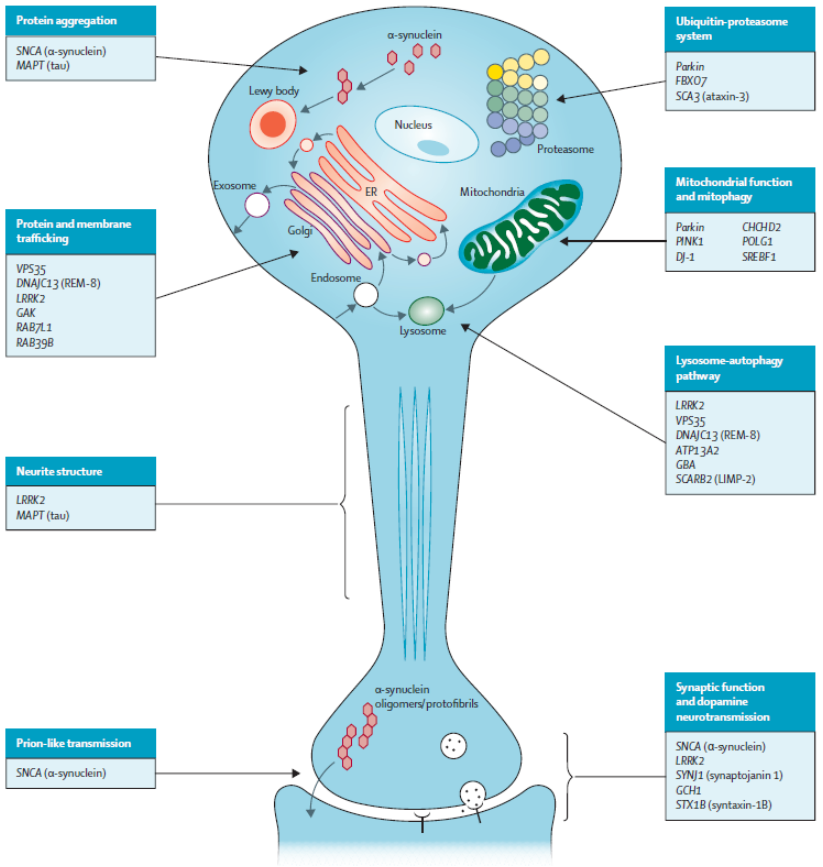

Figure 4. Cellular processes involved in the pathogenesis of Parkinson's disease (Modified from Kalia et al., Lancet, 2015).

3.3.4. Altered RNA metabolism in PD

The importance of RNA metabolism in PD has been recently emphasized. Alterations of translational regulation of disease-causing gene products has been investigated. In particular, several familial PD genes, including LRRK2, PINK1, Parkin, and eIF4G1 [150, 151], have been shown to interact with components of the translation initiation machinery or interact with modulators of the translation initiation process (miRNAs and signaling pathways).

Also, miRNAs play an important role in pathogenesis of PD by regulating the expression of target genes. In fact, hsa-miR-144, deregulated in brain samples of PD patients, modifies the expression of three genes associated with monogenic forms of PD (SNCA, PRKN, LRRK2) [152]. LRRK2 expression in the frontal cortex is also influenced by hsa-miR-205 [153], while SNCA in substantia nigra is targeted by has-miR-7,

downregulated in murine models of PD [154]. Alpha-synuclein is also reduced in substantia nigra and putamen because of the effect of hsa-miR-34b and hsa-miR-95 [155], that can further target DJ-1 and Parkin [156].

MiRNAs are not the only noncoding RNAs to have an impact on gene expression in PD. Also, lncRNAs seem to have an effect on genes involved in the pathogenesis of the disease. In fact, the loss or overexpression of PINK1 results in impaired dopamine release and motor deficits, and a human-specific ncRNA, NaPINK1, has been identified. It is transcribed from the antisense orientation of the PINK1 locus that has the ability to stabilize the expression of PINK1. In fact, NaPINK1 silencing results in the decreased expression of PINK1 in neurons [157]. Moreover, antisense Uchl1 RNA, a recently identified antisense transcript of the mouse ubiquitin carboxy-terminal hydrolase L1 gene (Uchl1), promotes the association of the overlapping sense protein-coding mRNA with active polysomes in the cytoplasm for translation. This activity is disrupted in rare cases of familial Parkinson's disease, and the loss of UCHL1 activity has also been reported in many neurodegenerative diseases [158].

4. AIMS

Neurodegenerative disorders are multifactorial diseases generated by the interplay between many different processes and molecules. In fact, despite progresses made in the study of diseases such as ALS, AD and PD, etiology of these pathologies remains uncertain. One of the emerging involved processes is RNA metabolism, both involving coding and noncoding transcripts. Dysregulation in gene expression and in transcription factor activity have emerged. In this context, we performed a whole transcriptome analysis in PBMCs of sALS, AD and PD patients compared to healthy controls that revealed two main concepts: a different grade of RNA metabolism impairment exists in these three disorders, where ALS appears to be the most affected one; a molecular classification of sALS patients, depending on subcellular localization of SOD1, reflects in different gene expression patterns.

Therefore, starting from these data, the aims of this work were:

1. To identify possible crossroads or deviations in the dysregulated genes and pathways of sALS, AD and PD. Our results pointed out a different degree of RNA metabolism and dysregulation involvement, highlighting a different role for lncRNAs and mRNAs regulation in the most relevant neurodegenerative disorders, offering an interesting starting point for future investigations on the pathogenic mechanisms involved.

2. To perform a transcriptome profiling with differential gene expression analysis in PBMCs of sALS patients divided in subgroup according to SOD1 subcellular localization. Based on our previous reports [95, 96], sALS patients can be classified into two groups based on the expression levels of nuclear SOD1: high nSOD1 and low nSOD1. Our aim was to further explore the molecular alterations that distinguish the two sALS subgroups and dissect the potential divergence at gene expression level. Our findings highlighted the importance of nuclear localization of soluble SOD1 as a protective mechanism in ALS patients. We reported differences in RNA regulation in the two groups of patients, leading to pathways conferring “protection” when nSOD1 was high, and “perturbation” of crucial biological systems when nSOD1was low. Also, investigating the possible effect of higher soluble nSOD1 and HSP70, we demonstrated that in this condition, DNA damage is reduced even under oxidative stress condition, thus confirming that nuclear mutant SOD1 aggregation may cause a loss of its protective activity in this cell compartment.

5. MATERIALS AND METHODS

5.1. Study subjects

After obtaining their written informed consent, 36 sALS, 6 AD and 6 PD patients, and 26 age- and sex-matched healthy controls (CTRL) were recruited. All the subjects were deep-sequenced and included in Real Time PCR experiments. ALS, AD and PD patients underwent clinical and neurologic examination at IRCCS Mondino Foundation (Pavia, Italy). ALS patients were diagnosed following the El Escorial criteria [159]. Only unmutated ALS patients were included in the study since our previous works highlighted interesting molecular features in this cohort [95, 110]. AD diagnosis was made according to the National Institute of Neurological and Communicative Disorders and Stroke and the AD and Related Disorders Association (NINCDS-ADRDA) criteria [117]. For PD, patients Movement Disorder Society (MDS) clinical diagnostic criteria were used [160]. All patients were analyzed to exclude any mutations in causative genes by whole exome sequencing. The control subjects were recruited at the Transfusional Service and Centre of Transplantation Immunology, Foundation San Matteo, IRCCS (Pavia, Italy). The study protocol to obtain PBMCs from patients and controls was approved by the Ethical Committee of the IRCCS Mondino Foundation (Pavia, Italy), (Codes 20200045392; n°20170001758; n°2020042334). All experiments were performed in accordance with relevant guidelines and regulations.

5.2. Peripheral Blood Mononuclear Cells isolation from blood samples

To isolate PBMCs, peripheral venous blood was layered over an equal volume of Ficoll Histopaque®-1077 (Sigma Aldrich) in a Falcon tube, following manufacturer's instructions, and centrifuged for 30 minutes at 950× g at room temperature (RT). Layers form, each containing different cell types. The second layer, characteristically white and cloudy, contains PBMCs, composed of ~80% lymphocytes and ~20% of monocytes. These cells were gently removed using a Pasteur pipette, added to 1X phosphate buffer saline solution (PBS) to wash off any remaining platelets, and pelleted at 1200× g for 10 minutes at room temperature (RT). The cell viability was estimated using trypan blue exclusion test.

5.3. RNA extraction

Total RNA from PBMCs was isolated by Trizol® reagent (Life Science Technologies) following the manufacturer's specifications. RNAs were quantified using a Nanodrop ND-100 Spectrophotometer (Nanodrop Technologies) and quality was checked with a 2100 Bioanalyzer (Agilent RNA 6000 Nano Kit). RNAs with a 260:280 ratio of ≥1.5 and an RNA integrity number of ≥8 were deep sequenced.

5.4. RNA sequencing

The transcriptome is the collection of all RNA molecules, including mRNAs, non-coding RNAs and small RNAs, in one cell or a population of cells. Understanding the transcriptome is essential for interpreting the functional elements of the genome, revealing the molecular constituents of cells and tissues, and for comprehending development and disease. The type and quantity of genes transcribed is dependent on the cell-type and its environment and is tightly regulated, thus the disruption of this regulatory process is often the cause of several diseases [161]. The key aims of transcriptomics are: 1) to catalogue all species of transcript, including mRNAs, non-coding RNAs and small RNAs; 2) to determine the transcriptional structure of genes, in terms of their start sites, 5′ and 3′ ends, splicing patterns and other post-transcriptional modifications; 3) to quantify the changing expression levels of each transcript during development and under different conditions [162].

The development of high-throughput approaches has enabled the interrogation of RNA sequences on a large scale [163]. RNA sequencing (RNA-seq) was developed more than a decade ago and since then has become a ubiquitous tool in molecular biology for the analysis of transcriptome. Basically, a population of RNA molecules is converted to a library of cDNA fragments; adapters are attached to one or both ends to allow sequencing reaction and barcodes are added to each fragment. Each molecule, with or without amplification, is then sequenced in a high-throughput manner to obtain sequences from one end (single-end sequencing) or both ends (pair-end sequencing). Paired-end sequencing allows the generation of a dataset with higher quality, suitable for the detection of gene fusions and for the characterization of novel splice isoforms. The reads are typically 30–400 bp, depending on the DNA sequencing technology used. Furthermore, Whole-Transcriptome analysis can also consider strand orientation, allowing the precise quantification of allele-specific expression.

Broader applications of RNA-seq have shaped our understanding of many aspects of biology, such as by revealing the extent of mRNA splicing and the regulation of gene expression by non-coding RNAs and enhancer RNAs. The adaptation and evolution of RNA-seq has been driven by technological developments and has enabled a richer and less biased view of RNA biology and the transcriptome [164]. Although RNA-seq is still a technology under development, it offers several key advantages over pre-existing technologies. First, unlike hybridization-based approaches, RNA-seq is not limited to detecting transcripts that correspond to existing genomic sequence, becoming crucial for

the discovery of unknown genes and novel transcript isoforms. In addition, it can reveal the precise location of transcription boundaries, to a single-base resolution. Furthermore, short reads from RNA-seq give information about how two exons are connected, whereas longer reads should reveal connectivity between multiple exons. These factors make RNA-seq useful for studying complex transcriptomes. In addition, RNA-seq can also reveal sequence variations as SNPs in the transcribed regions. This method has very low background signal because DNA sequences can be unambiguously mapped to unique regions of the genome [162].

5.4.1. RNA-seq workflow

The first challenge of RNA-seq is the designing of the experiment, where cost and accuracy must be balanced. Optimal number of biological and technical replicates must be chosen, together with the sequencing depth required to achieve reliable analysis. It is also remarkable the choice of "single-reads" or "paired-end" because this affects how the fragments are read, from only end to the other or from both ends. Where it is possible, a "paired-end" sequencing is recommended for increasing sequence coverage [165].

A typical RNA-seq experiment is structured in multiple steps: 1) Experimental Biology, 2) Computational Biology and 3) Systems Biology (Figure 5).

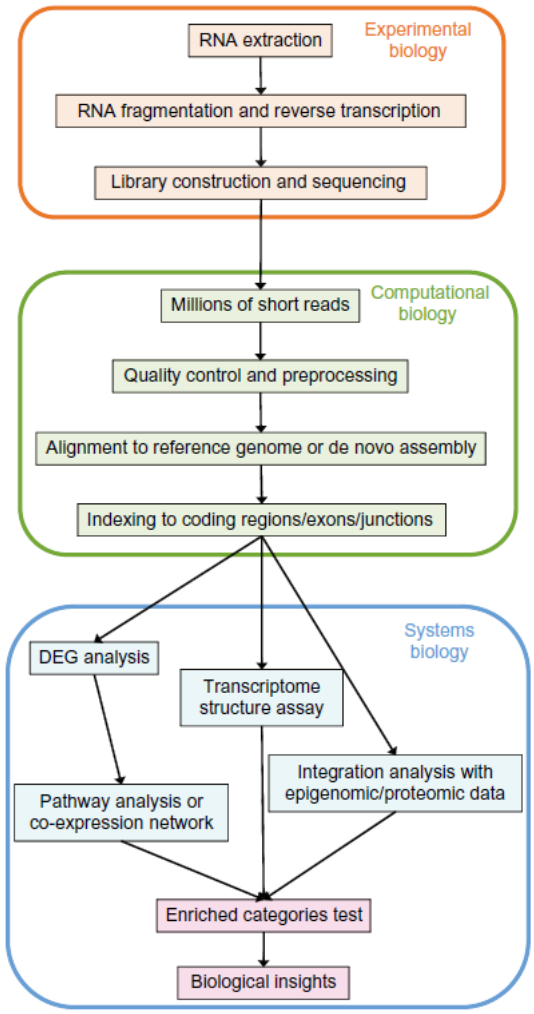

Figure 5. Overview of a typical RNA-seq workflow. The three main sections are presented in the different boxes: Experimental Biology (orange), Computational Biology (green) and System Biology (blue). The workflow starts from the sample preparation and continues to the sequencing and analysis steps as indicated by the arrows. [166]

Experimental Biology

The experimental step includes the choice of RNA extraction method and library preparation, that will result in millions of short reads from the Next Generation Sequencing (NGS) sequencer. RNA preparation methods may differ depending on sequencing platforms, RNA subtypes and sequencing purposes.

Isolation and purification of cellular RNAs is typically obtained by disrupting cells in the presence of detergents and chaotropic agents. After homogenization, RNA can be recovered and purified from the total cell lysate using either liquid-liquid partitioning or solid-phase extraction. Using a spectrophotometer, purity and yield of extracted RNA is measured. Furthermore, to assess the quality of samples to sequence, instruments such as Agilent Tape Station system, electrophoresis device that offer fast and reliable separation, sizing and quantification for quality control of DNA and RNA samples, can be used to detect signs of degradation that may affect the sequence reliability [167]. A crucial step prior to library preparation, is the removal of ribosomal RNA (rRNA) It consists of >80% of total RNA, thus if both mRNAs and noncoding RNAs are of interest for sequencing, it has to be depleted since it may cover the majority of obtained reads. Removal of rRNA can be achieved by several methods, such as hybridization, using oligos that are complementary to highly conserved l rRNA sequences [168].

Library preparation usually starts with RNA fragmentation (Figure 6). This happens because the majority of sequencing platforms only provide relatively short sequence reads (40-400bp). To test the effectiveness of the step, RNA can be evaluated on Tape Station. If the fragmentation is successful, RNA is converted into double-stranded complementary DNA (cDNA) for improving sequence coverage over the transcriptome. When libraries are prepared, their “multiplex” is pooled into a single sequencing reaction. Millions of sequence reads are produced in a single reaction by most high-throughput sequencers. Thus, to minimize time and expense multiple experiments or samples are sequenced together. To identify which experiment a given sequence comes from, each sample is prepared using adapters containing different tags, known as an index or barcode. Tags are made of short sequences (5-7 bp) that can be associated to the respective sample during downstream analysis. Last step before sequencing, is to assess the quality of cDNA libraries and quantify them. Also, the fragment size distribution of libraries is checked to be in the expected size range and free of artefacts deriving from ligation or PCR [169].

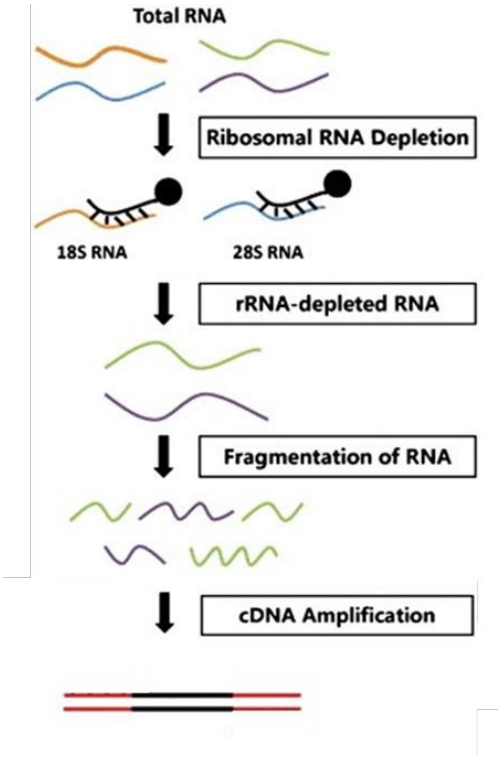

Figure 6. Workflow of RNA library preparation for sequencing: after total RNA isolation from the samples, rRNA depletion is performed. RNA is fragmented, adapter-ligated and reverse-transcribed into a cDNA library. Libraries are then amplified and sequenced. Generated reads are retained for downstream analysis (Modified from Cui et al., Genomics, 2010).

Suitable libraries can be sequenced at this point. Depending on the chosen sequencing platforms, different chemistries and technologies are exploited. For instance, Illumina NGS devices are based on an in vitro clonal amplification, called “bridge PCR”. Amplified fragments are then converted into single strands and sequenced through the different cleavable fluorescent dyes and reversible 3' blocker groups, added by the polymerase to complement the template fragments, that labels four kinds of nucleotides (ddATP, ddGTP, ddCTP, ddTTP). The fluorescent signal for each base is captured by a camera. On the contrary, Ion torrent technology approach is defined as "sequencing by synthesis". In this case, a new DNA strand, complementary to the target strand, is synthesized one base at a time. Hydrogen ions produced during the polymerization are detected on a chip. This method is faster and cheaper because it does not require a camera for fluorescence detection. However, it has limits in decoding repetitive sequences [170]. Lastly, PacBio sequencing is a method for real-time sequencing and does not require a pause between read steps. Four fluorescent-labelled nucleotides, which generate distinct emission spectrums, are added to the device and, as a base is held by the polymerase during DNA synthesis, a light pulse is produced that identifies the base [171].

Many sequencing platforms exist, but at the moment Illumina represents the leading platform for RNA-seq. Its technology enables deep sequencing, crucial for transcriptome studies, but also low error reads long enough for mapping to reference genomes and transcriptome assembly.

After sequencing, RNA-seq data are formatted in a FASTQ file, which includes sequences and base quality [172].

Computational Biology

Since RNA-seq is a complicated, multiple-step process involving sample preparation, fragmentation, purification, amplification, and sequencing, numerous erroneous sequence variants can be introduced. Hence, quality assessment is the first step of the bioinformatics pipeline of RNA-seq to perform on raw data to enable the assessment of the overall and per-base quality for each read in each sample [173]. Reads likely to contain multiple sequencing errors provide less biological information and are expected to hinder assembly and alignment. Therefore, a common filtering step is to discard reads or to remove the ends of the reads that containing low quality bases, base adapters, contamination or overrepresented sequences performing a "quality trimming" [166]. Then, suitable short reads are aligned to a reference genome or transcriptome assembly. In this way, reads are annotated and connected to gene families, individual transcripts, small RNAs or individual exons. Also, this allows to approximate the abundances of "elements" in the original samples [174]. For this aim, read counts obtained from mapping must be normalized for technical biases removal resulting from comparison in different sequencing depths experiments and differences in transcripts lengths [165].

Systems Biology

The purpose of many RNA-seq studies is to identify features of the transcriptome that are differentially expressed between or among groups of individuals or tissues that are different with respect to some condition [166]. Differential Gene Analysis (DGE) is performed for estimation of genes' differential expression between different conditions. It is obtained through read counts from which the fold change and p-value are calculated, considering sequencing depth and variability. Thus, both difference in the expression and significance are estimated and corrected for multiple testing [175]. DGE analysis is performed through different software, whose choice depends on sensitivity to specific parameters. Among many options, EBSeq and DESeq are two R package widely used for this kind of analysis.

Resulting dysregulated genes can be significant, which may lead to time-consuming literature searching for data interpreting. For this reason, pathway enrichment analysis

are usually performed to help in summarize large gene lists and in interpret the biological translation of RNA-seq results. These pathways result from the use of several statistical tests, which consider the number of genes detected in the experiment, their relative ranking and the number of genes annotated to a pathway of interest [176]. Gene Ontology is commonly used for this purpose, as well as KEGG, Ingenuity, Reactome or WikiPathway.

5.5. Library preparation for RNA-seq and bioinformatic data analysis

Sequencing libraries of sALS and AD patients and matched controls were prepared with the Illumina TruSeq Stranded RNA Library Prep kit, version 2, Protocol D, using 500 ng total RNA (Illumina). For PD patients and controls libraries it has been used the SENSE Total RNA-Seq Library Prep Kit (Lexogen, Vienna, Austria), starting from 200 ng total RNA. Quality of sequencing libraries was assessed by 2100 Bioanalyzer with a DNA1000 assay and DNA High Sensitivity assay (Agilent, Waldbronn, Germany). Before library generation, total RNA samples were processed by selective removal of rRNA (ribo-depletion). This is because the rRNA, making up more than 80% of total cellular RNA [177], was not the research focus, and its presence could greatly reduce the useful transcript coverage in the following sequencing step. A double-stranded cDNA library was then prepared via RNA fragmentation prior to the reverse transcription. After the generation of fragmented cDNA, sequencing adapters were ligated to both ends of the fragments. The quality of each library was assessed by 2100 Bioanalyzer with a "DNA High sensitivity" assay. Libraries were fluorometrically quantified using High Sensitivity ds DNA assay with Qubit device. The sequencing step was performed with NGS technologies using Illumina Genome Analyzer and the NextSeq 500/550 High Output v2.5 kit (150 cycles) produced by Illumina. RNA processing was carried out using Illumina NextSeq 500 Sequencing. FastQ files were generated via Illumina bcl2fastq2 (Version 2.17.1.14- http://support.illumina.com/downloads/bcl-2fastq-conversion-software-v217.html) starting from raw sequencing reads produced by Illumina NextSeq sequencer. Genes and transcripts intensities were computed using STAR/RSEM software [178] using GRCh38 (Gencode release 27) as a reference, using the "stranded" option. Differential expression analysis for mRNA was performed using R package EBSeq [179]. This tool was selected because of its superior performance in identifying isoforms differential expression [180]. Differential expression analysis for lncRNAs was performed with the R package DESeq [181]. Transcripts were considered differentially expressed and retained for further analysis with $|\log2(\text{disease sample/healthy control})| \geq 1$ and a FDR ≤ 0.1. We imposed minimum |Log2FC| of 1 and an FDR lower than 0.1 as thresholds to differentially expressed genes to maximize the sensitivity of this analysis.

5.6. Pathway analysis

Gene enrichment analysis was performed on coding genes [182]. We performed a Gene Ontology (GO) analysis for biological processes, cellular components and molecular function and KEGG pathway analysis (Kyoto Encyclopedia of Genes and Genomes http://www.genome.ad.jp/kegg) and Wikipathway (https://www.wikipathways.org/index.php/WikiPathways) via enrichR web tool [183, 184].

5.7. RT-PCR

Using human gene sequences available from NCBI (www.ncbi.nlm.nih.gov/nucleotide), PCR oligonucleotide for genes pairs (Table 4) were selected spanning introns to optimize amplification from mRNA templates and avoiding nonspecific amplification products, using NCBI's Primer- BLAST or online Primer 3.0. Total cDNAs were prepared from 500 ng using iScript™ Reverse Transcription Supermix for RT-qPCR (Bio-Rad). RT-PCR reactions included 200nM of each oligonucleotide, 7.5 µl of iQ SYBR Green Supermix (Bio-Rad), and 1 µL of cDNA template (or water control). Cycling conditions using a Bio-Rad CFX Real-Time thermocycler were 5 min denaturing at 95 °C, followed by 40 cycles of 95 °C (10 s) and 58 °C annealing (30 s). Cycle threshold (Ct) values was automatically recorded for each replicate qPCR reaction, and mean Ct values were normalized against those determined for GAPDH. Fold-expression differences relative to healthy controls will be determined using the 2ΔCt method. Significance of gene expression changes relative to controls was analyzed using one-way ANOVA (Kruskal-Wallis) and the Bonferroni post-test for all possible test pairings using Prism GraphPad 8.2.0 software (GraphPad Software). P-values (two tailed) with 95% confidence intervals was computed, and $P<0.05$ was considered statistically significant.

Gene	Forward	Reverse
GAPDH	5'-ATGGAAATCCCATCACCATCTT-3'	5'-CGCCCCACTTGATTTTGG-3'
HSPA1A	5'-CGACCTGAACAAGAGCATCA-3'	5'-AAGATCTGCGTCTGCTTGGT-3'
HSPA1B	5'-CCGAGAAGGACGAGTTTGAG-3'	5'-GCAGCAAAGTCCTTGAGTCC-3'
HSPH1	5'-CTCCCAAAGTGCTGGGATTA-3'	5'-CATCTTCACCCAGGAAGCAT-3'
HSF1	5'-GACATAAAGATCCGCCAGGA-3'	5'-CTGCACCAGTGAGATCAGGA-3'
ZEB1-AS1	5'-CACACGGTGCTTGTCTCACT-3'	5'-ATCTGTCAGCCGATGCTTCT-3'
IER3-AS1	5'-CGCCGAAGTCTCACACAGTA-3'	5'-ACTGCGGCAAAGTAGGAGAA-3'
ZBTB11-AS1	5'-TGCCAAAACACCACCTGTAA-3'	5'-AGCTGCCCATTGTCATTACC-3'
KIAA2013	5'-ATGGCATCCGCTACAAGAAC-3'	5'-GATGTAGAGCAGTGGCGTGA-3'
MYCBP	5'- TTGTACGGGTTCCCATGAAT-3'	5'- AACAGCACAGAAAGGCCAGT-3'
HDAC1	5'-GGAAATCTATCGCCCTCACA-3'	5'-AACAGGCCATCGAATACTGG-3'
VCL	5'-CTTTGCTGCTACAGGGGAAG-3'	5'-GGATATGGGACGGGAAGTTT-3'
TLN1	5'-CACCATGGTTGCACTTTCAC-3'	5'-CCCATTTCGGAGCATGTAGT-3'
MTRNR2L1	5'-CCGAGCAACATATGCTGAGA-3'	5'-CCTGGATTACTCCGGTCTGA-3'
MTRNR2L8	5'-TTGTATGAATGGCTCCACGA-3'	5'-CGAAATTTTTCACGCAGGTT-3'
SCARNA2	5'-GTGCAGGGTGAGTGTGAGTG-3'	5'-GCAGGAGGAGAGCTTTTCAT-3'
TBC1D3	5'-ATCGAGCGTACAAGGGAATG-3'	5'-CCGTATCGATCCCTGAAGAA-3'
RP1-29C18.9	5'-GATTTGCATGTGTGGATTGC-3'	5'-AAAGTTAGCCCCAACGACCT-3'

Table 4. Primers used for RT-PCR.

5.8. Subcellular fractionation

To separate the soluble cytoplasmic fraction (SCF) and the soluble nuclear fraction (SNF) of the cellular proteins, subcellular fractionation of PBMCs was performed according to the method of Schreiber and colleagues [185], with some modifications. After cells have been washed with ice-cold 1X PBS, the cellular pellet was resuspended in ice-cold hypotonic lysis buffer (10 mM HEPES, pH 7.9, 10 mM KCl, 0.1 mM EDTA, 1 mM dithiothreitol, 0.5 mM phenylmethylsulfonyl fluoride, 1% of protease and phosphatase inhibitor cocktail). Cells were allowed to swell on ice for 25 min, after which 25 µL of 10% Nonidet NP-40 (Fluka, St. Gallen, Switzerland) was added. Samples were vortexed and centrifuged at the maximum speed. The supernatant, containing the cytoplasm proteins, was collected and stored at –80 ◦C until the use. The nuclear pellets were resuspended in ice-cold hypertonic nuclear extraction buffer (20 mM HEPES, pH 7.9, 0.4 M NaCl, 1 mM EDTA, 1 mM dithiothreitol, 1 mM phenylmethylsulfonyl fluoride, 1% of protease and phosphatase inhibitor cocktail), and incubated on ice for 20 min with agitation. The nuclear extracts were then centrifuged at

the maximum speed for 5 min at 4 ◦C and the supernatant containing the nuclear proteins was collected and frozen at –80 ◦C.

5.9. BCA Protein assay

Protein concentration of previously extracted samples was determined using bicinchoninic acid (BCA) method (Sigma-Aldrich) and BSA (bovine serum albumin). A solution of copper (Cu^{+2}) and BCA was prepared and 20 µl of this solution are mixed with 2,5 µl of an intermediate dilution of each sample. The BCA assay relies on two reactions. First, the peptide bonds in protein reduce Cu^{2+} ions from the copper (II) sulphate to Cu^{+}. The amount of Cu^{2+} reduced is proportional to the amount of protein present in the solution. Next, two molecules of bicinchoninic acid chelate with each Cu+ ion, forming a purple-colored complex that strongly absorbs light at a wavelength of 562 nm. The sample was incubated at 37°C, temperature requested for the formation of peptide bonds involved in reaction complex development. Protein quantification was determined using Nanodrop ND-100 Spectrophotometer (Nanodrop Technologies).

5.10. Western Blotting analysis

A Western blotting analysis was performed by SDS–polyacrylamide gel electrophoresis (SDS-PAGE). Thirty µg of nuclear and cytoplasm proteins were loaded onto 12.5% SDS–PAGE gel (Bio-Rad). After electrophoresis, samples were transferred to nitrocellulose membrane (Bio-Rad) using a liquid transfer apparatus (Bio-Rad). Nitrocellulose membranes were treated with a blocking solution (5% of non-fat dry milk in TBS-T buffer, 10 mM Tris-HCl, 100 mM NaCl, 0.1% Tween, pH 7.5) to block unspecific protein binding sites and incubated with primary antibody overnight at 4 °C. SOD1 (sc-11407), PCNA (sc-56), HSF1 (sc-17757), all from Santa-Cruz. HSP70 (ab2787), HSPH1 (ab109624), pHSF1 (ab76076), all from Abcam. GAPDH (GTX100118), GeneTex. Immunoreactivity was detected using donkey anti-rabbit or anti-mouse secondary peroxidase-conjugated antibody (GE Healthcare) and bands were visualized using enhanced chemiluminescence detection kit (ECL Select, Ge Healthcare). Both primary and secondary antibodies were removed from the membrane by means of stripping solution (mercaptoethanol, 2% SDS, and 62.5 mM Tris/HCl, pH 6.7), and then processed as described above. Densitometric analysis of the bands was performed using the ImageJ software (version number 1.51, http://rsb.info.nih.gov/ij/) and statistical analysis were performed using one-way ANOVA (Kruskal-Wallis) and the Bonferroni post-test for all possible test pairings using Prism GraphPad 8.0.2 software (GraphPad Software). P-values (two tailed) with 95% confidence intervals was computed, and $P<0.05$ was considered statistically significant.

5.11. Immunofluorescence

1×10^5 cells were placed on a poly-L-Lysine slide (Thermo Fisher Scientific) and incubated at 37 °C to allow cell attachment to the slide. Cells were rinsed with 1X PBS and then fixed using a solution of 4% PFA/1X PBS. Fixed cells were washed with 1X PBS and treated with a blocking solution (5% normal goat serum in 0.1% Tween-PBS) for 1 h to block unspecific protein binding sites, cells were then incubated ON at 4 °C with primary antibodies: mouse monoclonal Anti-Histone H3 (tri methyl K27) antibody (ab6002); Abcam. Cells were washed with 1X PBS and incubated at RT for 1 h with secondary antibodies: CFTM 594 goat anti-mouse (Sigma). Both primary and secondary antibodies were prepared in blocking buffer. Finally, samples were washed with 1X PBS, mounted with Prolong® Gold antifade reagent with DAPI (Invitrogen), dried, nail-polished and images were acquired by confocal microscopy (Olympus Fluoview FV10i).

5.12. Comet Assay

For DNA damage study, comet assay was performed in PBMCs of controls, High nSOD1 and Low nSOD1 sALS patients, treated with 500 μM H_2O_2 or with 500 μM H_2O_2 (Sigma) + 50 μM VER (Sigma) (HSP70 inhibitor) treatment followed by 30' stress recovery phase. Approximately 10^4 cells were collected and centrifuged at 2000 x g for 5 min, the supernatant was discarded, and the pellet was suspended in 0.75% low-melting-point agarose (Sigma-Aldrich). The cell suspension was placed onto microscope slides coated with a layer of 1% agarose in 1X PBS. Slides were immersed in alkaline lysis buffer (2.5 M NaCl, 0.1 M EDTA, 10 mM Tris, pH 10) for 1 h at 4 °C and put in a horizontal electrophoresis tank, filled with cold electrophoresis buffer (0.3 M NaOH, 1 mM EDTA, pH 13), and equilibrate for 40 min before starting electrophoresis (run conditions: 300 mA, 25 V, 30 min at 4 °C). Slides were neutralized with 0.4 M Tris, pH 7.5 for 15 min at 4 °C, covered and stored in a humidity chamber. After the addition of the nuclear dye Hoechst (Sigma), individual cells or 'Comets' were analyzed using a fluorescence microscope (Axio Imager 2, Zeiss). Comet length was measured using CaspLab (1.2.3beta2 version) [186] and values were analyzed using one-way ANOVA (Kruskal-Wallis) and the Bonferroni post-test for all possible test pairings using Prism GraphPad 8.0.2 software (GraphPad Software, San Diego, CA). P-values (two tailed) with 95% confidence intervals was computed, and $P<0.05$ was considered statistically significant.

6. RESULTS

6.1. Amount of Differentially Expressed mRNAs and lncRNAs vary in sALS, AD and PD

Following RNA-sequencing experiments, the analysis of Differential Expressed (DE) genes was conducted. Coding and non-coding genes with a |log2(disease sample/healthy control)| ≥ 1 and a FDR ≤ 0.1 were considered differentially expressed and retained for downstream analysis. Both the amount of DE genes and their biotype were heterogenous among the three groups. A summary of these results is shown in Table 5. The number of DE transcripts found in these three pathological conditions is the first line of evidence of different RNA involvement among the different diseases. In fact, in sALS the total number of affected genes is 380, while in AD it is 25 and in PD only 5. It is also important to highlight that both in sALS and PD, the majority of DE genes belongs to non-protein coding class, but in AD only 4 transcripts out of 23 do not encode for proteins. By analyzing the DE genes lists, none were shared amongst these pathologies, but further bioinformatics and literature searches allowed us to identify some common features that will be highlighted later on.

	sALS		AD		PD	
	mRNA	lncRNA	mRNA	lncRNA	mRNA	lncRNA
Upregulated	57	183	8	3	0	1
Downregulated	30	110	11	1	1	3
Total	87	293	19	4	1	4

Table 5. Number of mRNAs and lncRNAs differentially expressed and statistically significant in PBMCs of sALS, AD and PD patients compared to healthy controls. Upregulated, downregulated and total are reported. (Modified from Garofalo et al., Int. J. Mol. Sci., 2020).

6.1.1. Amyotrophic Lateral Sclerosis

Through RNA-seq data analysis, 380 genes were found DE in sALS patients, 293 of which were lncRNAs (183 upregulated and 110 downregulated genes). Concerning the class of lncRNA, antisense lncRNA were 184 out of 293, 81 out of 293 were lincRNAs and the remaining 28 were classified as processed transcripts or intronic sense RNAs. About coding genes, 87 DE mRNAs were identified, 30 of which were downregulated

whereas 57 were upregulated. Expression levels of all dysregulated mRNAs and lncRNAs in sALS and healthy subjects are separately represented in heat-maps (Figure 7A-B). Different expression profiles in sALS and healthy controls can be visibly distinguished. The most deregulated coding genes were KIAA2013, HDAC1 and MYCBP. KIAA2013 is an uncharacterized protein and HDAC1 is an histone deacetylase, that has already been associated to ALS because of its altered expression [187]. Moreover, MYCBP is the binding protein of the well characterized oncogene MYC [188]. When considering the top 10 of DE lncRNAs our data showed an interesting deregulation of antisense (AS) RNAs related to genes involved in transcription regulation pathways such as ZEB1-AS and ZBTB11-AS. Also, XXbac-BPG252P9.10 is described as the antisense transcript of IER3, involved in transcription. Interestingly, some of the sense genes regulated by the DE AS lncRNAs in sALS are already linked to neurodegenerative disease, such as UBXN7-AS [189], ATG10-AS38 [190] and ADORA2A-AS [191].

6.1.2. Alzheimer's Disease

A total of 23 DE genes has emerged in AD patients, 19 of which were protein coding genes (8 upregulated and 11 downregulated) and 4 of which were non-coding genes, with 3 upregulated lincRNAs and one downregulated small nucleolar RNA. The expression rate of both coding and non-coding genes in AD population versus matched healthy controls was shown in a single heat-map since the total number of DE in AD is limited (Figure 7C). A neat separation between the two groups is visible despite the low number of DE genes, indicating a disease-specific gene expression pattern.

Interestingly, we found coding genes already associated to AD such as TLN1 [192], and four nuclear pseudogenes (MTRNR2L6, MTRNR2L1, MTRNR2L10 and MTRNR2L8) of the mitochondrial MT-RNR2 gene [193]. VCL was also upregulated. This gene encodes for a protein involved in a pathway associated to Aβ toxicity [194] and associates to TLN1 [195]. When looking at the deregulated lncRNAs, three upregulated lincRNAs were found: CH507-513H4.4, CH507-513H4.6, CH507-513H4.3. These are novel transcripts, similar to YY1 Associated Myogenesis RNA 1 (YAM1) and they are reported as AD associated in LncRNADisease v2.0 Database [196].

6.1.3. Parkinson's Disease

Only 5 genes were found DE in PD patients, 4 of which were downregulated (1 protein coding, 1 small nucleolar RNA, 1 sense intronic transcript and 1 lincRNA) and one of which was an upregulated lincRNA. The heat-map reporting DE mRNAs and lncRNAs in showed in Figure 7D. The protein coding gene TBC1D3 has been associated to

generation of basal neural progenitors [197]. The lncRNAs found in PD patients are currently not associated to specific pathways.

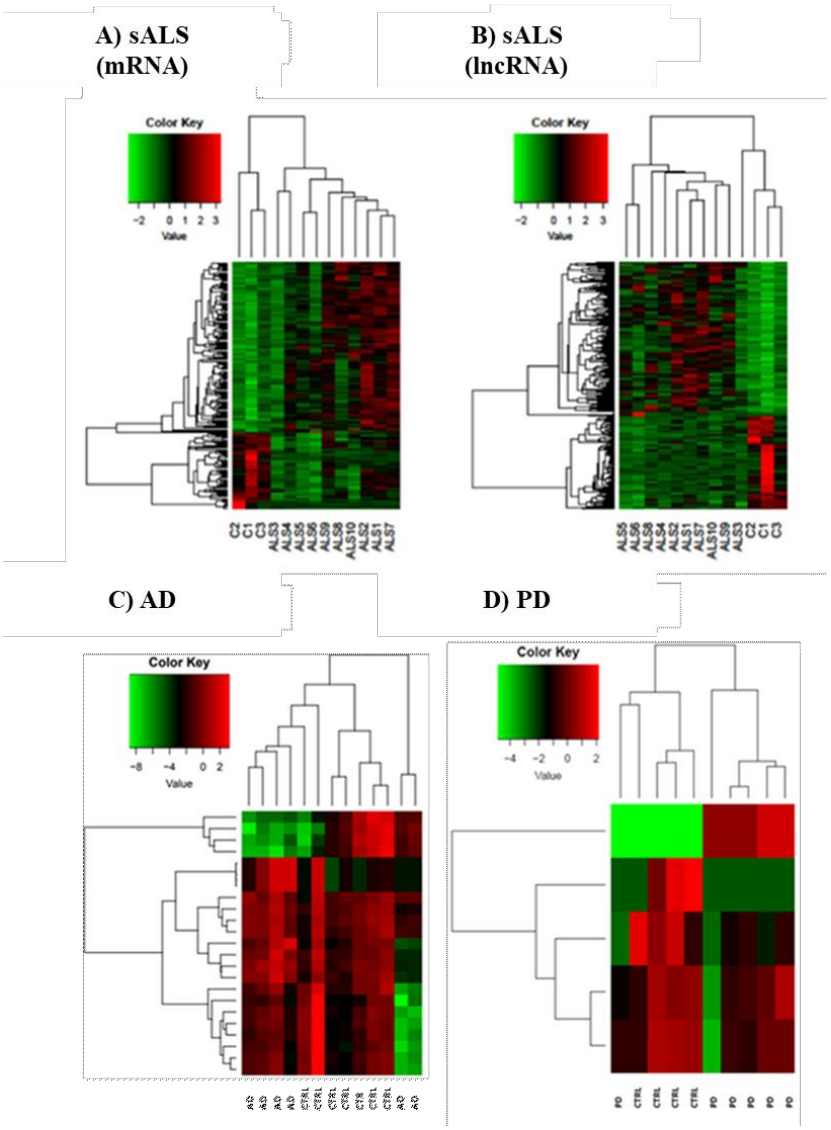

Figure 7. Heatmaps showing expression profiles and clusters of differently expressed genes in sALS, AD, PD compared to healthy controls. For sALS group (n=10; CTRL n=3), differentially expressed mRNAs are shown in panel A, while sALS differentially expressed lncRNAs are shown in panel B. Heatmaps representing both DE mRNAs and lncRNAs in AD (C) and PD (D) are shown. For both AD and PD heatmaps, 6 patients' samples and 6 CTRL were used. All comparisons are given between the disease state and the control samples. We considered as differentially expressed only genes showing |log2(disease sample/healthy donor)| ≥ 1 and a False Discovery Rate ≤ 0.1. (Modified from Garofalo et al., Int. J. Mol. Sci., 2020).

6.1.4. Validation of deregulated coding and non-coding genes

For qPCR validation, we selected specific mRNAs and lncRNAs. We selected the DE RNAs to be validated considering their Fold Change (FC), their previously description as "known" antisense and processed transcripts and a balance between up- and downregulated transcripts.

Transcripts validated in sALS are reported in Figure 8. Those validated in AD are reported in Figure 9 and PD validated ones are shown in Figure 10. Because of the pertinency of DE genes found in sALS patients, we extended validation on a larger cohort of these category of patients: 30 sALS and 30 healthy controls PBMCs underwent lncRNAs confirmation, while 10 sALS and 10 healthy controls PBMCs underwent mRNAs validation.

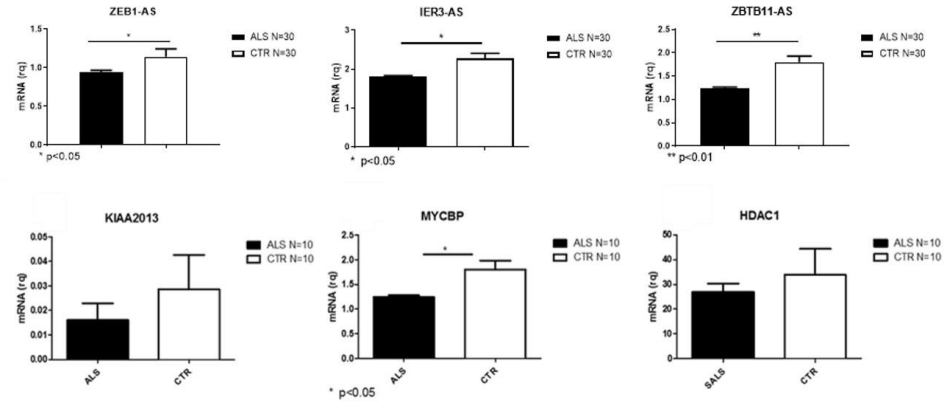

Figure 8. Validation through RT-PCR of DE transcripts in PBMCs from a larger cohort of sALS and CTRL (n=30 for lncRNAs and n=10 for coding RNAs. *p<0.05, **p<0.001. (Modified from Garofalo et al., Int. J. Mol. Sci., 2020).

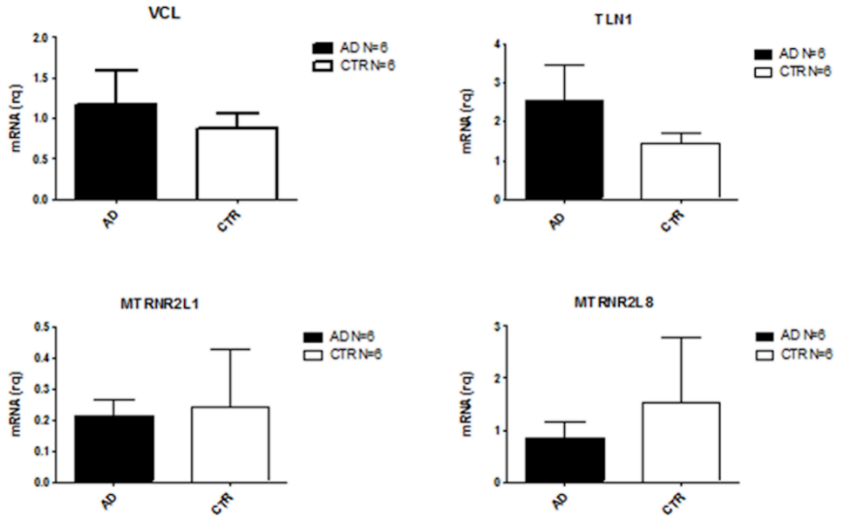

Figure 9. Validation through RT-PCR of DE transcripts in PBMCs from AD and CTRL. (Modified from Garofalo et al., Int. J. Mol. Sci., 2020).

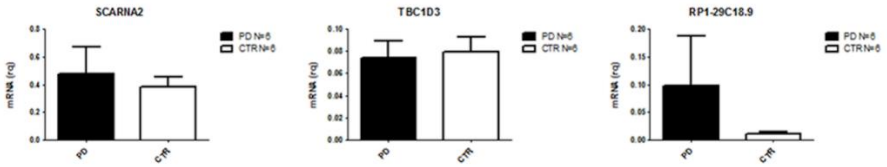

Figure 10. Validation through RT-PCR of DE transcripts in PBMCs from PD and CTRL. (Modified from Garofalo et al., Int. J. Mol. Sci., 2020).

6.1.5. mRNA pathway analysis

Amyotrophic Lateral Sclerosis

Cancer-related pathways, longevity pathway and atherosclerosis resulted from KEGG pathway analysis of DE mRNA in sALS patients (Figure 11).

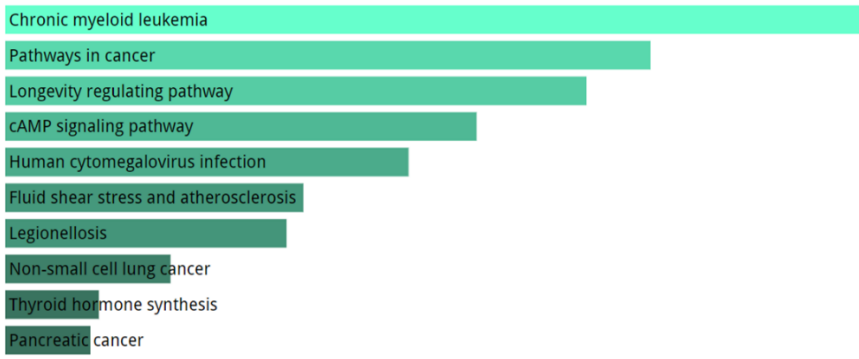

Figure 11. KEGG pathway analysis performed using DE genes in sALS group compared to healthy controls. Top 10 KEGG terms are showed. The significance of the specific gene-set term is represented by the length of the bar. The significance of the term is indicated by the brightness of the bar's color (the brighter, the more significant). Significance for $p<0.004$-0.05. (Modified from Garofalo et al., Int. J. Mol. Sci., 2020).

Intracellular transport, ROS response and regulation of transcription are the GO Biological Processes terms enriched in this group of patients (Figure 12A). The most enriched GO terms in Molecular Function database were activin binding, transcription factor activity, NF-kappaB binding and activating transcription factor binding and DNA binding (Figure 12B). Moreover, enriched GO terms for Cellular Component were integral component of plasma membrane and chromatin (Figure 12C).

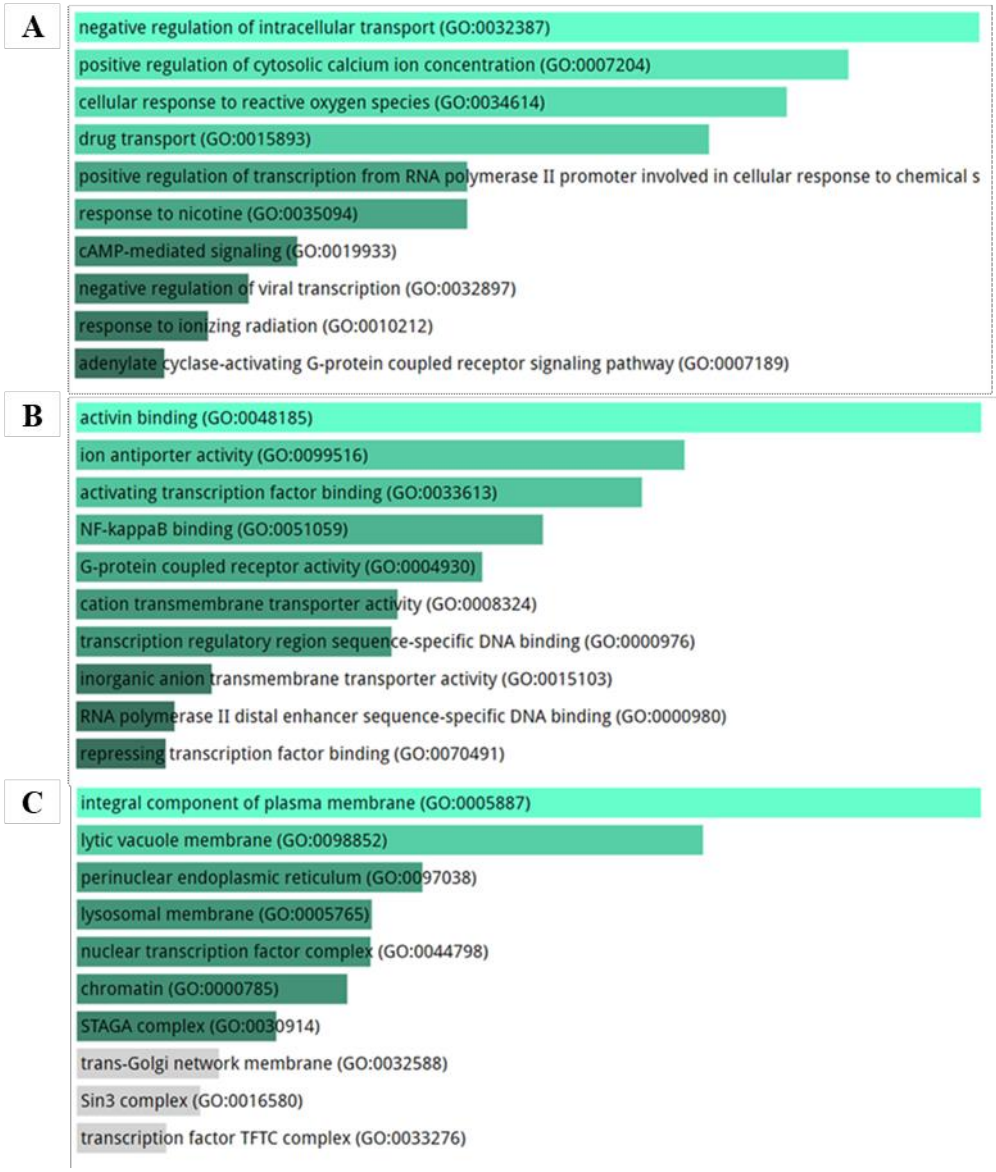

Figure 12. Gene Ontology analysis of DE genes in sALS patients compared to healthy controls. TOP10 enriched GO terms are showed. Biological process (A), molecular function (B) and cellular component (C). The length of the bar represents the significance of that specific gene-set or term. The brighter the color, the more significant that term is, and the grey color refers to non-significant terms. Significance for $p<0.003$-0.05. (Modified from Garofalo et al., Int. J. Mol. Sci., 2020).

Alzheimer's disease

DE genes in analyzed with KEGG pathways highlighted terms related to ribosome, focal adhesion and atherosclerosis (Figure 13).

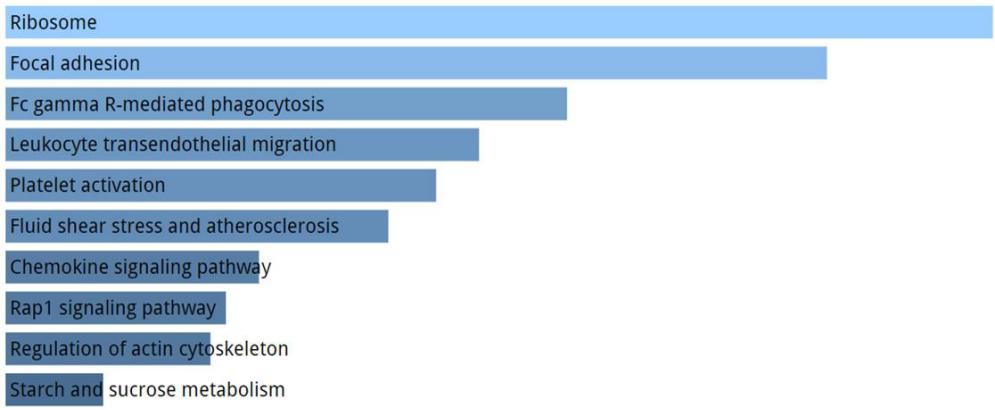

Figure 13. KEGG pathway analysis performed using DE genes in AD group compared to healthy controls. Top 10 KEGG terms are showed. The significance of the specific gene-set term is represented by the length of the bar. The significance of the term is indicated by the brightness of the bar's color (the brighter, the more significant). Significance for $p<0.0007$-0.05. (Modified from Garofalo et al., Int. J. Mol. Sci., 2020).

Exocytosis and protein targeting membrane represent GO enriched terms for Biological Process (Figure 14A), Function analysis resulted in ribosome and focal adhesion those for GO Molecular (Figure 14B) and phosphorylase and oxidase activity are enriched terms for Cellular Component (Figure 14C).

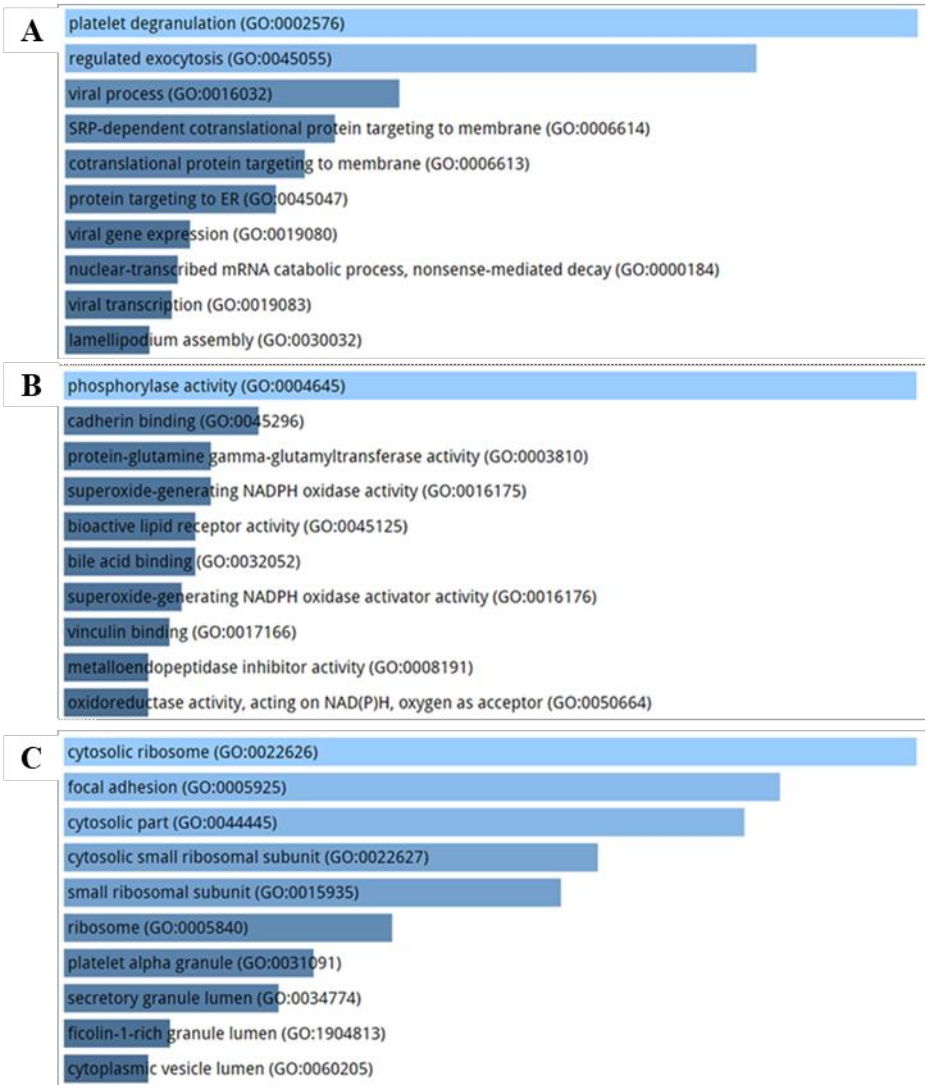

Figure 14. Gene Ontology analysis of DE genes in AD patients compared to healthy controls. TOP10 enriched GO terms are showed. Biological process (A), molecular function (B) and cellular component (C). The significance of the specific gene-set term is represented by the length of the bar. The significance of the term is indicated by the brightness of the bar's color (the brighter, the more significant) Significance for p< 0.00001-0.05. (Modified from Garofalo et al., Int. J. Mol. Sci., 2020).

We performed KEGG pathway and GO terms enrichment analysis for DE in sALS and AD patients compared to healthy controls [182]. This analysis was not conducted for PD patients because of the low number of DE genes found in this group. We found no common DE gene in the three cohorts of patients (Figure 15). Nevertheless, some shared features related to KEGG and GO were reported (Table 6).

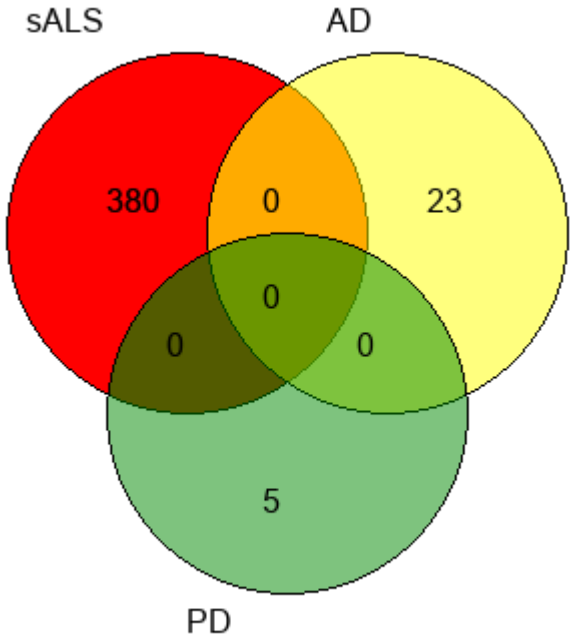

Figure 15. DE genes in common among the three pathologies showed in Venn diagram. No common deregulated gene emerged from DE analysis. (Modified from Garofalo et al., Int. J. Mol. Sci., 2020).

KEGG/GO term	sALS	AD
Dilated cardiomyopathy (DCM)	ADCY9	ITGA2B
	PLN	
	A2M	
Complement and coagulation cascades	F2RL2	F13A1
Fluid shear stress and atherosclerosis	RELA	NCF1
	ACVR2A	ITGA2B
	NFE2L2	
Cellular response to reactive oxygen species	MPV17L	NCF1
	RELA	
	NFE2L2	
Protein localization cell surface	SMURF1	VCL

Table 6. Enriched KEGG or GO terms shared among sALS and AD patients. In the first column the term is reported; in the columns relative to each disease the genes with the highest fold change involved in each term are reported, in green those upregulated, in red those downregulated. (Modified from Garofalo et al., Int. J. Mol. Sci., 2020).

6.2. Enlargement of sALS patients cohort

Because of the relevance of transcriptomic analysis in sALS patients, we have expanded the cohort of these subjects and sequenced 12 controls and 26 sALS patients.

Genes with $|\log2(\text{disease sample/healthy donor})| \geq 1$ and a False Discovery Rate ≤ 0.1 were considered DE and retained for further analysis (181). We found a total of 236 DE genes in PBMCs of sALS patients compared to healthy controls Table 7).

Transcript ID	log2FoldChange	Gene Name	Gene Biotype
ENSG00000259753	6,814706087	RP11-290H9.2	protein_coding
ENSG00000267520	3,654382745	RP11-373L24.1	3prime_overlapping_ncRNA
ENSG00000213197	2,532059755	AC012066.1	processed_pseudogene
ENSG00000205456	2,123347417	TP53TG3D	protein_coding
ENSG00000122877	1,902033379	EGR2	protein_coding
ENSG00000159189	1,77060126	C1QC	protein_coding
ENSG00000225964	1,714183701	NRIR	antisense
ENSG00000248810	1,52265559	RP11-362F19.1	lincRNA
ENSG00000108950	1,421431088	FAM20A	protein_coding
ENSG00000269897	1,416004453	COMMD3-BMI1	protein_coding
ENSG00000240563	1,331939839	L1TD1	protein_coding
ENSG00000105376	1,331929632	ICAM5	protein_coding
ENSG00000187536	1,329409565	TPM3P7	processed_pseudogene
ENSG00000188282	1,286286055	RUFY4	protein_coding
ENSG00000213172	1,278178875	RP1-228H13.2	processed_pseudogene
ENSG00000265690	1,272670259	RP11-5A19.5	protein_coding
ENSG00000279035	1,272553926	RP11-649A18.3	TEC
ENSG00000234076	1,242732935	TPRG1-AS1	lincRNA
ENSG00000225217	1,214902994	HSPA7	unprocessed_pseudogene
ENSG00000161643	1,201838667	SIGLEC16	transcribed_unprocessed_pseudogene
ENSG00000227382	1,198699742	EIF4A2P2	processed_pseudogene
ENSG00000280181	1,187022948	RP11-629N8.4	TEC
ENSG00000162512	1,177016502	SDC3	protein_coding
ENSG00000275793	1,171908524	RMBP3	protein_coding
ENSG00000171115	1,159182547	GMAP8	protein_coding
ENSG00000244682	1,155542197	FCGR2C	polymorphic_pseudogene
ENSG00000073737	1,154019304	DHRS9	protein_coding
ENSG00000276718	1,151152659	RP1-102E24.10	antisense
ENSG00000246731	1,149240179	MGC16275	antisense
ENSG00000167968	1,148492673	DNASE1L2	protein_coding
ENSG00000168874	1,147003798	ATOH8	protein_coding
ENSG00000234534	1,130597734	CSNK1G2P1	processed_pseudogene
ENSG00000198019	1,129224212	FCGR1B	protein_coding
ENSG00000088827	1,116508839	SIGLEC1	protein_coding
ENSG00000248863	1,112326554	RP11-83A24.1	transcribed_processed_pseudogene
ENSG00000174327	1,103627325	SLC16A13	protein_coding
ENSG00000283088	1,102914499	CTD-2331H12.8	protein_coding
ENSG00000267265	1,087182516	CTC-550B14.7	antisense
ENSG00000281887	1,08495997	GIMAP1-GIMAP5	protein_coding
ENSG00000121858	1,0819863	TNFSF10	protein_coding
ENSG00000214455	1,077442693	RCN1P2	processed_pseudogene
ENSG00000134247	1,076081906	PTGFRN	protein_coding
ENSG00000114737	1,06075246	CISH	protein_coding
ENSG00000260368	1,057293006	RP11-521I2.3	sense_overlapping
ENSG00000272625	1,050803195	RP11-737O24.5	antisense
ENSG00000280537	1,049587984	RP11-33O4.2	protein_coding
ENSG00000275111	1,049107374	ZNF2	protein_coding
ENSG00000113555	1,040011165	PCDH12	protein_coding
ENSG00000134824	1,035727475	FADS2	protein_coding
ENSG00000244357	1,033379296	RN7SL145P	misc_RNA
ENSG00000162396	1,026530029	PARS2	protein_coding
ENSG00000214465	1,023056761	SMARCE1P6	processed_pseudogene
ENSG00000276255	1,019936569	RP5-881P19.7	lincRNA
ENSG00000144290	-1,007383892	SLC4A10	protein_coding
ENSG00000162591	-1,010122937	MEGF6	protein_coding
ENSG00000274943	-1,019529502	RP11-351C21.2	sense_intronic
ENSG00000139890	-1,019805336	REM2	protein_coding
ENSG00000107719	-1,021597069	PALD1	protein_coding
ENSG00000100024	-1,085286559	UPB1	protein_coding
ENSG00000267457	-1,095324428	RP5-837J1.4	lincRNA
ENSG00000100433	-1,103262597	KCNK10	protein_coding

Transcript ID	log2FoldChange	Gene Name	Gene Biotype
ENSG00000110046	-1,12314372	ATG2A	protein_coding
ENSG00000118503	-1,131983427	TNFAIP3	protein_coding
ENSG00000258738	-1,160040835	RP11-73E17.2	antisense
ENSG00000178538	-1,183382764	CA8	protein_coding
ENSG00000179094	-1,18349776	PER1	protein_coding
ENSG00000257242	-1,188250849	LINC01619	processed_transcript
ENSG00000278356	-1,203148156	RP11-372B4.3	sense_intronic
ENSG00000244617	-1,211929904	ASPRV1	protein_coding
ENSG00000266677	-1,217047856	RP11-258F1.1	antisense
ENSG00000182326	-1,222000425	C1S	protein_coding
ENSG00000232811	-1,257784099	RP11-96K19.2	antisense
ENSG00000130635	-1,330578833	COL5A1	protein_coding
ENSG00000221949	-1,332974569	LINC01465	lincRNA
ENSG00000218713	-1,360598689	RP1-34L19.1	processed_pseudogene
ENSG00000265975	-1,363958482	CTB-41I6.2	lincRNA
ENSG00000275743	-1,377208434	TRBV14	TR_V_gene
ENSG00000137331	-1,42889208	IER3	protein_coding
ENSG00000270681	-1,436005416	RP11-372K14.2	antisense
ENSG00000267365	-1,462078162	KCNJ2-AS1	antisense
ENSG00000183625	-1,4725602	CCR3	protein_coding
ENSG00000174885	-1,472713218	NLRP6	protein_coding
ENSG00000269927	-1,478461081	RP6-91H8.3	lincRNA
ENSG00000120875	-1,481617086	DUSP4	protein_coding
ENSG00000100906	-1,503803687	NFKBIA	protein_coding
ENSG00000272256	-1,517741893	RP11-489E7.4	antisense
ENSG00000258082	-1,523454676	RP11-443B7.3	lincRNA
ENSG00000129038	-1,539255069	LOXL1	protein_coding
ENSG00000105855	-1,573698313	ITGB8	protein_coding
ENSG00000232891	-1,650011784	RP11-136K14.1	sense_intronic
ENSG00000213085	-1,678521988	CFAP45	protein_coding
ENSG00000175793	-1,71734418	SFN	protein_coding
ENSG00000126266	-1,731259262	FFAR1	protein_coding
ENSG00000264204	-1,754222564	AGAP7P	unprocessed_pseudogene
ENSG00000154928	-1,784469918	EPHB1	protein_coding
ENSG00000073150	-1,852536261	PANX2	protein_coding
ENSG00000149516	-1,918416781	MS4A3	protein_coding
ENSG00000114656	-1,924025266	KIAA1257	protein_coding
ENSG00000076706	-1,926117716	MCAM	protein_coding
ENSG00000012223	-1,937181715	LTF	protein_coding
ENSG00000205710	-2,005772416	C17orf107	protein_coding
ENSG00000115602	-2,008173095	IL1RL1	protein_coding
ENSG00000140287	-2,032423401	HDC	protein_coding
ENSG00000196549	-2,105248385	MME	protein_coding
ENSG00000206047	-2,138078345	DEFA1	protein_coding
ENSG00000239839	-2,149390778	DEFA3	protein_coding
ENSG00000277632	-2,166987482	CCL3	protein_coding
ENSG00000276070	-2,194181056	CCL4L2	protein_coding
ENSG00000124469	-2,227824208	CEACAM8	protein_coding
ENSG00000250696	-2,258244	RP11-704M14.1	antisense
ENSG00000283239	-2,293833996	RP11-439C15.6	protein_coding
ENSG00000105205	-2,318440105	CLC	protein_coding
ENSG00000119121	-2,341201381	TRPM6	protein_coding
ENSG00000133048	-2,461670736	CHI3L1	protein_coding
ENSG00000182885	-2,665787264	ADGRG3	protein_coding
ENSG00000233896	-2,790558481	RP4-684O24.5	antisense
ENSG00000173868	-2,986068915	PHOSPHO1	protein_coding
ENSG00000123689	-3,061950257	G0S2	protein_coding
ENSG00000115009	-3,164674365	CCL20	protein_coding
ENSG00000154099	-3,197752878	DNAAF1	protein_coding
ENSG00000115008	-3,698906359	IL1A	protein_coding
ENSG00000130383	-5,266726702	FUT5	protein_coding
ENSG00000276232	-6,336185527	SCARNA10	sense_intronic

Table 7. Differentially expressed transcripts in sALS PBMC. Transcript ID, log2FoldChange, Gene Name and Gene Biotype are indicated. Transcripts with a minimum |Log2FC| of 1 and an FDR lower than 0.1 are shown.

We evaluated both the trend of these transcripts (up- or downregulated) and their biotype, shown in Table 8. Deregulated mRNA were 78 (29 upregulated and 49 downregulated), while lncRNA were only 21 (8 upregulated and 13 downregulated). A representation of DE transcripts is presented in the volcano plot in Figure 16.

	sALS		
	mRNA	**lncRNA**	**Other**
UP	29	8	16
DOWN	49	13	8
Sub-total	78	21	24
Total	123		

Table 8. Differentially expressed genes in sALS group are classified in relation to regulation (Up or Down). In "lncRNA" column, only antisense RNA and long intergenic noncoding RNA (lincRNA) are considered due to their interest in gene expression modulation. In "Other" column different biotype of noncoding RNAs are reported (processed pseudogenes, processed transcripts), not object of this work.

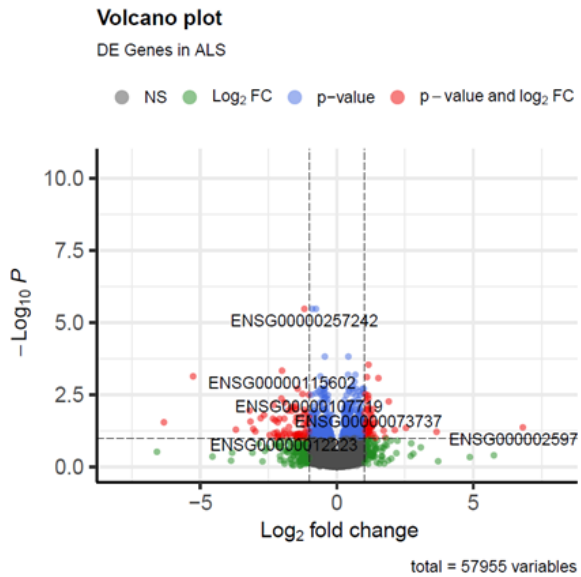

Figure 16. Volcano plot show DE genes. Red dots represent significant up- and downregulated genes which have |log2(fold change)|≥1 and a p-value ≤0.05. Blue, green and grey dots represent non-significant DE detected genes, because they do not satisfy both requirements. The top 6 DE genes are labelled (Ensembl ID).

The heatmap of top 60 DE genes in sALS compared to controls is shown Figure 17. The opposite expression pattern of genes in patients' group and control group is evident.

For further evaluating the distribution of all DE genes in the two class of subjects, we performed a Principal Component Analysis (PCA) (Figure 18). The spontaneous division of sALS patients and controls is clearly visible, meaning that the transcriptome of the two groups is condition specific.

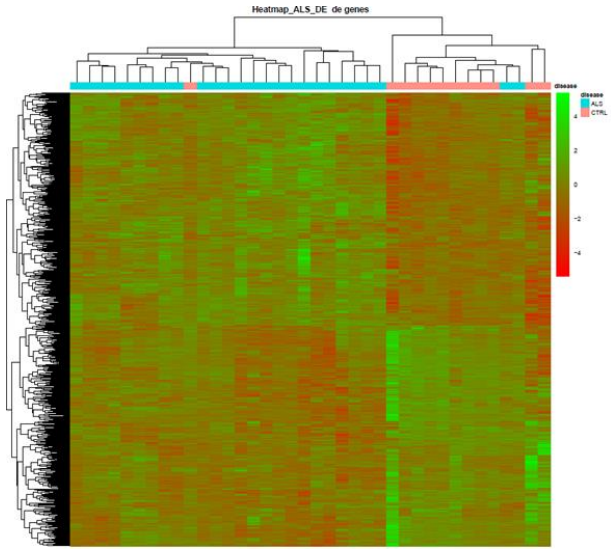

Figure 17. Expression profiles of differently expressed genes in ALS patients and healthy controls. Light blue labels indicate sALS patients, while pink ones indicate controls.

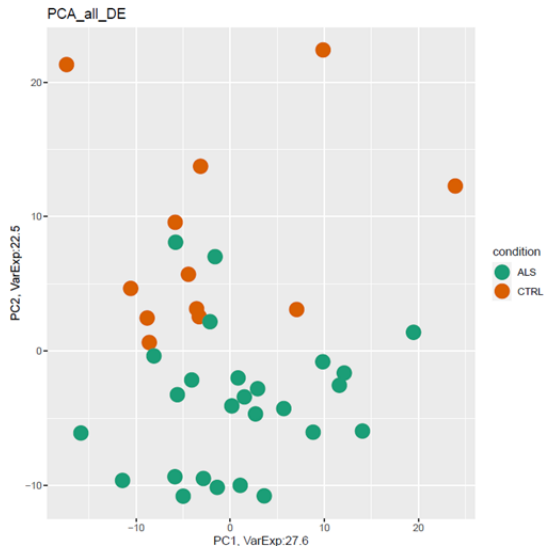

Figure 18. Principal Component Analysis (PCA) of all differentially expressed genes. sALS group are represented by green dots, while controls are shown as orange dots.

6.3 Whole transcriptome analysis in PBMCs of High and Low nSOD1 sALS patients and healthy matched controls

Patients suffering from sALS can be classified into two groups based on the expression levels of nuclear SOD1[95, 96]: High nSOD1 and Low nSOD1. Thus, we decided to perform a transcriptome profiling with differential gene expression analysis in PBMCs of these two sALS groups and matched healthy controls.

6.3.1. High and Low nuclear SOD1 sALS patients' classification

To group patients ALS population and matched controls in relation to nuclear SOD1 (nSOD1) levels, we classified High and Low nSOD1 by evaluating the levels of SOD1 protein in the nucleus of 12 healthy controls and 18 sALS patients through Western Blot analysis (Figure 19).

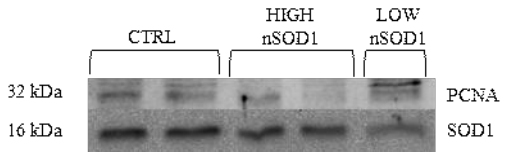

Figure 19. WB quantification of nSOD1 distribution in nuclei of PBMCs isolated from healthy controls (CTRL) and sALS patients.

The ratio between SOD1 and the nuclear Proliferating Cellular Nuclear Antigen 1 (PCNA1) was calculated for normalization (Table 9).

Patient	Age	Sex	Onset	SOD1/PCNA
M53	53	M	Spinal	1.935
F69	69	F	Spinal	1.673
M69	69	M	Spinal	2.021
F69	69	F	Spinal	1.807
F64	64	F	Spinal	2.903
M58	58	M	Spinal	4.456
M44	44	M	Spinal	3.395
F58	58	F	Bulbar	1.566
F66	66	F	Spinal	1.195
M65	65	M	Bulbar	1.319
M68	68	M	Spinal	1.275
F71	71	F	Spinal	0.718
F74	74	F	Bulbar	0.319
F70	70	F	Spinal	0.539
M66	66	M	Spinal	1.149
M72	72	M	Spinal	0.624
F89	89	F	Bulbar	0.492
F76	76	F	Bulbar	0.222

Table 9. Baseline characteristics of subjects recruited for this study. Male=44.4 %; Female=55.6%. Age (M ± SD) 66.72 ± 9.63). SOD1 and PCNA1 (reference nuclear protein)) ratio was calculated to separate High and Low nSOD patients. Threshold was set at 1.4.

Resulting data were used to define the threshold of 1.4 for distinguishing the High and Low nSOD1 groups [96]. The population distribution is represented in the violin plot shown in Figure 20. The mean value of the ratio between SOD1 and PCNA1 in CTRL and High nSOD1 samples was 1.66 and 2.26 respectively. Instead, in Low nSOD1, the mean value of the ration resulted to be 0.78. The density of Low nSOD1 values is more homogenous, while controls and High nSOD1 group show a similar distribution.

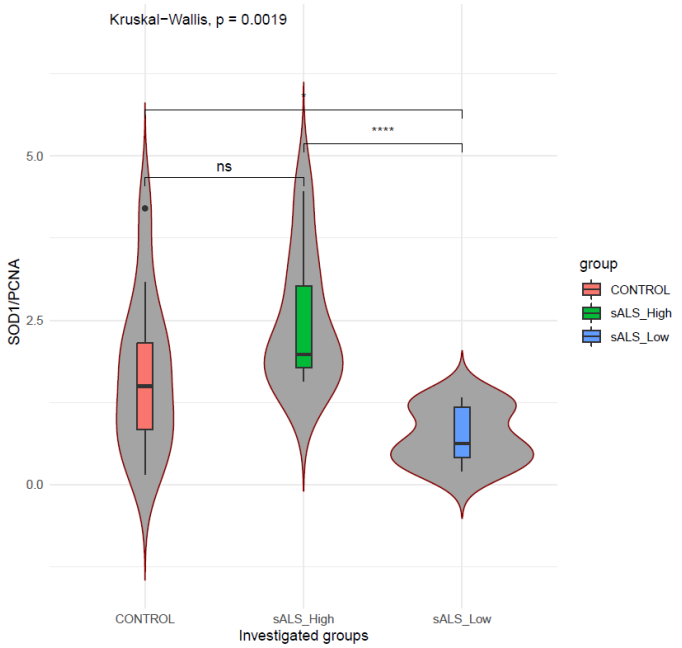

Figure 20. PBMCs of sALS patients differ for nSOD1 distribution. Violin plot with boxplot showing distribution of SOD1 in controls group (n=12; red), sALS patient group where nSOD1 is "High" (n=8; green) and sALS patients group with "Low" nSOD1 (n=10; bleu). Data were analyzed by Kruskall-Wallis test. ****$p < 0.005$; ns= non-significant.

Since patients selected for this study were age heterogenous, a linear regression model was realized on the basis of the age of patients and the SOD1 concentration in the nucleus (Figure 21A). We found that the levels of nSOD1 robustly decrease with age (p-value=0.0021). This data may confirm the putative protective role of SOD1 in nucleus since its presence is lost during aging. We also considered sex as possibly affecting nSOD1 concentration without observing any significant correlation (Figure 21B). No statistically significant incidence of sex (Figure 21B), age of onset, disease duration or other clinical parameters exist in correlation with SOD1 presence in the nucleus of sALS patients.

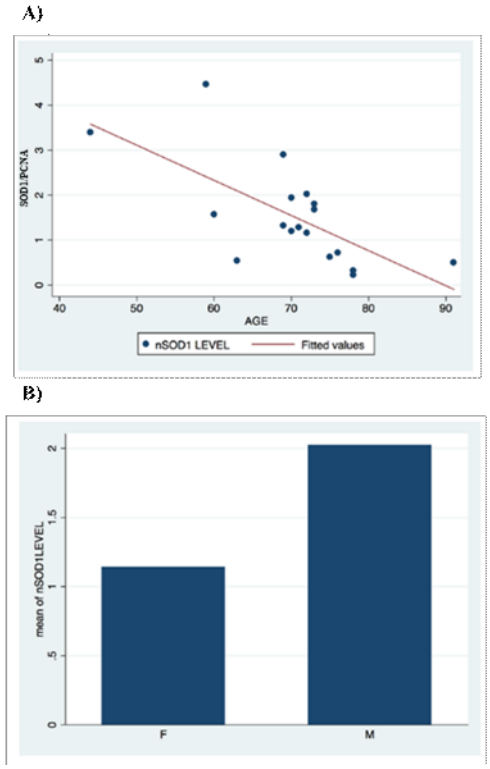

Figure 21. Levels of nSOD1 corelate with patients' aging. A) Scatter plot of age vs nSOD1 levels in patients considered for this work; p-value=0.0021; R^2=0.4456. nSOD1 amount is age dependent. B) Histogram showing nSOD1 levels in all patients classified according to sex. F= females, M = Males. No incidence of sex exists in relation to SOD1 levels in the nucleus of sALS patients.

6.3.2. RNA-sequencing data of High and Low nSOD1 sALS patients' and healthy controls' PBMCs

We performed RNA-seq analysis to investigate the transcriptome profiles in PBMCs of sALS patients (n = 18), classified in High nSOD1 (n = 8) and Low nSOD1 (n = 10) based on nuclear SOD1 ratio, and age/sex matched healthy controls (CTRL) (n = 12). The number of uniquely mapped reads per each sample, resulting from the RNA-seq experiment, is represented in the Figure 22.

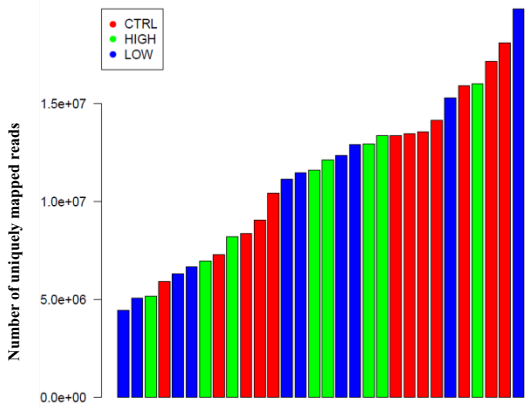

Figure 22. Uniquely mapped reads count per each sample. Red bars represent CTRL, green bars represent High nuclear SOD1 samples, blue bars represent Low nuclear SOD1 samples.

Genes with |log2(disease sample/healthy donor)|≥1 and a False Discovery Rate ≤ 0.1 were considered differentially expressed and retained for further analysis [198].

We detected DE transcripts in PBMCs in the two subgroups of subjects: sALS patients with High nSOD1 and sALS patients with Low nSOD1. Both groups were compared with healthy controls. In Low nSOD1 patients, we found a total of 62 DE genes (Table 10), 35 coding (20 upregulated and 15 downregulated) and 27 noncoding genes respect to healthy controls. Among the noncoding genes, 14 were lncRNA (9 upregulated and 5 downregulated).

Transcript ID	log2FoldChange	Gene Name	Gene Biotype	Transcript ID	log2FoldChange	Gene Name	Gene Biotype
ENSG00000282960	7.52131557043765	KDM4C	protein_coding	ENSG00000188282	1.18570434284884	RUFY4	protein_coding
ENSG00000213197	3.43318968024838	AC012066.1	processed_pseudogene	ENSG00000258056	1.12385840146588	RP11-644F5.11	antisense
ENSG00000113361	3.00036926599837	CDH6	protein_coding	ENSG00000183773	1.08332436905338	AIFM3	protein_coding
ENSG00000205456	2.53512639275729	TP53TG3D	protein_coding	ENSG00000088881	1.07305484919398	EBF4	protein_coding
ENSG00000108950	2.52453286905801	FAM20A	protein_coding	ENSG00000272908	1.05750802461125	RP11-121A8.1	lincRNA
ENSG00000160307	2.42937741396295	S100B	protein_coding	ENSG00000279672	1.05279843661825	CMB9-55F22.1	TEC
ENSG00000278558	2.42472842821478	TMEM191B	protein_coding	ENSG00000228140	1.03601102734597	RP3-467K16.4	lincRNA
ENSG00000267342	2.29936464816193	RP11-552F3.10	antisense	ENSG00000197182	1.01390517105201	MIRLET7BHG	lincRNA
ENSG00000178115	2.04808456161896	GOLGA8Q	protein_coding	ENSG00000227032	1.00130120553494	RPS2P36	processed_pseudogene
ENSG00000248810	1.97245744012298	RP11-362F19.1	lincRNA	ENSG00000251867	-1.8889163144791	RP11-48B3.5	antisense
ENSG00000179071	1.94853286778044	CCDC89	protein_coding	ENSG00000155090	-1.29119167656028	KLF10	protein_coding
ENSG00000265690	1.69865070287264	RP11-5A19.5	protein_coding	ENSG00000175985	-1.34024220813713	PLEKHD1	protein_coding
ENSG00000213172	1.55873488377518	RP1-228H13.2	processed_pseudogene	ENSG00000274943	-1.39791792460496	RP11-351C21.2	sense_intronic
ENSG00000225217	1.51587206743831	HSPA7	unprocessed_pseudogene	ENSG00000105855	-1.7233577156103	ITGB8	protein_coding
ENSG00000168874	1.49183756412985	ATOH8	protein_coding	ENSG00000154928	-1.97846639716329	EPHB1	protein_coding
ENSG00000167123	1.4837029499073	CERCAM	protein_coding	ENSG00000273338	-2.00581553510598	RP11-386I14.4	antisense
ENSG00000277887	1.47463149202592	SNORA50C	snoRNA	ENSG00000183625	-2.033818502528	CCR3	protein_coding
ENSG00000182584	1.42667506474105	ACTL10	protein_coding	ENSG00000115602	-2.24329928981437	IL1RL1	protein_coding
ENSG00000279035	1.41749572299054	RP11-649A18.3	TEC	ENSG00000149516	-2.40878002447957	MS4A3	protein_coding
ENSG00000267265	1.35440619037764	CTC-550B14.7	antisense	ENSG00000246363	-2.42386858944451	RP11-13A1.1	lincRNA
ENSG00000113555	1.34982712725523	PCDH12	protein_coding	ENSG00000196549	-2.51448439700376	MME	protein_coding
ENSG00000234534	1.32798325159191	CSNK1G2P1	processed_pseudogene	ENSG00000149534	-2.72219915817	MS4A2	protein_coding
ENSG00000174327	1.31263293223441	SLC16A13	protein_coding	ENSG00000140287	-2.98037532537816	HDC	protein_coding
ENSG00000260852	1.29499104645243	FBXL19-AS1	antisense	ENSG00000259717	-3.05787307358582	LINC00677	lincRNA
ENSG00000246731	1.29434272200613	MGC16275	antisense	ENSG00000105205	-3.12858532843734	CLC	protein_coding
ENSG00000244682	1.28846469571542	FCGR2C	polymorphic_pseudogene	ENSG00000124469	-3.15277182309077	CEACAM8	protein_coding
ENSG00000281887	1.26629588706563	GIMAP1-GIMAP5	protein_coding	ENSG00000204455	-3.25588473635444	TRIM51BP	unprocessed_pseudogene
ENSG00000196159	1.24812256098341	FAT4	protein_coding	ENSG00000250696	-3.48129785669236	RP11-704M14.1	antisense
ENSG00000171914	1.24215111349475	TLN2	protein_coding	ENSG00000005108	-3.60714266160544	THSD7A	protein_coding
ENSG00000250995	1.22891519249441	RP13-128O4.3	processed_pseudogene	ENSG00000119121	-3.74960547589506	TRPM6	protein_coding
ENSG00000206811	1.1942733692373	SNORA10	snoRNA	ENSG00000134827	-3.79351543723891	TCN1	protein_coding

Table 10. Differentially expressed transcripts in Low nSOD1 group. Transcript ID, log2FoldChange, Gene Name and Gene Biotype are indicated. Transcripts with a minimum |Log2FC| of 1 and an FDR lower than 0.1 are shown.

In High nSOD1 patients, we found only 25 DE genes versus controls (Table 11). Coding genes were 15, (12 upregulated and 3 downregulated), 10 were noncoding genes of which 4 lncRNA (2 upregulated and 2 downregulated).

Transcript ID	log2FoldChange	Gene Name	Gene Biotype
ENSG00000167680	4.41141153396196	SEMA6B	protein_coding
ENSG00000204388	3.98858942876702	HSPA1B	protein_coding
ENSG00000135094	3.24161490612005	SDS	protein_coding
ENSG00000280046	2.70188427795239	RP11-1099M24.6	TEC
ENSG00000204389	2.03299955046361	HSPA1A	protein_coding
ENSG00000225964	1.90193935607654	NRIR	antisense
ENSG00000139354	1.88481211809689	GAS2L3	protein_coding
ENSG00000168386	1.79171274414036	FILIP1L	protein_coding
ENSG00000246731	1.57637117434868	MGC16275	antisense
ENSG00000260401	1.56340394144516	RP11-800A3.4	sense_overlapping
ENSG00000260368	1.50323340586512	RP11-521I2.3	sense_overlapping
ENSG00000134247	1.40550554950708	PTGFRN	protein_coding
ENSG00000120694	1.25930759944865	HSPH1	protein_coding
ENSG00000114737	1.21658625634824	CISH	protein_coding
ENSG00000182580	1.17317696051547	EPHB3	protein_coding
ENSG00000178718	1.07270037190965	RPP25	protein_coding
ENSG00000212719	1.01344397191424	C17orf51	protein_coding
ENSG00000257242	-1.07500240173783	LINC01619	processed_transcript
ENSG00000053524	-1.11229105846428	MCF2L2	protein_coding
ENSG00000238090	-1.12883860990823	AC006195.2	processed_pseudogene
ENSG00000198590	-1.15812827035902	C3orf35	lincRNA
ENSG00000062524	-1.2658181952968	LTK	protein_coding
ENSG00000157985	-1.27285771604886	AGAP1	protein_coding
ENSG00000232811	-1.79322447224647	RP11-96K19.2	antisense
ENSG00000218713	-2.37708149831829	RP1-34L19.1	processed_pseudogene

Table 11. Differentially expressed transcripts in High nSOD1 group. Transcript ID, log2FoldChange, Gene Name and Gene Biotype are indicated. Transcripts with a minimum |Log2FC| of 1 and an FDR lower than 0.1 are shown.

Outcomes of DE analysis are summarized in Table 12 and biotype of detected transcripts is represented in Figure 23.

	Low nSOD1			High nSOD1		
	mRNA	lncRNA	Other	mRNA	lncRNA	Other
UP	20	9	11	12	2	3
DOWN	15	5	2	3	2	3
Sub-total	35	14	13	15	4	6
Total	62			25		

Table 12. Differentially expressed genes in each group are classified in relation to regulation (Up or Down). In “lncRNA” column, only antisense RNA and long intergenic noncoding RNA (lincRNA) are considered due to their interest in gene expression modulation. In “Other” column different biotype of noncoding RNAs are reported (processed pseudogenes, processed transcripts), not object of this work.

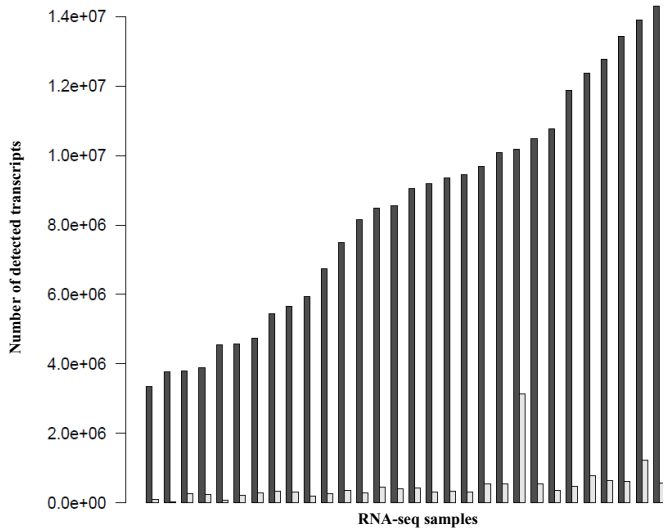

Figure 23. Number of detected transcripts per sample for coding (dark grey bars) and non-coding RNAs (light grey bars).

We considered the resulting transcripts separately for each group and realized volcano plots (Figure 24A,B) to highlight all statistically significant DE genes in the two ALS subgroups.

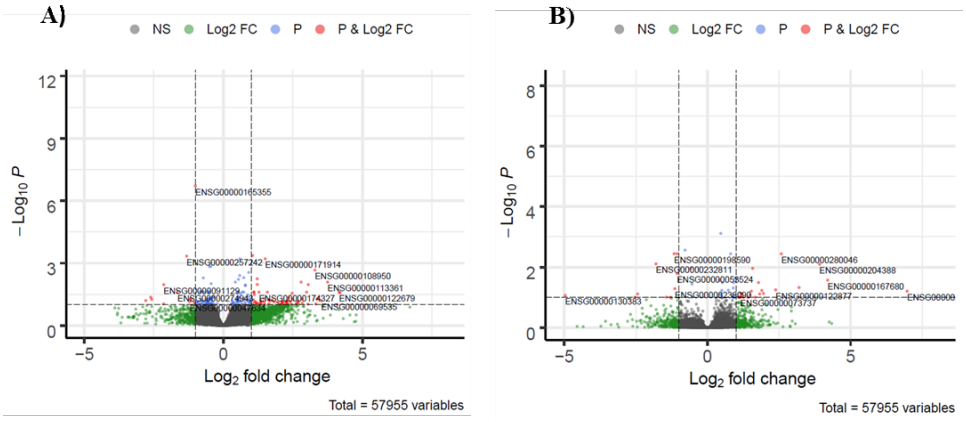

Figure 24. Volcano plots. Panel (A) shows DE genes in Low nSOD1 patients, while panel (B) shows DE genes in High nSOD1 patients. Red dots represent significant up- and downregulated genes which have |log2(fold change)|≥1 and a p-value ≤0.05. Blue, green and grey dots represent non-significant DE detected genes, because they do not satisfy both requirements. The top 11 DE genes are labelled (Ensembl ID).

Heat-maps of top 60 DE genes in both groups are shown in Figure 25C,D. It clearly appears that both groups, Low and High nSOD1, have different gene expression profiles compared to healthy controls. We then compared DE genes of the two sALS groups to highlight common transcripts. We only detected one common DE gene in the two groups (Figure 25E), that is an antisense lncRNA (MGC16275; Fold Change (FC) Low nSOD1: 1.29; FC High nSOD1: 1.58).

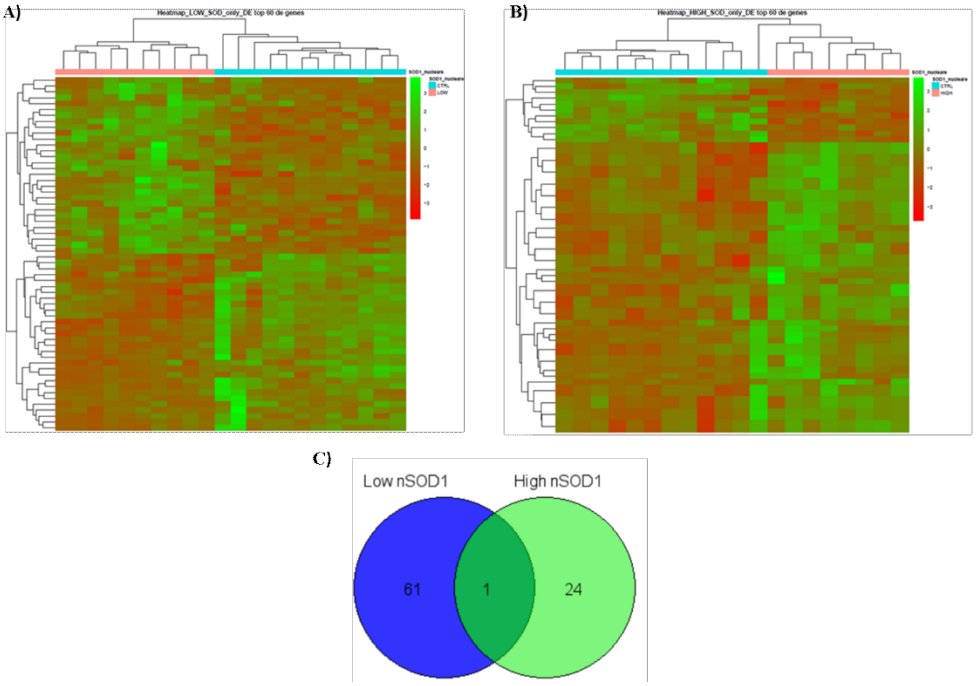

Figure 25. Differential expression analysis in Low and High nSOD1 PBMCs of sALS patients**.** *Heat-maps.* Expression profiles of differently expressed genes in ALS patients and healthy controls. Panel (A) compares RNAs in Low nSOD1 patients and the control samples, while panel (B) compares RNAs in High nSOD1 patients and the control samples. *Venn diagram*. Differentially expressed genes in common among the two nSOD1 ALS groups (C).

We performed a Principal Component Analysis (PCA) of DE genes in the two sALS groups and healthy controls (Figure 26). A neat and gradual division of patients is present. Both Low and High groups separate from healthy controls and interestingly the High nSOD1 group, already described as the "less affected" group [96], is similar to controls group. In Table 13, we have reported DE genes involved in DNA repair processes. KDM4C and TP53TG3D were found upregulated in Low nSOD1group,

HSPA1A, HSPA1B, FILIP1L and PTGFRN were found upregulated in High nSOD1 group.

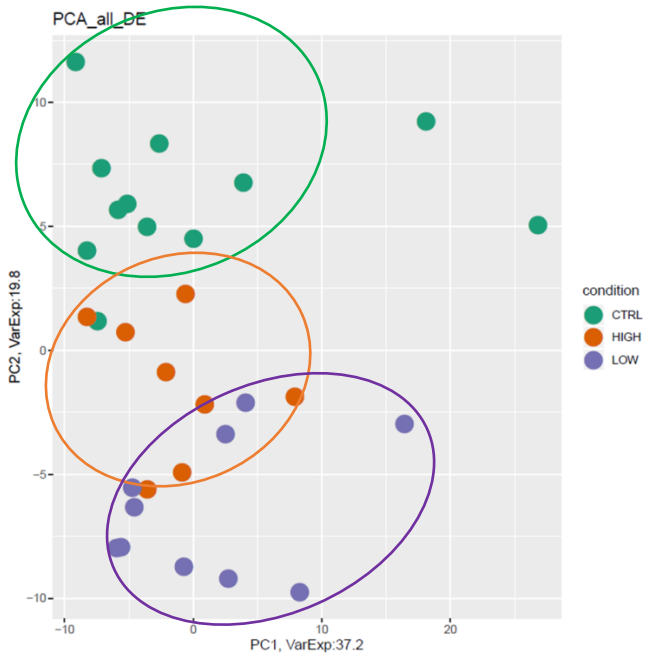

Figure 26. Principal Component Analysis (PCA) of all differentially expressed genes. Both Low nSOD1 (in purple) and High nSOD1 (in orange) groups separate from healthy controls (CTRL in green) and interestingly the High nSOD1 group is closer to controls group.

Low nSOD1		**High nSOD1**	
Gene	**Fold Change**	**Gene**	**Fold Change**
KDM4C	7.52	HSPA1B	3.99
TP53TG3D	2.53	HSPA1A	2.00
		FILIPL1	1.79
		PTGFRN	1.41

Table 13. Genes involved in DNA damage process in Low nSOD1 and in High nSOD1 are reported together with their Fold Change.

6.3.3. Evaluation of Histone 3 methylation

Because of the strong difference in gene expression that we observed in the two sALS subgroups, and the upregulation of lysine demethylase 4C (KDM4C) in Low nSOD1 group, we evaluated through immunofluorescence the tri-methylation of Histone 3 (H3) in PBMCs. We studied the expression of both H3K9me3, which is a direct substrate of KDM4C, and H3K27me3, which is not [199]. Both these histone modifications are transcriptional suppressive [200]. However, no differences were present in H3K9me3 between the two groups, or with healthy controls (data not shown). Nevertheless, as shown in Figure 27, in patients with High nSOD1 the amount of H3K27me3 is higher compared with Low nSOD1 groups. This is in agreement with the lower number of DE genes we found in High nSOD1 group. This evidence highlights a potential link between nSOD1 levels and H3 methylation with subsequent effect on epigenetic regulation of gene expression, leading to altered cellular processes.

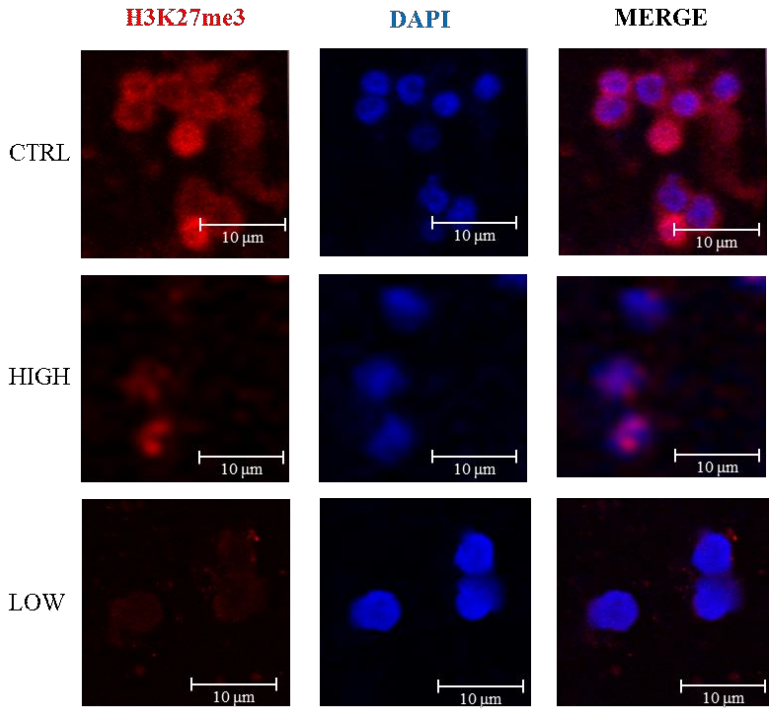

Figure 27. High nSOD1 induces the increase of H3K27 methylation. Representative images of tri-methylation of Histone 3 on the Lysine 27 (H3K27me3) investigated through immunofluorescence in PBMCs of controls, High nSOD1 and Low nSOD1 patients.

6.3.4. mRNA pathway analysis

To further explore the mechanisms underlying the differences observed in the two sALS groups, GO terms enrichment analysis for DE genes in High nSOD1 and Low nSOD1 patients compared to healthy controls have been performed for both upregulated and downregulated DE genes together. Concerning Low nSOD1 patients, the GO biological process enriched terms are related to sensory perception of pain, neurogenesis, regulation of skeletal muscle satellite cell proliferation, retinal ganglion cell axon guidance, regulation of cytokine production involved in immune response and central nervous system neuron axonogenesis (Figure 28A). The GO cellular component enriched terms highlight the involvement of granules and Golgi network (Figure 28B), while those belonging to molecular functions include cytokine receptor activity, Tau protein binding, RAGE receptor binding and Ephrin receptor activity (Figure 28C). RAGE receptor binding term results from the deregulation of S100B, a Ca^{2+} binding protein involved in a vast number of intracellular and extracellular effects in the brain [201], already reported as increased in both human and mouse ALS spinal cord tissues display transcript and protein levels of both RAGE and S100B [202].

With regards to High nSOD1 group' DE genes, the GO biological process enriched terms include response to unfolded proteins, cellular response to heat and positive regulation of tumor necrosis factor-mediated signaling pathway (Figure 28D). With respect to cellular component, the most enriched GO terms include aggregosome, centriole, microtubule and ribonuclease P complex (Figure 28E). The most enriched GO terms for molecular function are related to RING finger domain, ATPase activity, histone deacetylase binding and transmembrane receptor protein tyrosine kinase activity (Figure 28F).

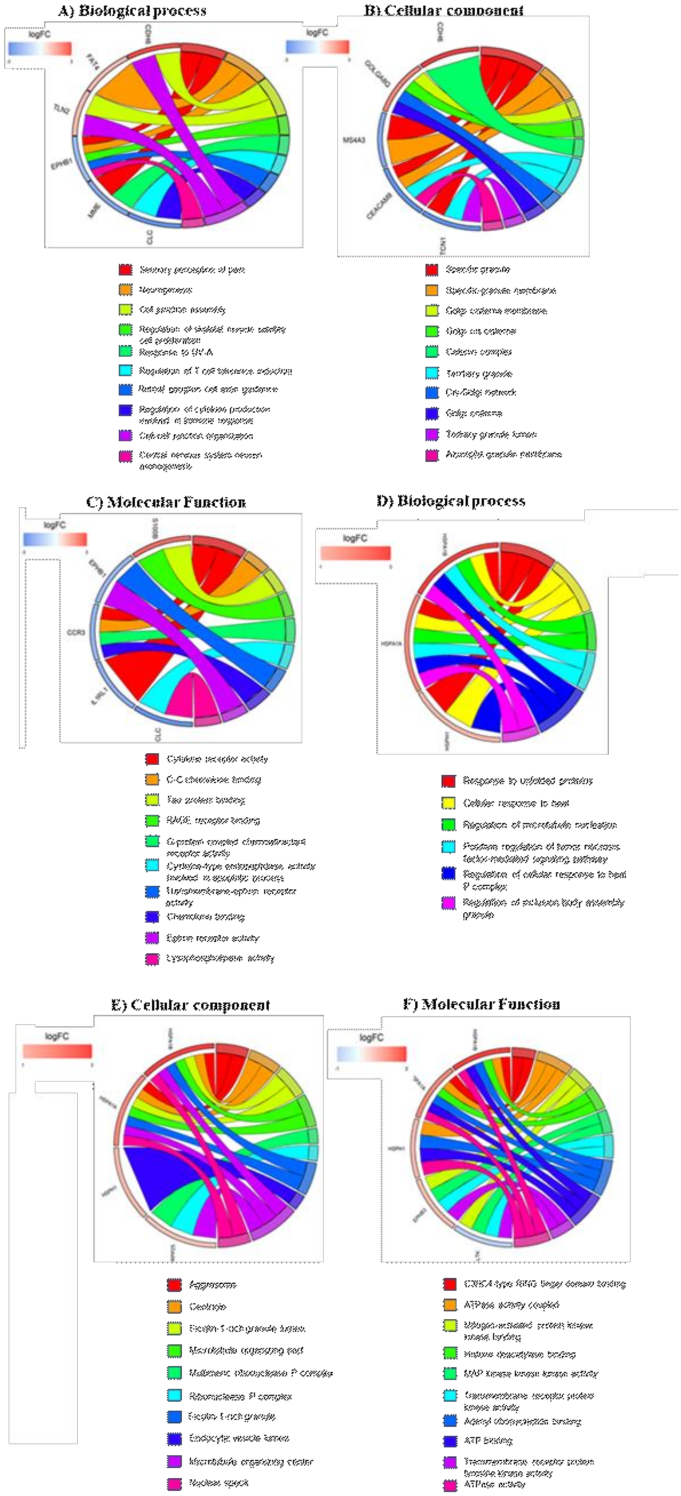
A) Biological process
logFC
B) Cellular component
logFC
Specific granule
Tertiary granule
Cis-Golgi network
Golgi cisterna
C) Molecular Function
logFC
Cytokine receptor activity
C-C chemokine binding
D) Biological process
logFC
Response to unfolded protein
Cellular response to heat
E) Cellular component
logFC
Aggresome
Centriole
F) Molecular Function
logFC
ATP binding
ATPase activity

Figure 28. Chord plot showing significantly enriched GO terms for Biological Process (A,D), Cellular Component (B,E) and Molecular Function (C,F) in Low (A,B,C) and in High (D,E,F) nSOD1. On the left of the plot, the genes contributing to that enrichment, arranged in order of their logFC, which is displayed in descending intensity of red squares for the upregulated genes, and blue squares for the downregulated ones. The genes are linked to their assigned terms via coloured ribbons.

We also analyzed the involved pathways resulting from DE genes using both KEGG and Wikipathways databases. DE genes in Low nSOD1 group submitted to KEGG analysis revealed the involvement of PI3K-Akt signaling pathway, axon guidance, Alzheimer disease and interaction of cytokines with their receptors, together with many pathways strictly related to the sample tissue (Figure 29A). Interestingly, the same analysis conducted in High nSOD1 group, showed the alteration of pathways related to protein processing in endoplasmic reticulum and endocytosis. Also, axon guidance and RNA transport were affected in this cohort of patients (Figure 29B). The same analysis carried out exploiting Wikipathways database, showed also different pathways in the two groups. For instance, in Low nSOD1 group, DE genes appear to be involved in amino acid biosynthesis and in spinal cord injury (Figure 29C). While, in High nSOD1 group, the activated pathways are related to nuclear receptors and apoptosis modulation (Figure 29D).

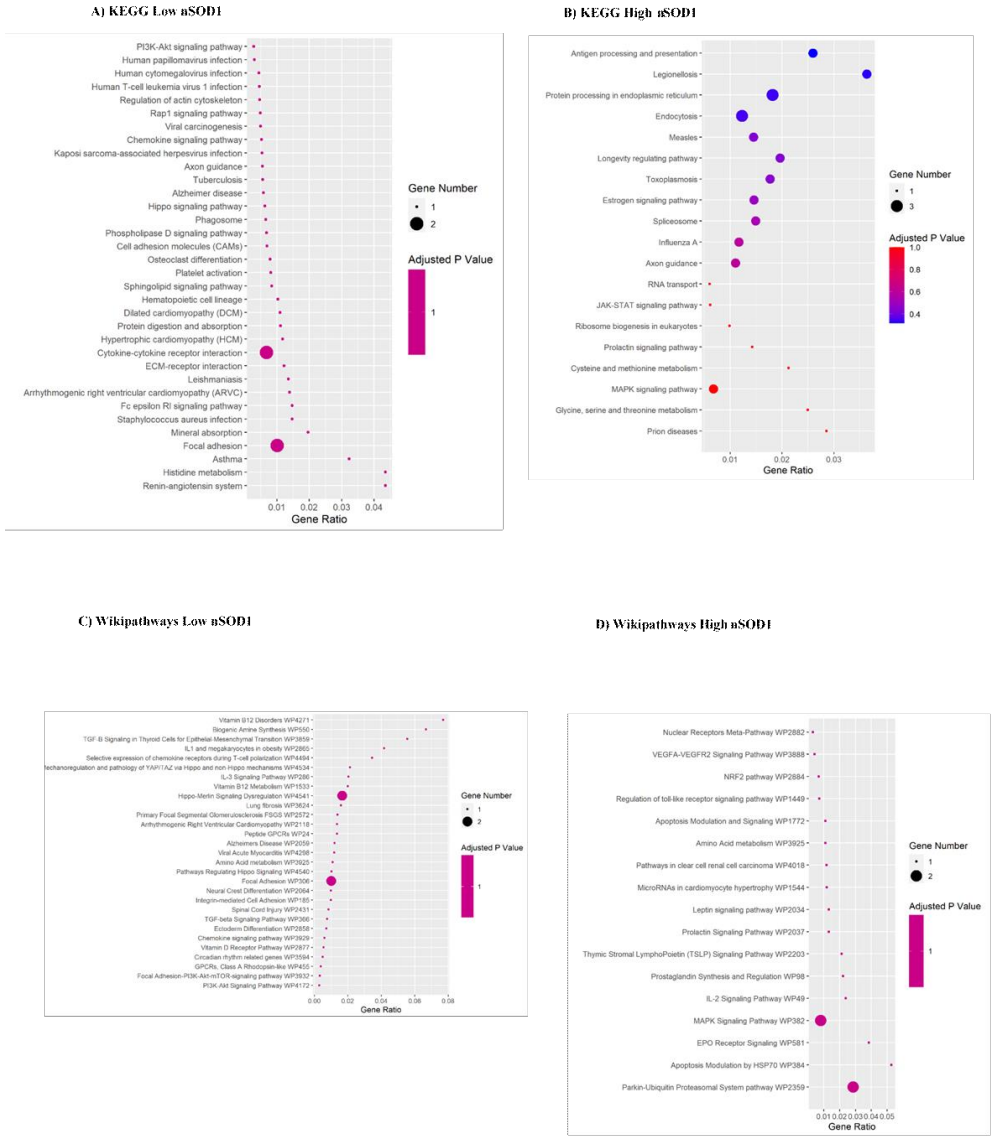

Figure 29. Dot plot shows the dysregulated KEGG and Wikipathways pathways (FDR <0.1) enriched for Low (A,C) and High (B,D) nSOD1 patients. The size of the dot is based on gene count enriched in the pathway, and the colour of the dot shows the pathway enrichment significance. Gene ratio: the ratio of resulting DE genes correlated to a KEGG pathway to the number of annotated genes per KEGG pathway in the database. The p-value is computed from the Fisher exact test which is a proportion test that assumes a binomial distribution and independence for probability of any gene belonging to any set.

6.3.4. Heat Shock Proteins and DNA damage evaluation in PBMCs

We found heat shock proteins (HSPs) to be upregulated in RNA-seq in High nSOD1 patients (Figure 28; Table 11. Of note HSPs play an important role in the maintenance of both protein homeostasis and DNA integrity [203]. Thus, we evaluated both HSPA1A, HSPA1B (both transcribed by HSP70 genes) and HSPH1 mRNAs expression (Figure 30A,B,C) and protein levels in PBMCs (Figure 30D,E,F). Levels of HSPA1A and HSPA1B mRNAs result significantly increased in High nSOD1 patients compared to those with Low nSOD1, while no significant alterations are observed in HSPH1 gene through RT-PCR. Concerning Western Blot analysis, levels of HSP70 and HSPH1 are higher in patients with High nSOD1 compared to those with Low nSOD1. We also measured the levels of the transcription factor HSF1 that regulates the expression of heat shock genes [204]. When triggered, HSF1 becomes trimerized and phosphorylated, and then translocated into the nucleus where it binds to conserved heat shock-responsive DNA elements (HSEs) to upregulate genes coding for HSPs [204]. Levels of both HSF1 transcript and protein were not altered (Figure 31A,B), while the phosphorylation of HSF1 protein at S326 is higher in patients with High nSOD1 compared to both Low nSOD1 patients and healthy controls (Figure 31C,D). These results show a greater activation of HSP70 and HSPH1 in PBMCs of patients with High nSOD1 distribution.

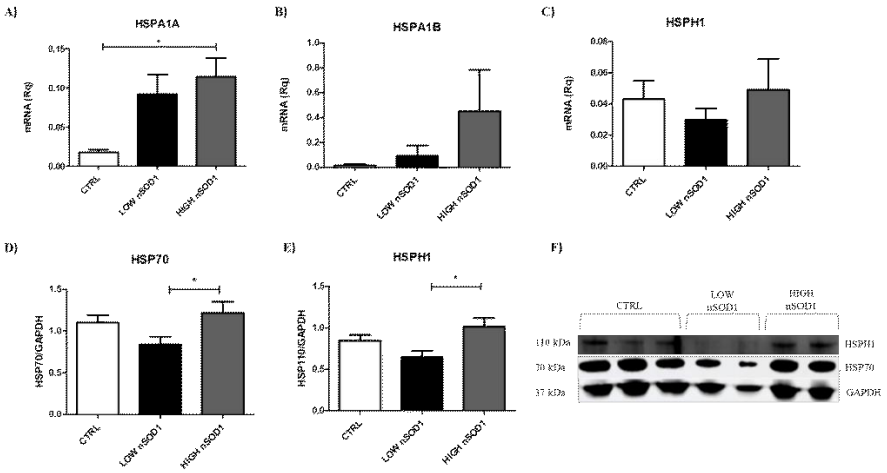

Figure 30. High nSOD1 show an increase of heat shock proteins. Validation of HSPs**.** A,B,C) RT-PCR of HSPA1A, HSPA1B and HSPH1 in PBMCs of CTRL, Low nSOD1 and High nSOD1 sALS patients. Data were analyzed by ANOVA (n = 3) followed by Bonferroni post-test. * $p < 0.05$. Levels of HSPA1A and HSPA1B mRNAs are higher in patients with High nSOD1 confirming RNA-seq results, while no significant alterations are observed in HSPH1 mRNAthrough qPCR. D,E,F) WB analysis for evaluating expression of HSP70s, HSPH1 in sALS PBMCs. Data were analyzed by ANOVA (n = 3) followed by Bonferroni post-test. * $p < 0.05$. Levels of HSP70 and HSPH1 are higher in patients with High nSOD1 compared to those with Low nSOD1.

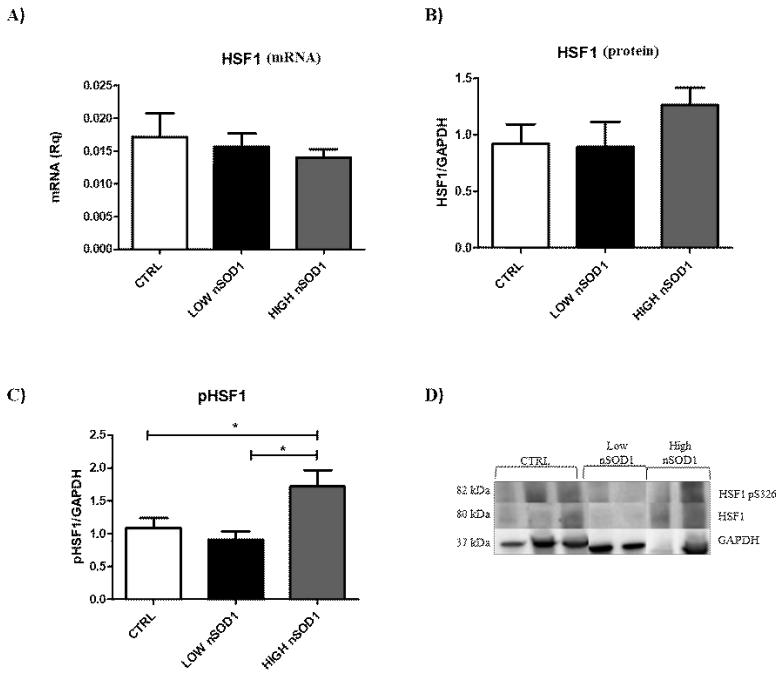

Figure 31. Phosphorylation of HSF1 is increased in High nSOD1 PBMCs of ALS patients. A) RT-PCR of HSF1 mRNA in PBMCs of CTRL, Low nSOD1 and High nSOD1 sALS patients. B) WB analysis of HSF1 protein. Their levels do not change. C,D) WB analysis for the study of HSF1phosphorylation at Serine 326. Levels of phosphorylated HSF1 at S326 are higher in patients with High nSOD1 compared to those with Low nSOD1 and to healthy controls. Data were analyzed by ANOVA (n = 3) followed by Bonferroni post-test. * $p < 0.05$.

To demonstrate the protective role of SOD1 and its relationship with HSP70 in the nucleus, we performed Comet assay in PBMCs of controls, High nSOD1 and Low nSOD1 sALS patients (Figure 33A-C). Comet length was measured for cells in basal conditions, cells treated with H_2O_2 (5 minutes of 500 μM H_2O_2) followed by 30' of stress recovery and cells undergone 1h of 50 μM VER (HSP70 inhibitor) treatment plus 5' of 500 μM H_2O_2 treatment followed by 30' of stress recovery. An increased comet length, indicating DNA damage, was observed in basal conditions in patients with Low nSOD1compared to High nSOD1 (Figure 33A,B). This increase is also visible in Low nSOD1compared to controls, while it was not evident in PBMCs of patients with High nSOD1 (Figure 33A,C). In healthy subjects, the treatment with H_2O_2 (5'; 500 μM) + VER (1h; 50 μM) visibly increased DNA damage compared to both basal conditions cells and control cells treated with H_2O_2 alone. This indicates that HSP70 is implicated in the recovery phase, and its inhibition strongly affects dsDNA repair. In High nSOD1 patients, as in the healthy controls, no significant variation was highlighted comparing basal cells and cells treated with H_2O_2 (5'; 500 μM), meaning that the upregulation of HSP70 restored normal DNA repair during the recovery phase. On the contrary, the

inhibition of HSP70 with VER (1h; 50 μM) prevented the recovery from the damage. Lastly in Low nSOD1 PBMCs no significant variation was observed in terms of Comet length (Figure 33A,C). This suggest that HSP70 are not sufficiently expressed, as their inhibition does not contribute to DNA damage increase, present regardless of treatments.

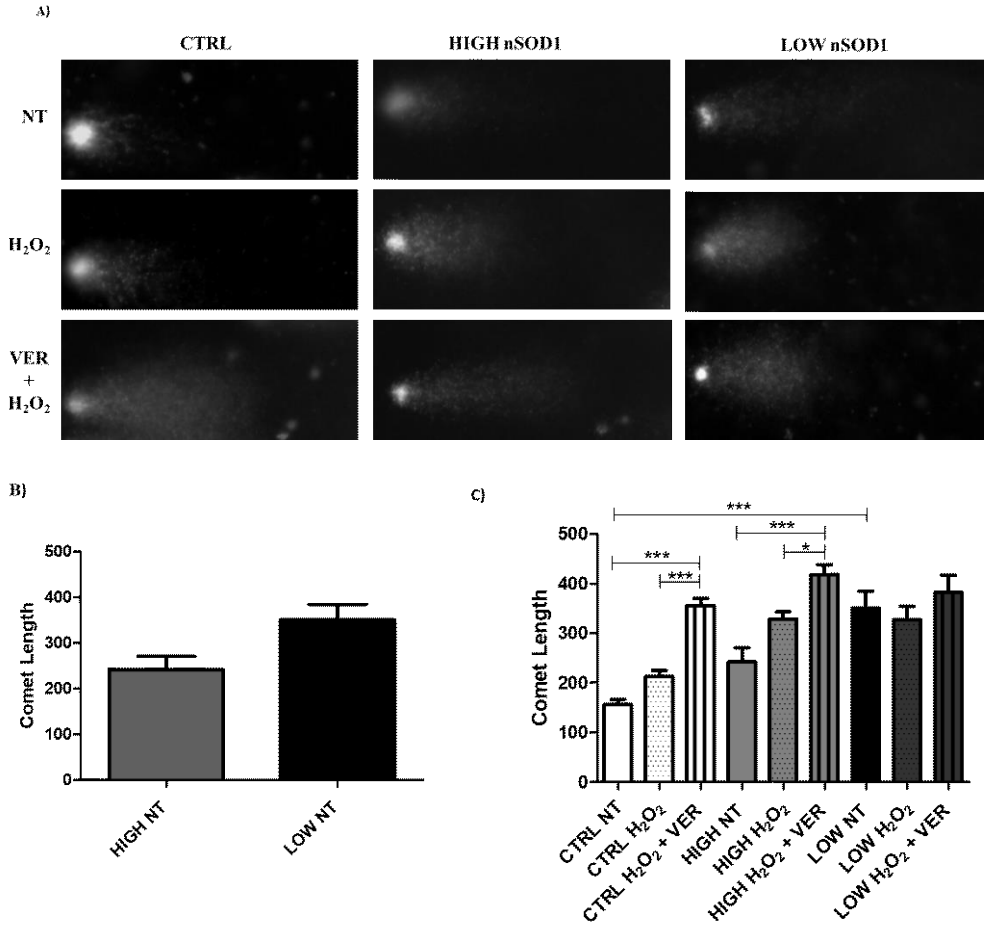

Figure 33. HSP70 is involved in DNA damage protection in PBMCs of sALS patients. A) Protective role of nuclear SOD1 against DNA damage in PBMCs. Controls, High and Low nSOD1 PBMCs underwent basal evaluation (NT; Not Treated), or H_2O_2 (5'; 500 μM) treatment followed by recovery or H_2O_2 (5'; 500 μM) + VER (1h; 50 μM) treatment followed by recovery. B) Comet assay quantification by comet length. Data were analyzed by unpaired t test (p value=0.063). An increased comet length, indicating DNA damage, was observed in basal conditions in patients with Low nSOD1compared to High nSOD1 patients. C) Comet assay quantification by comet length. Data were analyzed by ANOVA (n = 3) followed by Bonferroni post-test. * $p < 0.05$ and *** $p < 0.001$. An increased comet length, indicating DNA damage, was observed in basal conditions in patients with Low nSOD1compared to controls. Treatment with H_2O_2 (5'; 500 μM) + VER (1h; 50 μM) visibly increased DNA damage compared to both basal conditions cells and cells treated with H_2O_2 (5'; 500 μM) only in healthy controls. In High nSOD1 patients, no significant variation was highlighted comparing basal cells and cells treated with H_2O_2 (5'; 500 μM), meaning that upregulation of HSP70 restored normal DNA repair during recovery phase. Inhibition of H_2O_2 (5'; 500 μM) with VER (1h;

50 μM) prevented the re-establishment of this mechanism. In the end, in Low nSOD1 PBMCs no significant variation was observed in terms of comet length.

7. DISCUSSION

The complete biological context of disease pathogenesis can be investigated thanks to transcriptome analysis that allows the study of gene expression profile. Moreover, regulatory ncRNAs have been studied because of their involvement in onset of several diseases, such as cancer and neurodegenerative disorders. Hence, we conducted a profiling study of lncRNAs and mRNAs in human PBMCs from sALS patients, AD patients, PD patients, and healthy controls exploiting RNA-Sequencing technique, with the aim of understanding effects of these molecules on the pathogenesis of these diseases. The deep screening of transcripts in sALS, AD and PD patients allowed us to both highlight transcriptome alterations due to the pathological condition and to assess whether a shared deregulation was present in coding/noncoding RNAs.

No common DE genes emerged in the three cohorts of patients. Nonetheless, we found shared feature related to KEGG and GO terms that were reported for sALS and AD, but not in PD patients where the low number of DE genes impeded the enrichment analysis.

“Dilated cardiomyopathy”, “complement and coagulation cascade” and “fluid shear stress” are the deregulated pathways in sALS and AD patients that emerged through KEGG analysis. Genes related to these pathways are not the same for the two disease and moreover, in sALS they are both up- and downregulated, while in AD only downregulated. The same happens also for GO analysis, where the enrichment of “cellular response to reactive oxygen species” and “protein localization to cell surface” were observed. Again, response to ROS in only enriched by two genes upregulated and one downregulated in sALS.

No overlapping terms were found between and the two other pathologies. Nevertheless, when consulting KEGG pathways related to AD downregulated DE RNAs, the term “Parkinson’s disease” aroused. In fact, one of the downregulated genes in AD was NDUFV2, previously described as a genetic variation promoting a mild form of Parkinsonism with a similar prognosis to idiopathic PD [205].

Pathways resulted from KEGG analysis of sALS and AD DE genes are highly relevant for neurodegeneration pathophysiology. Indeed, heart failure in both AD, because of Aβ amyloid accumulation in the heart [206], and ALS, because of sympathetic hyperactivity that leads to cardiac death [207] are pertinent with the term “dilated cardiomyopathy” resulting from enrichment analysis. Also, “complement and coagulation cascades” emerged from DE genes in both groups of patients. A tight balance between protective and toxic effect is crucial to regulate these cascades. In fact, the signaling of these processes might be compromised promoting cellular damage [208] when subjected to

molecular stress typical of neurodegeneration. Finally, "cellular response to reactive oxygen species" resulted from cellular processes in GO analysis. This outcome is highly relevant in the context of neurodegenerative disease, since oxidative stress is one of the most investigated molecular alterations that affect patients affected by neurodegeneration [209, 210].

Interestingly, we found a very small number of DE genes in PD patients' PBMCs. The deregulation of noncoding genes in CNS of patients suffering from these disease has been reported [211]. However, despite being present in peripheral blood, the expression of these molecules is not altered when compared to healthy controls [212, 213]. Only 5 genes were DE in our cohort. One of them was TBC1D3, we found it downregulated in our analysis and it is not associated to any typical PD molecular alteration. Nonetheless, it has been reported as a promoter of basal neural progenitors generation, and as inductor of cortical folding in mice [197]. We found an independently transcribed lincRNA as upregulated, which is SCARNA2 (small Cajal body-specific RNA 2) [214]. Two other ncRNAs were found downregulated, namely RP1-29C18.9 and RP1-29C18.8, but there is nothing reported in literature concerning their potential implication in PD.

We concluded that there is a different involvement of RNA metabolism in Alzheimer's disease, Amyotrophic Lateral Sclerosis and Parkinson's disease, because the differences in the amount of DE genes we found shows that a milder transcriptional machinery involvement is present in AD and PD compared to ALS. Despite this imbalance, some molecular features common amongst them are present.

Thus, considering the results we obtained, a more extensive study of coding and noncoding genes modulation was necessary for sALS patients, that is the group showing the greater number of DE genes.

In fact, after extending the cohort of these patients, we observed a further significance of gene expression alteration in ALS. A total of 123 DE genes was found and two different gene expression patterns resulted for sALS and healthy controls.

Based on our previous reports [95, 96], sALS patients can be classified into two groups based on the expression levels of nuclear SOD1[95, 96]: High nSOD1 and Low nSOD1. To further explore the molecular alterations that distinguish the two sALS subgroups and dissect the potential divergence at gene expression level, we performed a transcriptome profiling with differential gene expression analysis in PBMCs of these two sALS groups and matched healthy controls.

Our results clearly indicate a distance in the gene expression patterns between all sALS individuals and controls, confirming the implication of sALS disease on RNA metabolism [110]. Nevertheless, we have also shown that the RNA expression profile of High nSOD1 patients is more similar to the one of healthy controls, compared to the Low nSOD1 subgroup. Moreover, it is remarkable that despite of being patients affected

by the same disease, we found only one common deregulated gene in PBMCs among the two groups, the antisense lncRNA MGC16275. This lncRNA is still uncharacterized and has been found to be broadly expressed in many tissues with relevance in the brain and by an integration study of transcriptomics and antibody-based proteomics [215]**.** We observed a greater number of DE genes in Low nSOD1 group, this may be explained by the poor presence of SOD1 in the nucleus and by the weak methylation we observed on H3, marker of loss of transcription suppression [199].

These data are consistent with our previous studies demonstrating molecular differences among the two patients' subgroups [95, 96]. This is also supported by the greater number of dysregulated coding and non-coding transcripts that were found in Low nSOD1 cells, indicating more dysregulated cellular processes in these patients.

For better understanding the transcriptomic-phenotypic relation that may exists in ALS, we evaluated the concentration of nSOD1 in patients with their age or sex and we demonstrated that nSOD1 decreases with ageing, while sex does not seem to affect protein behavior.

Since SOD1 may act as a protective protein in the nucleus by preventing DNA damage [216] we have investigated the profiles of genes involved in DNA repair processes in the two subgroups of patients. Gene database/literature research was performed, and we reported 6 genes implicated in genomic stability maintenance (Table 13). KDM4C and TP53TG3D were found upregulated in Low nSOD1group. The former is not directly involved in DNA integrity maintenance, but its expression is induced by p53, a central player in cellular DNA damage responses [217]. KDM4C has been found associated with chromatin during mitosis. This association is accompanied by a decrease in the mitotic levels of H3K9me3. Moreover, an research work showed its implication in cell senescence [218, 219]. In High nSOD1 group, the genes related to DNA damage and repair mechanisms found upregulated were 4. The most upregulated were HSPA1A and HSPA1B, both belonging to HSP70 family. These heat shock proteins, known for their role in the maintenance of protein homeostasis [220], are also induced in response to DNA-damaging agents, facilitating DNA repair [221, 222]. Also, in High nSOD1 group FILIP1L resulted upregulated. This is a gene that shares similarities to bacterial SbcC ATPase DNA repair protein [223]. The expression of FILIP1L is dependent of ATM/ATR [224] found activated in SH-SY5Y exposed to oxidative stress [96]. The fourth gene found upregulated in this group was PTGFRN. It has been demonstrated that the downregulation of this gene leads to reduced DNA-damage sensing [225]. These results suggest that patients with higher concentration of nSOD1 show an enhanced activation of genes involved in DNA integrity maintenance, corroborating our previous study demonstrating a higher damaged DNA in Low nSOD1 patients.

Interestingly, HSPA1A, is overexpressed in High nSOD1 patients. HSPA1A folding activity can be regulated by other chaperones that also act as nucleotide-exchange factors such as HSPH1, HSPH2, HSPH3 [226]. Notably, in High nSOD1 samples we have further detected the upregulation of HSPH1 mRNA, and moreover, we also confirmed HSP70 and HSPH1 proteins upregulation. In Low nSOD1 group, we did not detect any alteration in the expression of HSPA1A, HSPH1 or any other heat shock protein transcripts levels. Several studies have additionally addressed the HSPs direct involvement in the DNA-damage response [221, 227, 228]. They can regulate DNA repair signaling pathways and are required to stabilize core components of DNA repair mechanisms. Altered expression levels of HSPs could lead to impaired DNA damage detection as well as delayed repair [229]. HSP70s, which include HSPA1A and HSPA1B, strongly accumulate in the nucleus upon formation of DNA single strand breaks caused by metabolic reactive oxygen species production. As whole these observations strongly support our hypothesis that high levels of nSOD1 can modulate the activity of factors involved in DNA damage protection. In fact, we demonstrated that upon oxidative stress only healthy controls and High nSOD1 cells were able to restore DNA integrity. However, when we inhibited the activity of HSP70s, DNA damage was increased in controls and in High nSOD1 PBMCs.

The detection of altered S100B transcript levels in PBMCs of Low nSOD1 patients might explain their worse prognosis. In fact, S100B is a Ca^{2+} binding protein involved in a vast number of intracellular and extracellular effects in the brain [201]. It is passively released from damaged and/or necrotic cells and it increases oxidative stress through binding to RAGE (receptor for advanced glycation end products) [201]. It has already been demonstrated that both human and mouse ALS spinal cord tissues display increased transcript and protein levels of both RAGE and S100B [202]. Our results indicate that S100B transcript upregulation is solely present in Low nSOD1 PBMCs and thus it might therefore exert its toxic activity on cell survival and aggravate the ALS pathology exclusively in this subgroup.

Epigenetic modifications and resulting effects on gene expression regulation factors are crucial for neuronal populations integrity, as demonstrated for repressor element 1-silencing transcription factor (REST) in ageing [230]. We observed a strong difference of gene expression in the two sALS subgroups. Thus, we also evaluated the amount of H3K27me3, an important marker of gene expression repression [199]. In fact, in High nSOD1 PBMCs, tri-methylation is greater than Low nSOD1 group, in accordance with the lower number of DE genes found in these patients. In Low nSOD1 group, the tri-methylation is much lower, partially explaining the higher number of DE genes emerged from our analysis. However, H3K27me3 is not the specific substrate of KDM4C [231], which was upregulated in Low nSOD1 patients. The data related to histone methylation need to be further evaluated to highlight the effect of SOD1 sub-cellular localization on epigenetic modifications. In fact, these modifications could be affected by nSOD1,

responsible of maintaining intact the state of chromatin and its epigenetic features. When nSOD1 is low, the balance is lost, and a strong deregulation is observed.

In conclusion, this thesis highlights how High nSOD1 levels activates HSP70 family genes able to positively affect survival and adversely Low nSOD1 levels influence cell viability in PBMCs of sALS patients. This could possibly explain the differences in disease severity and duration observed in the two patients' sub-groups. Further investigations are needed to better corroborate the proposed mechanism, its cellular implications and regulation. Moreover, our findings could suggest these genes as potential future targets for ALS treatment.

8. REFERENCES

1. Liscic RM, Breljak D. Molecular basis of amyotrophic lateral sclerosis. Prog Neuro-Psychopharmacology Biol Psychiatry. 2011;35:370–2.

2. Mejzini R, Flynn LL, Pitout IL, Fletcher S, Wilton SD, Akkari PA. ALS Genetics, Mechanisms, and Therapeutics: Where Are We Now? Frontiers in Neuroscience. 2019;13.

3. Katz JS, Dimachkie MM, Barohn RJ. Amyotrophic Lateral Sclerosis: A Historical Perspective. Neurologic Clinics. 2015;33:727–34.

4. Rowland LP. How Amyotrophic Lateral Sclerosis Got Its Name The Clinical-Pathologic Genius of Jean-Martin Charcot. https://jamanetwork.com/.

5. Gordon PH. Amyotrophic lateral sclerosis: An update for 2013 clinical features, pathophysiology, management and therapeutic trials. Aging and Disease. 2013;4:295–310.

6. Shellikeri S, Karthikeyan V, Martino R, Black SE, Zinman L, Keith J, et al. The neuropathological signature of bulbar-onset ALS: A systematic review. Neuroscience and Biobehavioral Reviews. 2017;75:378–92.

7. Pasinelli P, Brown RH. Molecular biology of amyotrophic lateral sclerosis: Insights from genetics. Nature Reviews Neuroscience. 2006;7:710–23.

8. Ingre C, Roos PM, Piehl F, Kamel F, Fang F. Risk factors for amyotrophic lateral sclerosis. Clin Epidemiol. 2015;7:181–93.

9. Safety and efficacy of edaravone in well defined patients with amyotrophic lateral sclerosis: a randomised, double-blind, placebo-controlled trial. Lancet Neurol. 2017;16:505–12.

10. Mejzini R, Flynn LL, Pitout IL, Fletcher S, Wilton SD, Akkari PA. ALS Genetics , Mechanisms , and Therapeutics : Where Are We Now ? 2019;13 December:1–27.

11. van Es MA, Hardiman O, Chio A, Al-Chalabi A, Pasterkamp RJ, Veldink JH, et al. Amyotrophic lateral sclerosis. Lancet (London, England). 2017;390:2084–98.

12. Logroscino G, Piccininni M. Amyotrophic lateral sclerosis descriptive epidemiology: The origin of geographic difference. Neuroepidemiology. 2019;52:93–103.

13. Al-Chalabi A, Hardiman O. The epidemiology of ALS: A conspiracy of genes, environment and time. Nature Reviews Neurology. 2013;9:617–28.

14. Oskarsson B, Gendron TF, Staff NP. Amyotrophic Lateral Sclerosis: An Update for 2018. Mayo Clinic Proceedings. 2018;93:1617–28.

15. Robberecht W, Philips T. The changing scene of amyotrophic lateral sclerosis. Nat Rev Neurosci. 2013;14:248–64.

16. Rosen DR, Siddique T, Patterson D, Figlewicz DA, Sapp P, Hentati A, et al. Mutations in Cu/Zn superoxide dismutase gene are associated with familial amyotrophic lateral sclerosis. Nature. 1993;362:59–62.

17. Mathis S, Goizet C, Soulages A, Vallat JM, Masson G Le. Genetics of amyotrophic lateral sclerosis: A review. J Neurol Sci. 2019;399 February:217–26.

18. Kirby J, Al Sultan A, Waller R, Heath P. The genetics of amyotrophic lateral sclerosis: current insights. Degener Neurol Neuromuscul Dis. 2016;:49.

19. Corcia P, Couratier P, Blasco H, Andres CR, Beltran S, Meininger V, et al. Genetics of amyotrophic lateral sclerosis. Revue Neurologique. 2017;173:254–62.

20. Zarei S, Carr K, Reiley L, Diaz K, Guerra O, Altamirano PF, et al. A comprehensive review of amyotrophic lateral sclerosis. Surg Neurol Int. 2015;6:171.

21. Chou C-C, Zhang Y, Umoh ME, Vaughan SW, Lorenzini I, Liu F, et al. TDP-43 pathology disrupts nuclear pore complexes and nucleocytoplasmic transport in ALS/FTD. Nat Neurosci. 2018;21:228–39.

22. Kok JR, Palminha NM, Dos Santos Souza C, El-Khamisy SF, Ferraiuolo L. DNA damage as a mechanism of neurodegeneration in ALS and a contributor to astrocyte toxicity. Cell Mol Life Sci. 2021.

23. Kruman II, Pedersen WA, Springer JE, Mattson MP. ALS-linked Cu/Zn-SOD mutation increases vulnerability of motor neurons to excitotoxicity by a mechanism involving increased oxidative stress and perturbed calcium homeostasis. Exp Neurol. 1999;160:28–39.

24. Blokhuis AM, Groen EJN, Koppers M, Van Den Berg LH, Pasterkamp RJ. Protein aggregation in amyotrophic lateral sclerosis. Acta Neuropathologica. 2013;125:777–94.

25. Basso M, Samengo G, Nardo G, Massignan T, D'Alessandro G, Tartari S, et al. Characterization of detergent-insoluble proteins in ALS indicates a causal link between nitrative stress and aggregation in pathogenesis. PLoS One. 2009;4.

26. Ciechanover A, Kwon YT a. Degradation of misfolded proteins in neurodegenerative

diseases: therapeutic targets and strategies. Experimental & molecular medicine. 2015;47:e147.

27. Wijesekera LC, Leigh PN. Amyotrophic lateral sclerosis. Orphanet J Rare Dis. 2009;4.

28. Osellame LD, Blacker TS, Duchen MR. Cellular and molecular mechanisms of mitochondrial function. Best Pract Res Clin Endocrinol Metab. 2012;26:711–23.

29. Faes L, Callewaert G. Mitochondrial dysfunction in familial amyotrophic lateral sclerosis. Journal of Bioenergetics and Biomembranes. 2011;43:587–92.

30. Fujita K, Yamauchi M, Shibayama K, Ando M, Honda M, Nagata Y. Decreased cytochrome c oxidase activity but unchanged superoxide dismutase and glutathione peroxidase activities in the spinal cords of patients with amyotrophic lateral sclerosis. J Neurosci Res. 1996;45:276–81.

31. Bowling AC, Schulz JB, Brown RH, Flint Beal M. Rapid Communication Superoxide Dismutase Activity, Oxidative Damage, and Mitochondria1 Energy Metabolism in Familial and Sporadic Amyotrophic Lateral Sclerosis.

32. Goldsteins G, Keksa-Goldsteine V, Ahtoniemi T, Jaronen M, Arens E, Åkerman K, et al. Deleterious role of superoxide dismutase in the mitochondrial intermembrane space. J Biol Chem. 2008;283:8446–52.

33. Jaiswal MK, Keller BU. Cu/Zn superoxide dismutase typical for familial amyotrophic lateral sclerosis increases the vulnerability of mitochondria and perturbs Ca 2+ Homeostasis in SOD1G93A mice. Mol Pharmacol. 2009;75:478–89.

34. Browne SE, Yang L, DiMauro JP, Fuller SW, Licata SC, Beal MF. Bioenergetic abnormalities in discrete cerebral motor pathways presage spinal cord pathology in the G93A SOD1 mouse model of ALS. Neurobiol Dis. 2006;22:599–610.

35. Dupuis L, Gonzalez De Aguilar JL, Oudart H, De Tapia M, Barbeito L, Loeffler JP. Mitochondria in amyotrophic lateral sclerosis: A trigger and a target. Neurodegenerative Diseases. 2004;1:245–54.

36. Heath PR, Shaw PJ. Update on the glutamatergic neurotransmitter system and the role of excitotoxicity in amyotrophic lateral sclerosis. Muscle and Nerve. 2002;26:438–58.

37. Eisen A. Amyotrophic lateral sclerosis-evolutionary and other perspectives. Muscle and Nerve. 2009;40:297–304.

38. King AE, Woodhouse A, Kirkcaldie MTK, Vickers JC. Excitotoxicity in ALS:

Overstimulation, or overreaction? Experimental Neurology. 2016;275:162–71.

39. Shaw, al. CSF and Plasma Amino Acid Levels in Motor Neuron Disease: Elevation of CSF Glutamate in a Subset of Patients. 1995.

40. Bogaert E, D'ydewalle C, Van L, Bosch D. Amyotrophic Lateral Sclerosis and Excitotoxicity: From Pathological Mechanism to Therapeutic Target. 2010.

41. Grosskreutz J, Haastert K, Dewil M, Van Damme P, Callewaert G, Robberecht W, et al. Role of mitochondria in kainate-induced fast Ca2+ transients in cultured spinal motor neurons. Cell Calcium. 2007;42:59–69.

42. Martin LJ. Biology of mitochondria in neurodegenerative diseases. In: Progress in Molecular Biology and Translational Science. Elsevier B.V.; 2012. p. 355–415.

43. Tortarolo M, Grignaschi G, Calvaresi N, Zennaro E, Spaltro G, Colovic M, et al. Glutamate AMPA receptors change in motor neurons of SOD1G93A transgenic mice and their inhibition by a noncompetitive antagonist ameliorates the progression of amytrophic lateral sclerosis-like disease. J Neurosci Res. 2006;83:134–46.

44. Kawahara Y, Ito K, Sun H, Aizawa H, Kanazawa I, Kwak S. Glutamate receptors: RNA editing and death of motor neurons. Nature. 2004;427:801.

45. Milanese M, Zappettini S, Onofri F, Musazzi L, Tardito D, Bonifacino T, et al. Abnormal exocytotic release of glutamate in a mouse model of amyotrophic lateral sclerosis. J Neurochem. 2011;116:1028–42.

46. Bonifacino T, Musazzi L, Milanese M, Seguini M, Marte A, Gallia E, et al. Altered mechanisms underlying the abnormal glutamate release in amyotrophic lateral sclerosis at a pre-symptomatic stage of the disease. Neurobiol Dis. 2016;95:122–33.

47. Fray AE, Ince PG, Banner SJ, Milton ID, Usher PA, Cookson MR, et al. The expression of the glial glutamate transporter protein EAAT2 in motor neuron disease: An immunohistochemical study. Eur J Neurosci. 1998;10:2481–9.

48. Boehmer C, Palmada M, Rajamanickam J, Schniepp R, Amara S, Lang F. Post-translational regulation of EAAT2 function by co-expressed ubiquitin ligase Nedd4-2 is impacted by SGK kinases. J Neurochem. 2006;97:911–21.

49. Lin CG, Bristol LA, Jin L, Dykes-hoberg M, Crawford T, Clawson L, et al. Aberrant RNA Processing in a Neurodegenerative Disease : the Cause for Absent EAAT2 , a Glutamate Transporter , in Amyotrophic Lateral Sclerosis. 1998;20:589–602.

50. Rao SD, Yin HZ, Weiss JH. Disruption of Glial Glutamate Transport by Reactive Oxygen Species Produced in Motor Neurons. 2003;23:2627–33.

51. Dewil PVDM, Bosch WRL Van Den. Excitotoxicity and Amyotrophic Lateral. 2005;:147–59.

52. Ii JAW, Banerjee R, Gunawardena S. Axonal Transport and Neurodegeneration : How Marine Drugs Can Be Used for the Development of Therapeutics. 2016.

53. Hirata H, Hinoda Y, Shahryari V, Deng G, Tanaka Y, Tabatabai ZL, et al. Genistein downregulates onco-miR-1260b and upregulates sFRP1 and Smad4 via demethylation and histone modification in prostate cancer cells. Br J Cancer. 2014;110:1645–54.

54. Corbo M, Hays AP. Peripherin and neurofilament protein coexist in spinal spheroids of motor neuron disease. J Neuropathol Exp Neurol. 1992;51:531–7.

55. Williamson TL, Cleveland DW. Slowing of axonal transport is a very early event in the toxicity of ALS-linked SOD1 mutants to motor neurons. 1999;2.

56. Zhang B, Tu P, Abtahian F, Trojanowski JQ, Lee VM. Neurofilaments and Orthograde Transport Are Reduced in Ventral Root Axons of Transgenic Mice that Express Human SOD1 with a G93A Mutation. 1997;139:1307–15.

57. Vos KJ De, Hafezparast M. Neurobiology of Disease Neurobiology of axonal transport defects in motor neuron diseases : Opportunities for translational research ? Neurobiol Dis. 2017. doi:10.1016/j.nbd.2017.02.004.

58. Letournel F, Bocquet A, Dubas F, Barthelaix A, Eyer J. Stable Tubule Only Polypeptides (STOP) Proteins Co-Aggregate with Spheroid Neurofilaments in Amyotrophic Lateral Sclerosis. 2003. https://academic.oup.com/jnen/article/62/12/1211/2609953.

59. Morfini GA, Bosco DA, Brown H, Gatto R, Kaminska A, Song Y, et al. Inhibition of Fast Axonal Transport by Pathogenic SOD1 Involves Activation of p38 MAP Kinase. PLoS One. 2013;8.

60. Liu J, Wang F. Role of neuroinflammation in amyotrophic lateral sclerosis: Cellular mechanisms and therapeutic implications. Frontiers in Immunology. 2017;8 AUG.

61. Roberts K, Zeineddine R, Corcoran L, Li WEN, Campbell IL, Yerbury JJ. Extracellular Aggregated Cu / Zn Superoxide Dismutase Activates Microglia to Give a Cytotoxic Phenotype. 2013;419 December 2012:409–19.

62. Volonté C, Apolloni S, Parisi C, Amadio S. Purinergic contribution to amyotrophic lateral sclerosis. Neuropharmacology. 2016;104:180–93.

63. Appel SH, Zhao W, Beers DR, Henkel JS, Askanas DV, Engel K. The Microglial-Motoneuron dialogue in ALS. 2011;:4–8.

64. Nagai M, Re DB, Nagata T, Chalazonitis A, Jessell TM, Wichterle H, et al. Astrocytes expressing ALS-linked mutated SOD1 release factors selectively toxic to motor neurons. Nat Neurosci. 2007;10:615–22.

65. Damme P Van, Bogaert E, Dewil M, Hersmus N, Kiraly D, Scheveneels W, et al. Astrocytes regulate GluR2 expression in motor neurons and their vulnerability to excitotoxicity. 2007. www.pnas.orgcgidoi10.1073pnas.0705046104.

66. Hensley K, Abdel-Moaty H, Hunter J, Mhatre M, Mhou S, Nguyen K, et al. Primary glia expressing the G93A-SOD1 mutation present a neuroinflammatory phenotype and provide a cellular system for studies of glial inflammation. J Neuroinflammation. 2006;3.

67. Beers DR, Henkel JS, Zhao W, Wang J, Appel SH. CD4 ⁺ T cells support glial neuroprotection , slow disease progression , and modify glial morphology in an animal model of inherited ALS. 2008.

68. Pollari E, Goldsteins G, Bart G, Koistinaho J, Giniatullin R. The role of oxidative stress in degeneration of the neuromuscular junction in amyotrophic lateral sclerosis. Frontiers in Cellular Neuroscience. 2014;8 MAY.

69. Lee Y, Morrison BM, Li Y, Lengacher S, Farah MH, Hoffman PN, et al. Oligodendroglia metabolically support axons and contribute to neurodegeneration. Nature. 2012;487:443–8.

70. Kim HJ, Taylor JP. Lost in Transportation: Nucleocytoplasmic Transport Defects in ALS and Other Neurodegenerative Diseases. Neuron. 2017;96:285–97.

71. Blokhuis AM, Groen EJN, Koppers M, Berg LH Van Den, Pasterkamp RJ. Protein aggregation in amyotrophic lateral sclerosis. 2013;:777–94.

72. Kitamura A, Yuno S, Muto H, Kinjo M. Different aggregation states of a nuclear localization signal-tagged 25-kDa C-terminal fragment of TAR RNA/DNA-binding protein 43 kDa. Genes Cells. 2017;22:521–34.

73. Penndorf D, Witte OW, Kretz A. DNA plasticity and damage in amyotrophic lateral sclerosis. Neural Regeneration Research. 2018;13:173–80.

74. Abugable AA, Morris JLM, Palminha NM, Zaksauskaite R. DNA repair and neurological disease : From molecular understanding to the development of diagnostics and model organisms ☆ , ☆☆. DNA Repair (Amst). 2019;81 July:102669. doi:10.1016/j.dnarep.2019.102669.

75. Niedzielska E, Smaga I, Gawlik M, Moniczewski A, Stankowicz P, Pera J, et al. Oxidative Stress in Neurodegenerative Diseases. Molecular Neurobiology.

2016;53:4094–125.

76. Bell KFS. Insight into a neuron's preferential susceptibility to oxidative stress. In: Biochemical Society Transactions. 2013. p. 1541–5.

77. Zheng M, Storz G. Redox sensing by prokaryotic transcription factors. Biochem Pharmacol. 2000;59:1–6.

78. Halliwell B. Role of Free Radicals in the Neurodegenerative Diseases Therapeutic Implications for Antioxidant Treatment.

79. Essa MM. The Benefits of Natural Products for Neurodegenerative Diseases.

80. Cobley JN, Fiorello ML, Bailey DM. 13 reasons why the brain is susceptible to oxidative stress. Redox Biology. 2018;15:490–503.

81. Contestabile A. Oxidative Stress in Neurodegeneration: Mechanisms and Therapeutic Perspectives. 2001.

82. Méndez-Armenta M, Nava-Ruíz C, Juárez-Rebollar D, Rodríguez-Martínez E, Yescas Gómez P. Oxidative stress associated with neuronal apoptosis in experimental models of epilepsy. Oxidative Medicine and Cellular Longevity. 2014;2014.

83. Halliwell B. Role of Free Radicals in the Neurodegenerative Diseases Therapeutic Implications for Antioxidant Treatment. 2001;18:685–716.

84. Andersen JK. Oxidative stress in neurodegeneration: Cause or consequence? Nat Rev Neurosci. 2004;10:S18.

85. Ren X, Zou L, Zhang X, Branco V, Wang J, Carvalho C, et al. Redox Signaling Mediated by Thioredoxin and Glutathione Systems in the Central Nervous System. Antioxidants and Redox Signaling. 2017;27:989–1010.

86. Smith T, Heger A, Sudbery I. UMI-tools: Modeling sequencing errors in Unique Molecular Identifiers to improve quantification accuracy. Genome Res. 2017;27:491–9.

87. Bozzo F, Mirra A, Carrì MT. Oxidative stress and mitochondrial damage in the pathogenesis of ALS: New perspectives. Neuroscience Letters. 2017;636:3–8.

88. Carrì MT, Valle C, Bozzo F, Cozzolino M. Oxidative stress and mitochondrial damage: Importance in non-SOD1 ALS. Frontiers in Cellular Neuroscience. 2015;9 FEB.

89. Saccon RA, Bunton-Stasyshyn RKA, Fisher EMC, Fratta P. Is SOD1 loss of function involved in amyotrophic lateral sclerosis? Brain. 2013;136:2342–58.

90. Gruzman A, Wood WL, Alpert E, Dharma Prasad M, Miller RG, Rothstein JD, et al. Common molecular signature in SOD1 for both sporadic and familial amyotrophic lateral sclerosis. 2007. www.pnas.org/cgi/content/full/.

91. Ezzi SA, Urushitani M, Julien JP. Wild-type superoxide dismutase acquires binding and toxic properties of ALS-linked mutant forms through oxidation. J Neurochem. 2007;102:170–8.

92. Paré B, Lehmann M, Beaudin M, Nordström U, Saikali S, Julien JP, et al. Misfolded SOD1 pathology in sporadic Amyotrophic Lateral Sclerosis. Sci Rep. 2018;8.

93. Gagliardi S, Cova E, Davin A, Guareschi S, Abel K, Alvisi E, et al. SOD1 mRNA expression in sporadic amyotrophic lateral sclerosis. Neurobiol Dis. 2010;39:198–203.

94. Cova E, Cereda C, Galli A, Curti D, Finotti C, Di Poto C, et al. Modified expression of Bcl-2 and SOD1 proteins in lymphocytes from sporadic ALS patients. Neurosci Lett. 2006;399:186–90.

95. Cereda C, Leoni E, Milani P, Pansarasa O, Mazzini G, Guareschi S, et al. Altered Intracellular Localization of SOD1 in Leukocytes from Patients with Sporadic Amyotrophic Lateral Sclerosis. PLoS One. 2013;8.

96. Bordoni M, Pansarasa O, Dell'Orco M, Crippa V, Gagliardi S, Sproviero D, et al. Nuclear Phospho-SOD1 Protects DNA from Oxidative Stress Damage in Amyotrophic Lateral Sclerosis. J Clin Med. 2019;8:729.

97. Tsang CK wa., Liu Y, Thomas J, Zhang Y, Zheng XFS. Superoxide dismutase 1 acts as a nuclear transcription factor to regulate oxidative stress resistance. Nat Commun. 2014;5:3446.

98. Alsultan AA, Waller R, Heath PR, Kirby J. The genetics of amyotrophic lateral sclerosis: current insights. Degener Neurol Neuromuscul Dis. 2016;6:49–64.

99. Kim HJ, Taylor JP. Lost in Transportation: Nucleocytoplasmic Transport Defects in ALS and Other Neurodegenerative Diseases. Neuron. 2017;96:285–97.

100. Jeong YH, Ling JP, Lin SZ, Donde AN, Braunstein KE, Majounie E, et al. Tdp-43 cryptic exons are highly variable between cell types. Mol Neurodegener. 2017;12.

101. Polymenidou M, Lagier-Tourenne C, Hutt KR, Huelga SC, Moran J, Liang TY, et al. Long pre-mRNA depletion and RNA missplicing contribute to neuronal vulnerability from loss of TDP-43. Nat Neurosci. 2011;14:459–68.

102. Freibaum BD, Chitta RK, High AA, Taylor JP. Global Analysis of TDP-43 Interacting Proteins Reveals Strong Association with RNA Splicing and Translation

Machinery research articles. 2010;:1104–20.

103. Gopal PP, Nirschl JJ, Klinman E, Holzbaurb ELF. Amyotrophic lateral sclerosis-linked mutations increase the viscosity of liquid-like TDP-43 RNP granules in neurons. Proc Natl Acad Sci U S A. 2017;114:E2466–75.

104. Birsa N, Bentham MP, Fratta P. Cytoplasmic functions of TDP-43 and FUS and their role in ALS. Seminars in Cell and Developmental Biology. 2020;99:193–201.

105. Ling S-C, Polymenidou M, Cleveland DW. Converging mechanisms in ALS and FTD: disrupted RNA and protein homeostasis. Neuron. 2013;79:416–38.

106. Bosco DA, Lemay N, Ko HK, Zhou H, Burke C, Kwiatkowski TJ, et al. Mutant FUS proteins that cause amyotrophic lateral sclerosis incorporate into stress granules. Hum Mol Genet. 2010;19:4160–75.

107. Kapeli K, Pratt GA, Vu AQ, Hutt KR, Martinez FJ, Sundararaman B, et al. Distinct and shared functions of ALS-associated proteins TDP-43, FUS and TAF15 revealed by multisystem analyses. Nat Commun. 2016;7.

108. Kamelgarn M, Chen J, Kuang L, Jin H, Kasarskis EJ, Zhu H. ALS mutations of FUS suppress protein translation and disrupt the regulation of nonsense-mediated decay. Proc Natl Acad Sci U S A. 2018;115:E11904–13.

109. Butti Z, Patten SA. RNA dysregulation in amyotrophic lateral sclerosis. Frontiers in Genetics. 2019;10 JAN.

110. Gagliardi S, Zucca S, Pandini C, Diamanti L, Bordoni M, Sproviero D, et al. Long non-coding and coding RNAs characterization in Peripheral Blood Mononuclear Cells and Spinal Cord from Amyotrophic Lateral Sclerosis patients. Sci Rep. 2018;8.

111. D'Erchia AM, Gallo A, Manzari C, Raho S, Horner DS, Chiara M, et al. Massive transcriptome sequencing of human spinal cord tissues provides new insights into motor neuron degeneration in ALS. Sci Rep. 2017;7.

112. Halliday G, Bigio EH, Cairns NJ, Neumann M, Mackenzie IRA, Mann DMA. Mechanisms of disease in frontotemporal lobar degeneration: gain of function versus loss of function effects. Acta Neuropathol. 2012;124:373–82.

113. Belzil V V, Gendron TF, Petrucelli L. RNA-mediated toxicity in neurodegenerative disease. Mol Cell Neurosci. 2013;56:406–19.

114. Bentmann E, Haass C, Dormann D. Stress granules in neurodegeneration--lessons learnt from TAR DNA binding protein of 43 kDa and fused in sarcoma. FEBS J. 2013;280:4348–70.

115. Ling SC, Polymenidou M, Cleveland DW. Converging mechanisms in als and FTD: Disrupted RNA and protein homeostasis. Neuron. 2013;79:416–38.

116. Anderson P, Ivanov P. tRNA fragments in human health and disease. FEBS Lett. 2014;588:4297–304.

117. McKhann GM, Knopman DS, Chertkow H, Hyman BT, Jack CRJ, Kawas CH, et al. The diagnosis of dementia due to Alzheimer's disease: recommendations from the National Institute on Aging-Alzheimer's Association workgroups on diagnostic guidelines for Alzheimer's disease. Alzheimers Dement. 2011;7:263–9.

118. Masters CL, Bateman R, Blennow K, Rowe CC, Sperling RA, Cummings JL. Alzheimer's disease. Nat Rev Dis Prim. 2015;1:15056.

119. Dartigues JF. Alzheimer's disease: a global challenge for the 21st century. Lancet Neurol. 2009;8:1082–3.

120. Lobo A, Launer LJ, Fratiglioni L, Andersen K, Di Carlo A, Breteler MM, et al. Prevalence of dementia and major subtypes in Europe: A collaborative study of population-based cohorts. Neurologic Diseases in the Elderly Research Group. Neurology. 2000;54 11 Suppl 5:S4—9. http://intl.neurology.org/cgi/content/full/54/11_suppl_5/S4.

121. Hendrie C, Hall S, Ph D, Hui SL, Unverzagt W, Rodenberg A, et al. Nigerian received accepted. :1485–92.

122. Chandra V, Ganguli M, Pandav R, Johnston J, Belle S, DeKosky ST. Prevalence of Alzheimer's disease and other dementias in rural India: the Indo-US study. Neurology. 1998;51:1000–8.

123. Ferri CP, Prince M, Brayne C, Brodaty H, Fratiglioni L, Ganguli M, et al. Global prevalence of dementia: a Delphi consensus study. Lancet (London, England). 2005;366:2112–7.

124. Mayeux R, Stern Y. Epidemiology of Alzheimer disease. Cold Spring Harb Perspect Med. 2012;2.

125. Goate A, Chartier-Harlin MC, Mullan M, Brown J, Crawford F, Fidani L, et al. Segregation of a missense mutation in the amyloid precursor protein gene with familial Alzheimer's disease. Nature. 1991;349:704–6.

126. Levy-Lahad E, Wasco W, Poorkaj P, Romano DM, Oshima J, Pettingell WH, et al. Candidate gene for the chromosome 1 familial Alzheimer's disease locus. Science. 1995;269:973–7.

127. Sherrington R, Froelich S, Sorbi S, Campion D, Chi H, Rogaeva EA, et al. Alzheimer's disease associated with mutations in presenilin 2 is rare and variably penetrant. Hum Mol Genet. 1996;5:985–8.

128. Carmona S, Hardy J, Guerreiro R, Lambert JC, Ibrahim-Verbaas CA, Harold D, et al. The genetics of Alzheimer disease. Science. 2001;148:569–74.

129. Annese A, Manzari C, Lionetti C, Picardi E, Horner DS, Chiara M, et al. Whole transcriptome profiling of Late-Onset Alzheimer's Disease patients provides insights into the molecular changes involved in the disease. Sci Rep. 2018;8:4282.

130. Giau V Van, Bagyinszky E, An SSA, Kim SY. Role of apolipoprotein E in neurodegenerative diseases. Neuropsychiatr Dis Treat. 2015;11:1723–37.

131. Han S, Miller JE, Byun S, Kim D, Risacher SL, Saykin AJ, et al. Identification of exon skipping events associated with Alzheimer's disease in the human hippocampus. BMC Med Genomics. 2019;12 Suppl 1:13.

132. Braggin JE, Bucks SA, Course MM, Smith CL, Sopher B, Osnis L, et al. Alternative splicing in a presenilin 2 variant associated with Alzheimer disease. Ann Clin Transl Neurol. 2019;6:762–77.

133. Ritter ML, Avila J, García-Escudero V, Hernández F, Pérez M. Frontotemporal Dementia-Associated N279K Tau Mutation Localizes at the Nuclear Compartment. Front Cell Neurosci. 2018;12:202. doi:10.3389/fncel.2018.00202.

134. Lacovich V, Espindola SL, Alloatti M, Pozo Devoto V, Cromberg LE, Čarná ME, et al. Tau Isoforms Imbalance Impairs the Axonal Transport of the Amyloid Precursor Protein in Human Neurons. J Neurosci. 2017;37:58–69.

135. Avramopoulos D, Szymanski M, Wang R, Bassett S. Gene expression reveals overlap between normal aging and Alzheimer's disease genes. Neurobiol Aging. 2011;32:2319.e27-34.

136. Antonell A, Lladó A, Altirriba J, Botta-Orfila T, Balasa M, Fernández M, et al. A preliminary study of the whole-genome expression profile of sporadic and monogenic early-onset Alzheimer's disease. Neurobiol Aging. 2013;34:1772–8.

137. Canchi S, Raao B, Masliah D, Rosenthal SB, Sasik R, Fisch KM, et al. Integrating Gene and Protein Expression Reveals Perturbed Functional Networks in Alzheimer's Disease. Cell Rep. 2019;28:1103—1116.e4. doi:10.1016/j.celrep.2019.06.073.

138. Morabito S, Miyoshi E, Michael N, Swarup V. Integrative genomics approach identifies conserved transcriptomic networks in Alzheimer's disease. Hum Mol Genet. 2020;29:2899–919.

139. Zhou X, Xu J. Identification of Alzheimer's disease-associated long noncoding RNAs. Neurobiol Aging. 2015;36:2925–31.

140. Liu T, Huang Y, Chen J, Chi H, Yu Z, Wang J, et al. Attenuated ability of BACE1 to cleave the amyloid precursor protein via silencing long noncoding RNA BACE1-AS expression. Mol Med Rep. 2014;10:1275–81.

141. Massone S, Ciarlo E, Vella S, Nizzari M, Florio T, Russo C, et al. NDM29, a RNA polymerase III-dependent non coding RNA, promotes amyloidogenic processing of APP and amyloid β secretion. Biochim Biophys Acta - Mol Cell Res. 2012;1823:1170–7. doi:10.1016/j.bbamcr.2012.05.001.

142. Li H, Zheng L, Jiang A, Mo Y, Gong Q. Identification of the biological affection of long noncoding RNA BC200 in Alzheimer's disease. Neuroreport. 2018;29:1061–7.

143. Bagyinszky E, Giau V Van, Shim K, Suk K, An SSA, Kim S. Role of inflammatory molecules in the Alzheimer's disease progression and diagnosis. J Neurol Sci. 2017;376:242–54.

144. Jost WH, Reichmann H. "An essay on the shaking palsy" 200 years old. J Neural Transm. 2017;124:899–900.

145. Shulman JM, De Jager PL, Feany MB. Parkinson's disease: Genetics and pathogenesis. Annu Rev Pathol Mech Dis. 2011;6:193–222.

146. Braak H, Del Tredici K, Rüb U, De Vos RAI, Jansen Steur ENH, Braak E. Staging of brain pathology related to sporadic Parkinson's disease. Neurobiol Aging. 2003;24:197–211.

147. Puschmann A. Monogenic Parkinson's disease and parkinsonism: Clinical phenotypes and frequencies of known mutations. Park Relat Disord. 2013;19:407–15. doi:10.1016/j.parkreldis.2013.01.020.

148. Kalia L V, Lang AE. Parkinson's disease. Lancet (London, England). 2015;386:896–912.

149. Bezard E, Przedborski S. A tale on animal models of Parkinson's disease. Mov Disord. 2011;26:993–1002.

150. Trancikova A, Mamais A, Webber PJ, Stafa K, Tsika E, Glauser L, et al. Phosphorylation of 4E-BP1 in the mammalian brain is not altered by LRRK2 expression or pathogenic mutations. PLoS One. 2012;7:e47784.

151. Liu S, Lu B. Reduction of protein translation and activation of autophagy protect against PINK1 pathogenesis in Drosophila melanogaster. PLoS Genet.

2010;6:e1001237.

152. Tatura R, Kraus T, Giese A, Arzberger T, Buchholz M, Höglinger G, et al. Parkinson's disease: SNCA-, PARK2-, and LRRK2- targeting microRNAs elevated in cingulate gyrus. Parkinsonism Relat Disord. 2016;33:115–21.

153. Cho HJ, Liu G, Jin SM, Parisiadou L, Xie C, Yu J, et al. MicroRNA-205 regulates the expression of Parkinson's disease-related leucine-rich repeat kinase 2 protein. Hum Mol Genet. 2013;22:608–20.

154. Junn E, Lee K-W, Jeong BS, Chan TW, Im J-Y, Mouradian MM. Repression of alpha-synuclein expression and toxicity by microRNA-7. Proc Natl Acad Sci U S A. 2009;106:13052–7.

155. Kabaria S, Choi DC, Chaudhuri AD, Mouradian MM, Junn E. Inhibition of miR-34b and miR-34c enhances α-synuclein expression in Parkinson's disease. FEBS Lett. 2015;589:319–25.

156. Rezaei O, Nateghinia S, Estiar MA, Taheri M, Ghafouri-Fard S. Assessment of the role of non-coding RNAs in the pathophysiology of Parkinson's disease. Eur J Pharmacol. 2021;896:173914. doi:10.1016/j.ejphar.2021.173914.

157. Chiba M, Kiyosawa H, Hiraiwa N, Ohkohchi N, Yasue H. Existence of Pink1 antisense RNAs in mouse and their localization. Cytogenet Genome Res. 2009;126:259–70.

158. Carrieri C, Forrest ARR, Santoro C, Persichetti F, Carninci P, Zucchelli S, et al. Expression analysis of the long non-coding RNA antisense to Uchl1 (AS Uchl1) during dopaminergic cells' differentiation in vitro and in neurochemical models of Parkinson's disease. Front Cell Neurosci. 2015;9:114.

159. Brooks BR. El Escorial World Federation of Neurology criteria for the diagnosis of amyotrophic lateral sclerosis. Subcommittee on Motor Neuron Diseases/Amyotrophic Lateral Sclerosis of the World Federation of Neurology Research Group on Neuromuscular Diseases and t. J Neurol Sci. 1994;124 Suppl:96–107.

160. Postuma RB, Berg D, Stern M, Poewe W, Olanow CW, Oertel W, et al. MDS clinical diagnostic criteria for Parkinson's disease. Mov Disord. 2015;30:1591–601.

161. Srivastava A, George J, Karuturi RKM. Transcriptome analysis. In: Encyclopedia of Bioinformatics and Computational Biology: ABC of Bioinformatics. Elsevier; 2018. p. 792–805.

162. Wang Z, Gerstein M, Snyder M. RNA-Seq: a revolutionary tool for transcriptomics. 2009.

163. Hrdlickova R, Toloue M, Tian B. RNA-Seq methods for transcriptome analysis. Wiley Interdisciplinary Reviews: RNA. 2017;8.

164. Stark R, Grzelak M, Hadfield J. RNA sequencing: the teenage years. Nature Reviews Genetics. 2019;20:631–56.

165. Giannopoulou EG, Elemento O, Ivashkiv LB. Use of RNA sequencing to evaluate rheumatic disease patients. Arthritis Research and Therapy. 2015;17.

166. Han Y, Gao S, Muegge K, Zhang W, Zhou B. Advanced applications of RNA sequencing and challenges. Bioinform Biol Insights. 2015;9:29–46.

167. Hussing C, Kampmann ML, Mogensen HS, Børsting C, Morling N. Quantification of massively parallel sequencing libraries - A comparative study of eight methods. Sci Rep. 2018;8:1–9.

168. Kraus AJ, Brink BG, Siegel TN. Efficient and specific oligo-based depletion of rRNA. Sci Rep. 2019;9:12281.

169. Head SR, Kiyomi Komori H, LaMere SA, Whisenant T, Van Nieuwerburgh F, Salomon DR, et al. Library construction for next-generation sequencing: Overviews and challenges. Biotechniques. 2014;56:61–77.

170. Bragg LM, Stone G, Butler MK, Hugenholtz P, Tyson GW. Shining a light on dark sequencing: characterising errors in Ion Torrent PGM data. PLoS Comput Biol. 2013;9:e1003031.

171. Rhoads A, Au KF. PacBio Sequencing and Its Applications. Genomics, Proteomics and Bioinformatics. 2015;13:278–89.

172. Dobin A, Davis CA, Schlesinger F, Drenkow J, Zaleski C, Jha S, et al. STAR: ultrafast universal RNA-seq aligner. Bioinformatics. 2013;29:15–21.

173. Yang IS, Kim S. Analysis of Whole Transcriptome Sequencing Data: Workflow and Software. Genomics Inform. 2015;13:119.

174. Yalamanchili HK, Wan Y-W, Liu Z. Data Analysis Pipeline for RNA-seq Experiments: From Differential Expression to Cryptic Splicing. Curr Protoc Bioinforma. 2017;59:11.15.1-11.15.21.

175. Dündar F, Skrabanek L, Zumbo P. Introduction to differential gene expression analysis using RNA-seq. 2015.

176. Reimand J, Isserlin R, Voisin V, Kucera M, Tannus-Lopes C, Rostamianfar A, et al. Pathway enrichment analysis and visualization of omics data using g:Profiler, GSEA, Cytoscape and EnrichmentMap. Nat Protoc. 2019;14:482–517.

177. Lindberg J, Lundeberg J. The plasticity of the mammalian transcriptome. Genomics. 2010;95:1–6. doi:10.1016/j.ygeno.2009.08.010.

178. Li B, Dewey CN. RSEM: Accurate transcript quantification from RNA-Seq data with or without a reference genome. BMC Bioinformatics. 2011;12.

179. Leng N, Dawson JA, Thomson JA, Ruotti V, Rissman AI, Smits BMG, et al. EBSeq: An empirical Bayes hierarchical model for inference in RNA-seq experiments. Bioinformatics. 2013;29:1035–43.

180. Carrara M, Lum J, Cordero F, Beccuti M, Poidinger M, Donatelli S, et al. Alternative splicing detection workflow needs a careful combination of sample prep and bioinformatics analysis. BMC Bioinformatics. 2015;16.

181. Love MI, Huber W, Anders S. Moderated estimation of fold change and dispersion for RNA-seq data with DESeq2. Genome Biol. 2014;15.

182. Subramanian A, Tamayo P, Mootha VK, Mukherjee S, Ebert BL, Gillette MA, et al. Gene set enrichment analysis: A knowledge-based approach for interpreting genome-wide expression profiles. 2005. www.pnas.orgcgidoi10.1073pnas.0506580102.

183. Chen EY, Tan CM, Kou Y, Duan Q, Wang Z, Meirelles GV, et al. Enrichr: interactive and collaborative HTML5 gene list enrichment analysis tool. 2013. http://amp.pharm.mssm.edu/Enrichr.

184. Kuleshov M V., Jones MR, Rouillard AD, Fernandez NF, Duan Q, Wang Z, et al. Enrichr: a comprehensive gene set enrichment analysis web server 2016 update. Nucleic Acids Res. 2016;44:W90–7.

185. Schreiber E, Matthias P, Miiller MM, Schaffner W. Rapid detection of octamer binding proteins with “mini-extracts”, prepared from a small number of cells. 1989. http://nar.oxfordjournals.org/.

186. Końca K, Lankoff A, Banasik A, Lisowska H, Kuszewski T, Góźdź S, et al. A cross-platform public domain PC image-analysis program for the comet assay. Mutat Res - Genet Toxicol Environ Mutagen. 2003;534:15–20.

187. Lazo-Gómez R, Ramírez-Jarquín UN, Tovar-Y-Romo LB, Tapia R. Histone deacetylases and their role in motor neuron degeneration. Front Cell Neurosci. 2013;7:243.

188. Kim T, Cui R, Jeon Y-J, Fadda P, Alder H, Croce CM. MYC-repressed long noncoding RNAs antagonize MYC-induced cell proliferation and cell cycle progression. Oncotarget. 2015;6:18780–9.

189. Guo X, Qi X. VCP cooperates with UBXD1 to degrade mitochondrial outer membrane protein MCL1 in model of Huntington's disease. Biochim Biophys acta Mol basis Dis. 2017;1863:552–9.

190. Lee JK, Shin JH, Lee JE, Choi E-J. Role of autophagy in the pathogenesis of amyotrophic lateral sclerosis. Biochim Biophys Acta. 2015;1852:2517–24.

191. Villar-Menéndez I, Porta S, Buira SP, Pereira-Veiga T, Díaz-Sánchez S, Albasanz JL, et al. Increased striatal adenosine A2A receptor levels is an early event in Parkinson's disease-related pathology and it is potentially regulated by miR-34b. Neurobiol Dis. 2014;69:206–14.

192. Castillo E, Leon J, Mazzei G, Abolhassani N, Haruyama N, Saito T, et al. Comparative profiling of cortical gene expression in Alzheimer's disease patients and mouse models demonstrates a link between amyloidosis and neuroinflammation. Sci Rep. 2017;7:17762.

193. Hashimoto Y, Niikura T, Tajima H, Yasukawa T, Sudo H, Ito Y, et al. A rescue factor abolishing neuronal cell death by a wide spectrum of familial Alzheimer's disease genes and Abeta. Proc Natl Acad Sci U S A. 2001;98:6336–41.

194. Grace EA, Busciglio J. Aberrant activation of focal adhesion proteins mediates fibrillar amyloid beta-induced neuronal dystrophy. J Neurosci. 2003;23:493–502.

195. Calderwood DA, Campbell ID, Critchley DR. Talins and kindlins: partners in integrin-mediated adhesion. Nat Rev Mol Cell Biol. 2013;14:503–17.

196. Bao Z, Yang Z, Huang Z, Zhou Y, Cui Q, Dong D. LncRNADisease 2.0: an updated database of long non-coding RNA-associated diseases. Nucleic Acids Res. 2019;47:D1034–7.

197. Ju X-C, Hou Q-Q, Sheng A-L, Wu K-Y, Zhou Y, Jin Y, et al. The hominoid-specific gene TBC1D3 promotes generation of basal neural progenitors and induces cortical folding in mice. Elife. 2016;5.

198. Zucca S, Gagliardi S, Pandini C, Diamanti L, Bordoni M, Sproviero D, et al. RNA-seq profiling in peripheral blood mononuclear cells of amyotrophic lateral sclerosis patients and controls. Sci Data. 2019;6.

199. Cai Y, Zhang Y, Loh YP, Tng JQ, Lim MC, Cao Z, et al. H3K27me3-rich genomic regions can function as silencers to repress gene expression via chromatin interactions. Nat Commun. 2021;12. doi:10.1038/s41467-021-20940-y.

200. Igolkina AA, Zinkevich A, Karandasheva KO, Popov AA, Selifanova M V., Nikolaeva D, et al. H3K4me3, H3K9ac, H3K27ac, H3K27me3 and H3K9me3 Histone

Tags Suggest Distinct Regulatory Evolution of Open and Condensed Chromatin Landmarks. Cells. 2019;8:1–16.

201. Donato R, Sorci G, Bianchi R, Riuzzi F, Tubaro C, Arcuri C, et al. S100B protein, a damage-associated molecular pattern protein in the brain and heart, and beyond. Cardiovascular Psychiatry and Neurology. 2010.

202. Juranek JK, Daffu GK, Wojtkiewicz J, Lacomis D, Kofler J, Schmidt AM. Receptor for advanced glycation end products and its inflammatory ligands are upregulated in amyotrophic lateral sclerosis. Front Cell Neurosci. 2015;9 DEC.

203. Dubrez L, Causse S, Borges Bonan N, Dumétier B, Garrido C. Heat-shock proteins: chaperoning DNA repair. Oncogene. 2020;39:516–29.

204. Barna J, Csermely P, Vellai T. Roles of heat shock factor 1 beyond the heat shock response. Cell Mol Life Sci. 2018;75:2897–916.

205. Nishioka K, Vilariño-Güell C, Cobb SA, Kachergus JM, Ross OA, Hentati E, et al. Genetic variation of the mitochondrial complex I subunit NDUFV2 and Parkinson's disease. Parkinsonism Relat Disord. 2010;16:686–7.

206. Troncone L, Luciani M, Coggins M, Wilker EH, Ho C-Y, Codispoti KE, et al. Aβ Amyloid Pathology Affects the Hearts of Patients With Alzheimer's Disease: Mind the Heart. J Am Coll Cardiol. 2016;68:2395–407.

207. Gdynia H-J, Kurt A, Endruhn S, Ludolph AC, Sperfeld A-D. Cardiomyopathy in motor neuron diseases. J Neurol Neurosurg Psychiatry. 2006;77:671–3.

208. Orsini F, De Blasio D, Zangari R, Zanier ER, De Simoni M-G. Versatility of the complement system in neuroinflammation, neurodegeneration and brain homeostasis. Front Cell Neurosci. 2014;8:380.

209. Dasuri K, Zhang L, Keller JN. Oxidative stress, neurodegeneration, and the balance of protein degradation and protein synthesis. Free Radic Biol Med. 2013;62:170–85.

210. Kim GH, Kim JE, Rhie SJ, Yoon S. The Role of Oxidative Stress in Neurodegenerative Diseases. Exp Neurobiol. 2015;24:325–40.

211. Wei C-W, Luo T, Zou S-S, Wu A-S. The Role of Long Noncoding RNAs in Central Nervous System and Neurodegenerative Diseases. Front Behav Neurosci. 2018;12:175.

212. Soreq L, Guffanti A, Salomonis N, Simchovitz A, Israel Z, Bergman H, et al. Long Non-Coding RNA and Alternative Splicing Modulations in Parkinson's Leukocytes Identified by RNA Sequencing. PLoS Comput Biol. 2014;10.

213. Elkouris M, Kouroupi G, Vourvoukelis A, Papagiannakis N, Kaltezioti V, Matsas

R, et al. Long Non-coding RNAs Associated With Neurodegeneration-Linked Genes Are Reduced in Parkinson's Disease Patients. Front Cell Neurosci. 2019;13:58.

214. Gérard M-A, Myslinski E, Chylak N, Baudrey S, Krol A, Carbon P. The scaRNA2 is produced by an independent transcription unit and its processing is directed by the encoding region. Nucleic Acids Res. 2010;38:370–81.

215. Fagerberg L, Hallström BM, Oksvold P, Kampf C, Djureinovic D, Odeberg J, et al. Analysis of the human tissue-specific expression by genome-wide integration of transcriptomics and antibody-based proteomics. Mol Cell Proteomics. 2014;13:397–406.

216. Sau D, De Biasi S, Vitellaro-Zuccarello L, Riso P, Guarnieri S, Porrini M, et al. Mutation of SOD1 in ALS: A gain of a loss of function. Hum Mol Genet. 2007;16:1604–18.

217. Vousden KH. Outcomes of p53 activation - Spoilt for choice. J Cell Sci. 2006;119:5015–20.

218. Kupershmit I, Khoury-Haddad H, Awwad SW, Guttmann-Raviv N, Ayoub N. KDM4C (GASC1) lysine demethylase is associated with mitotic chromatin and regulates chromosome segregation during mitosis. Nucleic Acids Res. 2014;42:6168–82.

219. Huang B, Wang B, Yuk-Wai Lee W, Pong U K, Leung KT, Li X, et al. KDM3A and KDM4C Regulate Mesenchymal Stromal Cell Senescence and Bone Aging via Condensin-mediated Heterochromatin Reorganization. iScience. 2019;21:375–90.

220. Mayer MP. Gymnastics of molecular chaperones. Molecular Cell. 2010;39:321–31.

221. Duan Y, Huang S, Yang J, Niu P, Gong Z, Liu X, et al. HspA1A facilitates DNA repair in human bronchial epithelial cells exposed to Benzo[a]pyrene and interacts with casein kinase 2. Cell Stress Chaperones. 2014;19:271–9.

222. Hunt CR, Dix DJ, Sharma GG, Pandita RK, Gupta A, Funk M, et al. Genomic Instability and Enhanced Radiosensitivity in Hsp70.1- and Hsp70.3-Deficient Mice. Mol Cell Biol. 2004;24:899–911.

223. Tandle AT, Mazzanti C, Alexander HR, Roberts DD, Libutti SK. Endothelial monocyte activating polypeptide-II induced gene expression changes in endothelial cells. Cytokine. 2005;30:347–58.

224. Lu H, Hallstrom TC. Sensitivity to TOP2 targeting chemotherapeutics is regulated by Oct1 and FILIP1L. PLoS One. 2012;7.

225. Aguila B, Morris AB, Spina R, Bar E, Schraner J, Vinkler R, et al. The Ig superfamily protein PTGFRN coordinates survival signaling in glioblastoma multiforme. Cancer Lett. 2019;462:33–42.

226. Serlidaki D, van Waarde MAWH, Rohland L, Wentink AS, Dekker SL, Kamphuis MJ, et al. Functional diversity between HSP70 paralogs caused by variable interactions with specific co-chaperones. J Biol Chem. 2020;295:7301–16.

227. Fang Q, Inanc B, Schamus S, Wang X, Wei L, Brown AR, et al. HSP90 regulates DNA repair via the interaction between XRCC1 and DNA polymerase β. Nat Commun. 2014;5:5513.

228. Katsogiannou M, Andrieu C, Baylot V, Baudot A, Dusetti NJ, Gayet O, et al. The functional landscape of Hsp27 reveals new cellular processes such as DNA repair and alternative splicing and proposes novel anticancer targets. Mol Cell Proteomics. 2014;13:3585–601.

229. Sottile ML, Nadin SB. Heat shock proteins and DNA repair mechanisms: an updated overview. Cell Stress Chaperones. 2018;23:303–15.

230. Lu T, Aron L, Zullo J, Pan Y, Kim H, Chen Y, et al. REST and stress resistance in ageing and Alzheimer's disease. Nature. 2014;507:448–54.

231. Shen H, Xu W, Lan F. Histone lysine demethylases in mammalian embryonic development. Exp Mol Med. 2017;49:1–7.